WOPM 2017

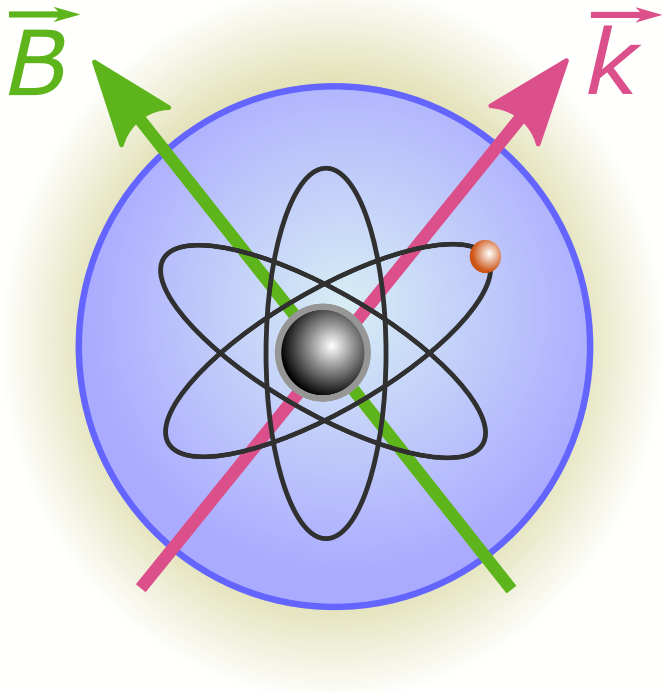

5th Workshop on Optically Pumped Magnetometers

University of Fribourg (Switzerland), August 21 - 22, 2017

BOOK OF ABSTRACTS

sponsored by:

Elekta

FRAP
Fribourg
Atomic Physics

Scientific Program Commitee:

Peter Schwindt (Chair, Sandia National Laboratories)
Svenja Knappe (University of Colorado & QuSpin Inc)
Tetsuo Kobayashi (Kyoto University)
Lauri Parkkonen (Aalto University & Elekta Oy)
Tilmann Sander (PTB Berlin)
Antoine Weis (University of Fribourg)

Local Organizing Committee:

Antoine Weis (Chair)
Victor Lebedev (Scientific secretary)
Zoran Grujić (Webmaster)
Theo Scholtes
Vladimir Dolgovskiy
Simone Colombo
Eliane Esseiva

Oral presentations

Monday, August 21st

#	Speaker	Title	Time
		Welcome and Introduction	08:30 – 08:50
		Session 1: Basic OPM research **Chair: Peter Schwindt / Dmitry Budker**	
T01	**Werner Heil**	Ultrasensitive ^{3}He NMR-Magnetometry for Measurements of High Magnetic Fields	08:50 – 09:10
T02	**Skyler Degenkolb**	Optical Magnetometry using Multiphoton Transitions and Polarized Nuclei	09:10 – 09:30
T03	**Volkmar Schultze**	The LSD-M_z Magnetometer – Working Principle, Properties and Applications	09:30 – 09:50
		Coffee break	09:50 – 10:30
T04	**Lu Deng**	Nonlinear Optical Wave Mixing Magnetometry	10:30 – 10:50
T05	**Michael Romalis**	Pulsed Scalar Atomic Magnetometer with Multi-Pass Cells	10:50 – 11:10
T06	**Ricardo Jimenez Martinez**	Precise signal-tracking with precessing spin ensembles	11:10 – 11:30
T07	**Witold Chalupczak**	Non-linear spin dynamics in atomic magnetometers	11:30 – 11:50
		Lunch	11:50 – 13:10
		Session 2: Novel OPM designs **Chair: Michael Romalis / Antoine Weis**	
T08	**Arne Wickenbrock**	Towards endoscopic magnetic field sensors based on diamonds for biomedical applications	13:10 – 13:30
T09	**Andreas Pollinger**	Flight Model Design of the Coupled Dark State Magnetometer for the China Seismo-Electromagnetic Satellite	13:30 – 13:50
T10	**Ilja Gerhardt**	Combination of Atomic Magnetometry with Solid State Samples	13:50 – 14:10
		Coffee break	14:10 – 14:50
T11	**Yosuke Ito**	A Simultaneous Multi-Location Measurement Method Based on Pump-Beam Modulation of Atomic Magnetometers by Electro-Optic Modulation	14:50 – 15:10
T12	**Thomas Kornack**	Towards a Practical Pulsed Magnetometer	15:10 – 15:30
T13	**Guzhi Bao**	Suppression of nonlinear Zeeman effect and heading error in earth-field alkali-vapor magnetometers	15:30 – 15:50
T14	**Stuart Ingleby**	Double Resonance Magnetometry in Arbitrarily Oriented Static Fields	15:50 – 16:10
		Posters	**16:10 – 18:10**
		Workshop dinner	**19:30 – ∞**

Oral presentations

Tuesday, August 22nd

#	Speaker	Title	Time
		Session 3: Biomagnetic Applications of OPMs Chair: Tilmann Sander / Lauri Parkkonen	
T15	**Tim Tierney**	Realising the advantages of OPM-MEG: Scanner casts and data modelling	08:30 – 08:50
T16	**Elena Boto**	OPM MEG with field nulling technology: Towards real world neuroimaging	08:50 – 09:10
T17	**Amir Borna**	Magnetoencephalography with a 20-Channel Optically Pumped Magnetometer Array	09:10 – 09:30
T18	**Joonas Iivanainen**	Quality of Visual Gamma-band Responses Measured with an Optically-pumped Magnetometer	09:30 – 09:50
		Coffee break	09:50 – 10:30
T19	**Sean Krzyzewski**	Development of a microfabricated optically-pumped magnetic gradiometer array for integration with a transcranial magnetic stimulation	10:30 – 10:50
T20	**Kaiyan He**	Magnetoencephalography with a Cs-Based High-Sensitivity Compact Atomic Magnetometer	10:50 – 11:10
T21	**Vishal Shah**	Towards Second-Generation Commercial OPMs for BioMagnetism	11:10 – 11:30
T22	**Kasper Jensen**	Quantum Optical Magnetometry for Biomedical Applications	11:30 – 11:50
		Lunch	11:50 – 13:10
		Session 4: Other Applications of OPMs Chair: Svenja Knappe / Tetsuo Kobayashi	
T23	**Theo Scholtes**	The Global Network of Optical Magnetometers for Exotic Physics searches	13:10 – 13:30
T24	**Derek Kimball**	Constraints on the coupling of the proton spin to gravity	13:30 – 13:50
T25	**Georg Bison**	Optical magnetometers for a next-generation neutron EDM experiment	13:50 – 14:10
		Coffee break	14:10 – 14:50
T26	**Midhat Farooq**	^{3}He Optical Magnetometer for the Absolute Calibration of Muon g-2 Magnetic Field Measurement	14:50 – 15:10
T27	**Simone Colombo**	Atomic Magnetometry Based Magnetic Particle Imaging (MPI)	15:10 –15:30
T28	**Rahul Mhaskar**	Applications of Miniature Scalar Atomic Magnetometers	15:30 –15:50
T29	**Valerio Biancalana**	Zero-to-Ultralow-Field-NMR spectroscopy with an atomic magnetometer in unshielded environment	15:50 – 16:10
		Posters	**16:10 – ∞**

Poster presentations

Part 1

Presenter	Title	#
	Section 1: OPM basic research	
Dong Sheng	Optically Pumped Magnetometry at USTC	**P01**
Victor Lebedev	Study of the Directional Dependence of Magnetic Resonance Signals in Orientation-Based Atomic Mx-Magnetometers	**P02**
Zoran Grujić	Accurate Cesium Magnetometer Based on Free Alignment Precession	**P03**
Morgan Mitchell	On the statistical sensitivity and quantum limits of spin noise spectroscopy	**P04**
Yongqi Shi	The Ground State Hanle Effect with Linearly-Polarized and Unpolarized Light	**P05**
Charikleia Troullinou	Towards a high-density squeezed-light magnetometer	**P06**
Carolyn O'Dwyer	Test System for Investigation of Geometry Dependent Systematic Effects in Double Resonance Magnetometry	**P07**
Rob IJsselsteijn	On the Heading Error of Various OPM Types	**P08**
Vira Bondar	Sensitive and stable Hanle-type 2D magnetometer	**P09**
Dominic Hunter	Chip-scale Atomic Magnetometer Based on Free Induction Decay for Ultra-low Magnetic Field Detection	**P10**
Michaela Ellmeier	Comparison of Two Sensor Designs for the Coupled Dark State Magnetometer	**P11**
François Beato	Laser frequency locking using a transversal magnetic field for helium-based magnetometers	**P12**
Lu Deng	Theory of Nonlinear Optical Wave Mixing Magnetometry	**P13**
	Section 2: Fundamental Science with OPM	
Peter Koss	A Potassium Magnetometry Based Current Source for the n2EDM Experiment at PSI	**P14**
Vincent Dumont	Cross-correlation analysis between Optically-Pumped Magnetometers for Dark Matter searches	**P15**
Hector Masia Roig	Description and Characterization of the Optical Magnetometer in Mainz Dedicated to the Global Network of Optical Magnetometers for Exotic Physics Searches (GNOME)	**P16**
Mikhail Padniuk	Self-compensating atomic magnetometer for searches of transient anomalous spin couplings	**P17**
Yunlan Ji	Detecting J-coupling in the gaseous molecule by spin-exchange optical pumping	**P18**

Poster presentations

Part 2

Presenter	Title	#
	Section 3: OPM Applications	
Vladimir Dolgovskiy	An Optically-Pumped Magnetometer for Field Mapping and Reconstruction of Distributed Source Locations	**P19**
Elena Boto	Multi-channel OPM-MEG during a visuo-motor task: induced responses and source localisation	**P20**
Sofie Meyer	Designing a cryogen-free MEG system for hippocampal recording	**P21**
Leonardo Duque-Muñoz	Estimating the geometry of OPM sensor arrays relative to the human brain	**P22**
Niall Holmes	Towards wearable OPM-MEG: Using bi-planar field nulling coils to allow subject movement	**P23**
George Roberts	Exploring Crosstalk in an Optically Pumped Magnetometer Array for Magnetoencephalography – Simulation and Experiment	**P24**
Tim Tierney	Accuracy and Reliability of a multi-channel OPM MEG System for presurgical planning	**P25**
Tilmann Sander	High subject throughput individualized OPM sensor array	**P26**
Tilmann Sander	Multivariate statistical analysis of OPM sensor array data	**P27**
Aaron Jaufenthaler	Exploiting Optically Pumped Magnetometer’s Flexibility To Optimize The Problem Conditioning In Magnetorelaxometry Imaging	**P28**
Gaëtan Lieb	Helium-based OPM for room-temperature bio-magnetic measurements	**P29**
Christoph Braun	Can Optically Pumped Magnetometers (OPM) Capture Neuromagnetic Activity of Peripheral Nerves and the Spinal Coord?	**P30**
Rasmus Zetter	Co-registration in On-scalp Magnetoencephalography Based on Optically-pumped Magnetometers	**P31**
Christian Schmidt	Optically pumped magnetic field camera – A proposal	**P32**
Dmitrii Altukhov	OPM versus SQUID Arrays in MEG Functional Connectivity Estimation: A Simulation Study	**P33**
Axel Thielscher	Wide-Field Imaging of Magnetic Fields Using Nitrogen-Vacancy Centers in Diamond: Estimation of required sensitivity and resolution	**P34**

Oral presentations

Ultrasensitive ^{3}He NMR-Magnetometry for Measurements of High Magnetic Fields

Werner Heil, Peter Blümler, Andreas Maul, Ernst Otten

Institute of Physics, University of Mainz, Staudingerweg 7, 55128 Mainz, Germany

In the talk a ^{3}He magnetometer is described capable to measure high magnetic fields (B > 0.1 T) with a relative accuracy of better than 10^{-12}. Our approach is based on the measurement of the free induction decay (FID) of gaseous, nuclear spin polarized ^{3}He following a resonant radio frequency pulse excitation. The measurement sensitivity can be attributed to the long coherent spin precession time T_2^* being of order minutes which is achieved for spherical sample cells in the regime of "motional narrowing" where the disturbing influence of field inhomogeneities is strongly suppressed. The ^{3}He gas is spin polarized in situ using a new, non-standard variant of the metastability exchange optical pumping. This magnetometer also provides precise measurements of magnetic field gradients in the sub pT/cm range extracted from the transverse relaxation rates.

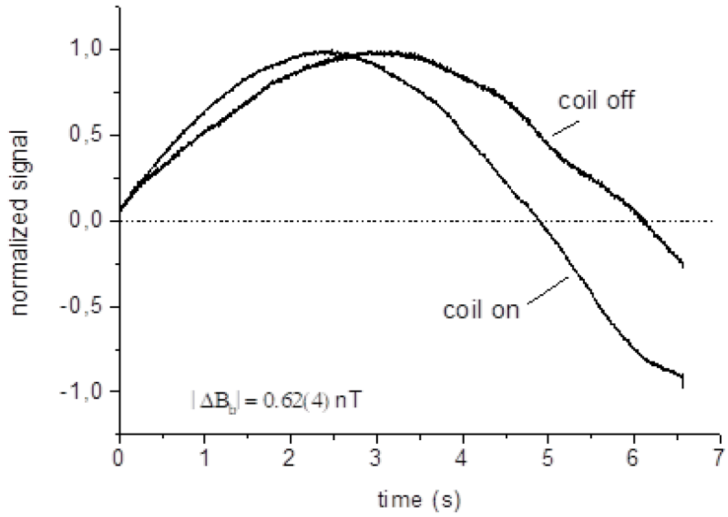

Fig. 1 Measured FID (normalized signal ; sampling rate: rs,0 = 620 Hz) of the beat frequency *fb* with and without preset magnetic field shifts of $\Delta B_{set} = 0.6$ nT added to the main B = 1.5 T field of the MR scanner. The characteristic time constant of the FID could be determined to be $T_2 \approx 70$ s. For technical reasons only 6.6 s of the FID could be recorded.

References

[1] C. Gemmel *et al.*, *Ultra-sensitive magnetometry based on free precession of nuclear spins*, Eur. Phys. J. D **57**, 303 (2010).
[2] A. Nikiel *et al.*, *Ultrasensitive ^{3}He magnetometer for measurements of high magnetic fields*, Eur. Phys. J. D **68**, 330 (2014).
[3] H.-C. Koch *et al.*, *Design and performance of an absolute ^{3}He/Cs magnetometer*, Eur. Phys. J. D **69**, 202 (2015).
[4] F. Allmendinger *et al.*, *Precise measurement of magnetic field gradients from free spin precession signals of ^{3}He and ^{129}Xe magnetometers*, Eur. Phys. J. D **71**, 98 (2017).

Optical Magnetometry using Multiphoton Transitions and Polarized Nuclei

Skyler Degenkolb[1], **Tim Chupp**[2], **Jaideep Singh**[3]

1. Institut Laue-Langevin, 71 avenue des Martyrs - CS 20156, 38042 Grenoble CEDEX 9, France
2. University of Michigan, 450 Church Street, Ann Arbor, Michigan 48109, USA
3. National Superconducting Cyclotron Laboratory, Michigan State University, 640 South Shaw Lane, East Lansing, Michigan 48824, USA

We present a novel approach to optical magnetometry, based on the use of multiphoton transitions in diamagnetic atoms to detect Larmor precession of spin-polarized nuclei. This technique promises several advantages in the context of low-energy precision measurements (especially permanent electric dipole moment searches), where magnetometer properties such as chemical reactivity, dielectric strength, and interaction cross-sections with other particles or atomic species are relevant in addition to intrinsic magnetic field sensitivity. Nuclear spins and non-linear optical excitation introduce new degrees of freedom, and evade limitations arising from rapid electronic decoherence that are typical in paramagnetic atomic systems.

We have demonstrated continuous-wave excitation of the ${}^1S_0 \to {}^2[5/2]_2$ two-photon transition in neutral xenon at 256nm, which represents a good experimental compromise between desirable material properties and the limitations of current laser technology. Proof-of-principle experiments have also been performed with two-photon transitions using continuous-wave and modelocked pulsed lasers at more convenient wavelengths, in ytterbium (808nm) and rubidium (778nm). We remark on the associated possibilities for efficient multiphoton excitation, spatial resolution, and absolute frequency stability that arise from the unique laser systems employed.

The LSD-Mz Magnetometer – Working Principle, Properties and Applications

Volkmar Schultze[1], **Rob IJsselsteijn**[1,2], **Ronny Stolz**[1]

1. Leibniz Institute of Photonic Technologies, Albert-Einstein-Straße 9, D-07745 Jena, Germany
2. Supracon AG, An der Lehmgrube 11, D-07751 Jena, Germany

We present an optically pumped magnetometer working in a new operational mode – the light-shift dispersed M_z (LSD-Mz) mode [1]. It uses light-narrowing (LN) [2] achieved by strong repumping of the lower hyperfine ground-state – $F = 3$ of the Cs-D1 line. In M_z configuration this enhances the absorption of the pump laser beam when the B1-field frequency approximates the Larmor frequency. At the same time, this high-power repumping induces a strong light-shift. In order to benefit from these features, we use two on-chip vapour cells with identical working conditions except for the antipodal circular polarisation of the pump light. The difference of the two absorption signals, which are shifted in opposite direction, has a dispersive character with zero crossing at the Larmor frequency, thus can be used for magnetic-field determination (Fig. 1).

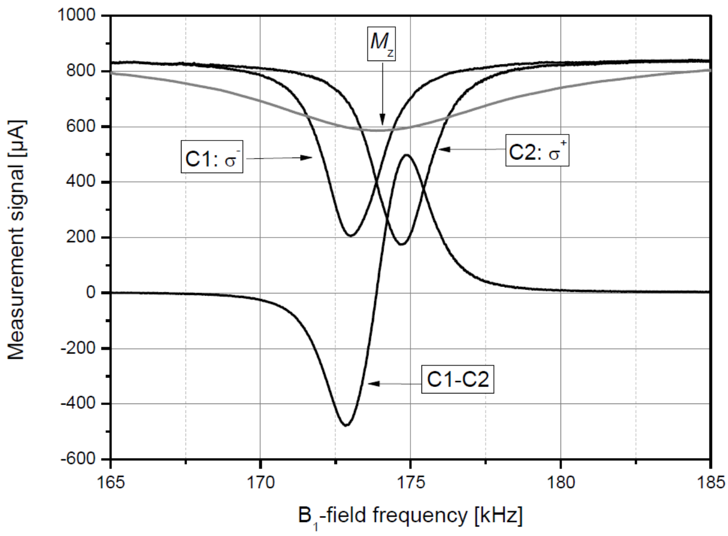

Fig. 1 M_z signals of two single cells (C1 and C2) pumped in the LN mode with different helicity of the circularly polarized light and their LSD-Mz difference signal (C1-C2), in dependence on the B_1-field frequency. A conventional M_z signal with pumping on F = 4 is shown for comparison. The B_0-field had a value of about 50 μT.

The LSD-Mz OPM offers various advantages: As a pure dc measurement it eliminates the problem of tuning the reference phase to the correct value in lock-in measurements like in the M_x configuration. Due to the preferred parallel orientation of pump light and measurement field B_0 almost all atoms are pumped into the stretched state. This increases the signal further. In consequence a good shot-noise limited magnetic-field resolution of about 10 $\mathrm{fT}/\sqrt{\mathrm{Hz}}$ is achieved with 50 mm^3 cell volumes despite the broad resonance of 1 kHz. As a positive consequence this, in turn, reflects in a corresponding high signal bandwidth. In contrast to SERF magnetometers [3] the LSD-Mz ones keep their magnetic-field resolution also for higher B_0 strengths like the Earth's magnetic field. Also the heading error can be kept low because the best signal quality is achieved in magnetic-field orientations around zero degree with respect to the pump beam direction. The price of these advantages is that low-frequency technical noise contributions like laser noise may degrade the measurement results. Due to the direct subtraction of the signals of two commonly operated vapour cells, a noise reduction is directly implemented in the LSD-Mz principle, however [4]. Further influences of various operational parameters on the LSD-Mz magnetometer performance will be shown and discussed.

References

[1] V. Schultze, B. Schillig, R. IJsselsteijn, T. Scholtes, S. Woetzel, and R. Stolz, *An Optically Pumped Magnetometer Working in the Light-Shift Dispersed M_z Mode*, Sensors **17**, 561 (2017).
[2] T. Scholtes, V. Schultze, R. IJsselsteijn, S. Woetzel, H.-G. Meyer, *Light-narrowed optically pumped M_x magnetometer with a miniaturized Cs cell*, Phys. Rev. A **84**, 043416 (2011); Erratum. **86**, 059904(E) (2012).
[3] I. K. Kominis, T. W. Kornack, J. C. Allred, M. V. Romalis, *A subfemtotesla multichannel atomic magnetometer*. Nature **422**, 596 (2003).
[4] V. Schultze, R. IJsselsteijn, H.-G. Meyer. *Noise reduction in optically pumped magnetometer assemblies*. Appl. Phys. B **100**, 717 (2010).

Nonlinear Optical Wave Mixing Magnetometry

Lu Deng[1], Yvonne Y. Li[2], Feng Zhou[1], Eric Zhu[1], E. W. Hagley[1]

1. National Institute of Standards and Technology, Gaithersburg, Maryland USA 20899
2. Department of Medical Oncology, Dana-Farber Cancer Institute, Harvard Medical School, Boston, MA USA 02115

Atomic magnetometers relying on the nonlinear magneto-optical rotation (NMOR) effect have achieved impressive weak magnetic field detection sensitivities [1-3]. In the semi-classical picture, different polarization components of a linearly-polarized probe field, with its two circular components forming a Λ-scheme, experience a different complex dispersion when traversing a magnetized medium, giving rise to an optical polarization rotation detectable using standard polarimetry methods. However, since each polarization component simultaneously undergoes one-photon absorption, and two-photon stimulated-emission processes, the symmetric nature of this single probe Λ-scheme is self-restricted by detailed balance, leading to a small NMOR effect.

An optical wave mixing process overcomes this self-limiting effect by introducing a second Zeeman-coherence manipulation channel (Fig. 1a), resulting in significant enhancement of the NMOR optical SNR (Fig. 1b) by using a counter-propagating beam configuration. In Fig. 1b we compare the NMOR signal of the usual single-beam Λ-scheme (blue trace) with the NMOR signal from the optical wave mixing scheme (red trace). Experimentally, we routinely observe more than 500-fold optical NMOR SNR enhancement using a wave mixing field intensity < 80 μW/cm^2, demonstrating the superior and robust performance of the new scheme.

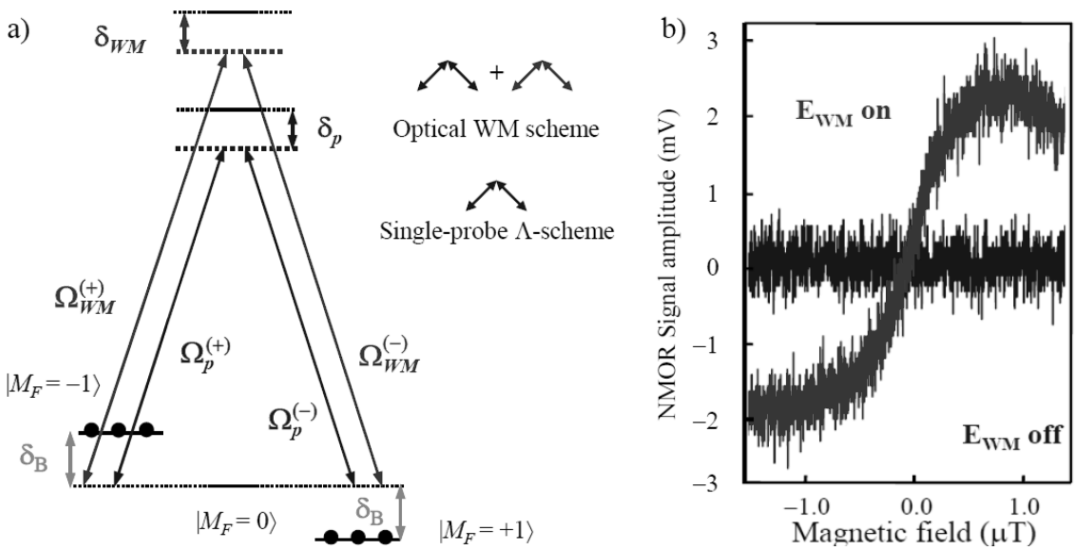

Fig. 1 Simplified optical wave mixing scheme (both channels) and the usual single-probe Λ-scheme (lower channel only). (b) NMOR signal at T=311K. Probe field: 20 μW/cm^2 (δ_P = -5 GHz, ^{87}Rb F = 2 to F = 1). WM field: 12 μW/cm^2 (δ_{WM} = -2 GHz, ^{87}Rb F = 2 to F = 1).

The Zeeman-coherence optical wave mixing scheme demonstrated here exhibits a superior optical SNR in extremely weak magnetic field detection. The physics behinds this novel performance is subtle and is partly related to ground state Zeeman coherence. The principle is also applicable to optical magnetometers where nonlinear optical polarization rotation is the central principle of the operation. Indeed, noticeable enhancement has been observed on a well-calibrated SERF-type magnetometer, raising the prospect of further improvement of the SNR of magnetometers operated on the similar principles. With further optical improvements, this new magnetometry scheme may enable a host of new applications, in fields such as bio-magnetism and fundamental particle physics, by eclipsing what current state-of-the-art technologies can presently offer.

References

[1] D. Budker and M. Romalis, *Optical Magnetometry*. Nature Phys. **3**, 227 (2007).
[2] I. K. Kominis, T.W. Kornack, J.C. Allred, and M. Romalis, *A subfemtotesla multichannel atomic magnetometer*. Nature **422**, 596 (2003).
[3] V.A. Sautenkov *et al.*, *Enhancement of magneto-optic effects via large atomic coherence in optically dense media*. Phys. Rev. A **62**, 023810 (2000).

Pulsed Scalar Atomic Magnetometer with Multi-pass Cells

V. G. Lucivero, N. D. McDonough, N. Dural, and M. V. Romalis

Physics Department, Princeton University, Princeton, NJ 08540, USA

I will review our recent work on scalar atomic magnetometers designed to operate with high sensitivity in Earth's magnetic field. In order to achieve high sensitivity in a compact sensor we arrange for the probe laser beam to pass many times through the atomic vapour by fabricating cells with internal high-reflectivity mirrors. In this regime we realize large optical rotation of the probe beam polarization, often well in excess of $\pi/4$ radians, and the polarization noise dominated by atomic quantum spin fluctuations [1]. We reduce spin-exchange relaxation of the alkali-metal vapour in the presence of a large magnetic field by initially creating a nearly fully-polarized atomic state with a short light pulse from a high power pump laser. In this regime the relaxation rate of the atomic vapour is not constant in time, it speeds up with time as the atoms lose their polarization. By operating in this non-Markovian regime we can take advantage of the spin quantum-non-demolition measurements performed by the probe laser in order to improve the overall sensitivity of the magnetometer [2].

In the past this approach has been limited by diffusion of atoms in the multi-pass cell [3]. As a result, the decay of the spin time-correlation function occurs much faster than the decay of the ensemble average spin polarization, because different atoms are sampled by the probe laser beam at different times. Recently we developed a new multi-pass cell geometry, shown in Fig. 1, which significantly reduces this problem by creating a more uniform intensity distribution of the probe laser in the multi-pass cell.

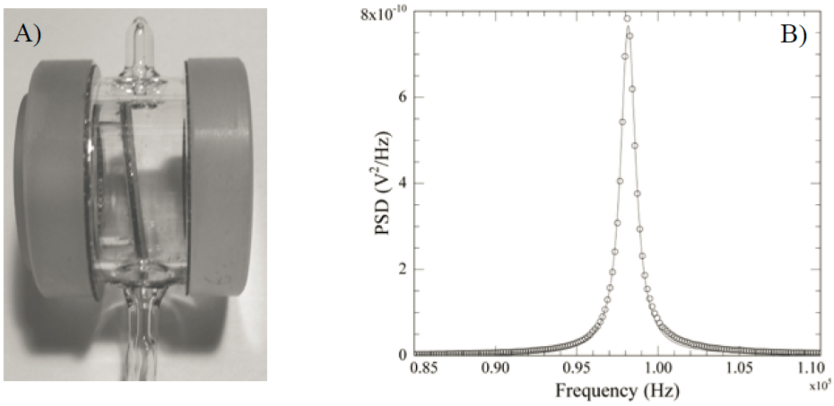

Fig. 1 A) A picture of a multi-pass cell assembled with anodic bonding using two spherical mirrors with high reflectivity coatings. One of the mirrors has a 200 μm hole for entrance and exit of the probe light. B) An example of the quantum spin noise spectrum with a Lorentzian fit. Diffusion effects result in distortions of the noise spectrum from a Lorentzian shape.

I will describe measurements of the spin time-correlation function, operation of the scalar magnetometer using the new multi-pass cells, and analysis of the fundamental noise sources limiting its performance.

References

[1] S. Li, P. Vachaspati, D. Sheng, N. Dural, and M. V. Romalis, *Optical rotation in excess of 100 rad generated by Rb vapor in a multipass cell*, Phys. Rev. A **84**, 061403 (2011).

[2] G. Vasilakis, V. Shah, and M. V. Romalis, *Stroboscopic Backaction Evasion in a Dense Alkali-Metal Vapor*, Phys. Rev. Lett. **106**, 143601 (2011).

[3] D. Sheng, S. Li, N. Dural, and M. V. Romalis, *Subfemtotesla Scalar Atomic Magnetometry Using Multipass Cells*, Phys. Rev. Lett. **110**, 160802 (2013).

Precise signal-tracking with precessing spin ensembles

Ricardo Jiménez-Martínez[1], Jan Kolodynski[1], Jia Kong[1], Charikleia Troullinou[1], Morgan W. Mitchell[1,2]

1. ICFO-Institut de Ciencies Fotoniques, The Barcelona Institute of Science and Technology, 08860 Castelldefels (Barcelona), Spain
2. ICREA – Institució Catalana de Recerca i Estudis Avançats, 08015 Barcelona, Spain

Many of the most compelling applications of atomic and optical interferometry study continuous, time-varying signals, such as in gravitational-wave detection [1] and bio-magnetic field sensing [2, 3] for instance. Moreover, many applications use such continuous measurements to control the measured system, as when a spectroscopy signal is fed back to a local oscillator in an atomic clock [4]. A central task in any such measurements is the *estimation* of the true signal from a noisy measurement record, a task that entails also giving uncertainties for the estimates. The choice of estimator leads to dynamical considerations not found in simpler measurement problems, for example a trade-off of time resolution versus precision. In control applications the choice is moreover fundamentally restricted to causal estimators, and practically limited to those that can be computed quickly. Tools from Bayesian statistics provide an elegant and natural framework to the estimation task in realtime. Of particular interest is the Kalman filter (KF) [5], and its extensions. To date KFs have been implemented in a number of interferometric sensors, for instance to enhance phase-tracking by light squeezing [6], and have been proposed to track quasi-static magnetic fields with optically-pumped magnetometers (OPM) [7]. However its experimental implementation and validation in alkali spin ensembles remains an open challenge, as a result optimal autonomous OPM are yet to be implemented. Here we describe our recent work and results aimed at implementing KFs with precessing alkali spin ensembles. Using KF we track the collective spin orientation of the atomic ensemble as well as stochastic and deterministic optical time-varying signals coupled to the spins. The prospects for integrating these techniques to track magnetic fields will be discussed as well.

References

[1] B.P. Abbot *et al.* (LIGO Scientific Collaboration and Virgo Collaboration), *Observation of Gravitational Waves from a Binary Black Hole Merger*, Phys. Rev. Lett. **116**, 061102 (2016).

[2] T. H. Sander, J. Preusser, R. Mhaskar, J. Kitching, L. Trahms, and S. Knappe, *Magnetoencephalography with a chip-scale atomic magnetometer*, Biomed. Opt. Express **3**, 981 (2012).

[3] G. Bison *et al.*, *A room temperature 19-channel magnetic field mapping device for cardiac signals*, Appl. Phys. Lett. **95**, 173701 (2009).

[4] A. D. Ludlow, M. M. Boyd, J. Ye, E. Peik, and P. O. Schmidt, *Optical atomic clocks*, Rev. Mod. Phys. **87**, 637 (2015).

[5] R. E. Kalman, *A New Approach to Linear Filtering and Prediction Problems*, Transactions of the ASME, Journal of Basic Engineering **82**, 35 (1960).

[6] H. Yonezawa *et al.*, *Quantum-Enhanced Optical-Phase Tracking*, Science **337**, 1514 (2012).

[7] J. Geremia, J. K. Stockton, A. C. Doherty, and H. Mabuchi, *Quantum Kalman Filtering and the Heisenberg Limit in Atomic Magnetometry*, Phys. Rev. Lett. **91**, 250801 (2003).

Non-linear spin dynamics in atomic magnetometers

R. Gartman[1], W. Chalupczak[1], G. Bevilacqua[2], Y. Dancheva[2], V. Biancalana[2]

1. National Physical Laboratory, Teddington, UK
2. Università di Siena, Siena, Italy

It is generally accepted that an optical probe and spin-exchange collisions, through so-called quantum back-action and decoherence respectively, introduce perturbations in the atomic system. We show that the non-linearities introduced by the optical probe (i.e. tensor light shift) as well as spin-exchange collisions generate novel atomic spin dynamics. This could lead to increase of the coherence lifetime and generation of the entanglement. The former will be demonstrated and discussed in context of so-called spin maser, while the latter on basis of Bell-Bloom pumping process, where the atomic coherences are created by a train of optical excitation pulses.

T08

Towards endoscopic magnetic field sensors based on diamonds for biomedical applications

Arne Wickenbrock[1,2], **Georgios Chatzidrosos**[1], **Huijie Zheng**[1], **Lykourgos Bougas**[1], **Dmitry Budker**[1,2,3]

1. Johannes Gutenberg-University, Mainz, Germany
2. Helmholtz Institut Mainz, Mainz, Germany
3. Department of Physics, University of California, Berkeley, CA 94720-7300, USA

We propose and report on the progress towards a miniaturized endoscopic magnetic field sensor based on color center ensembles in diamond. The unique design of the sensor enables spatially resolved in-vivo measurements of static and oscillating magnetic fields with a broad bandwidth and high sensitivity. An endoscopic magnetometer could boost the size of magnetic signals of the heart, the brain or other organs due to the reduced distance to the underlying current densities. The high-bandwidth of the device enables spatially resolved methods for tissue discrimination such as nuclear magnetic resonance or eddy-current detection in vivo.

We present the recent developments towards a miniaturized, highly sensitive magnetometer (Figure 1) that measures magnetic fields by monitoring cavity-enhanced absorption on the singlet transition of the negatively charged nitrogen-vacancy (NV) center in diamond under radio-frequency irradiation and optical pumping with a green laser. We achieve shot-noise limited performance with sensitivities better than 100 $\mathrm{pT}/\mathrm{Hz}^{1/2}$ [1].

Rapidly changing environment in the human body as well as exposure limits for electromagnetic radiation motivate the use of a microwave-free magnetometer. We demonstrated such a device based on a narrow magnetic feature due to the ground-state level anticrossing (GSLAC) of the NV center at a background field of 102 mT to measure magnetic fields without microwaves [2] (Figure 2).

Here, we report on the combination of this method with the miniaturized absorption-based magnetometer [3] and sketch a way towards a fully integrated device capable of first endoscopic measurements.

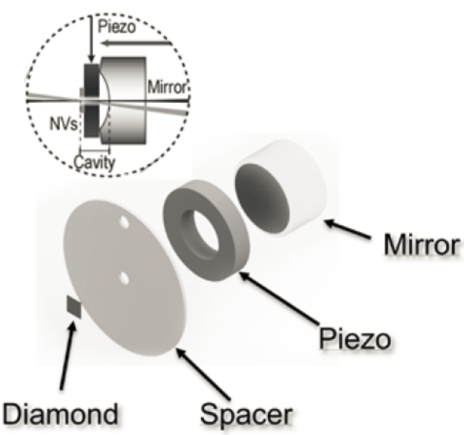

Fig. 1 Schematic of the absorption-based cavity-enhanced diamond magnetometer. The dimensions of the sensing volume are below (100x100x300) $\mu\mathrm{m}^3$.

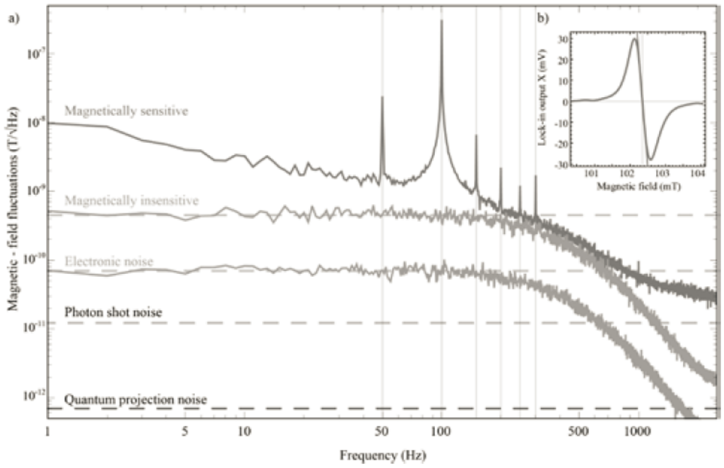

Fig. 2 Noise characterization of a microwave-free magnetometer. The inset shows the derivative of the GSLAC feature used to translate the measured signal into magnetic field.

References

[1] G. Chatzidrosos, A. Wickenbrock, L. Bougas, N. Leefer, T. Wu, K. Jensen, Y. Dumeige, and D. Budker, *Miniature cavity-enhanced diamond magnetometer*, in preparation.

[2] A. Wickenbrock, H. Zheng, L. Bougas, N. Leefer, S. Afach, A. Jarmola, V. M. Acosta, and D. Budker, *Microwave-free magnetometry with nitrogen-vacancy centers in diamond*, Appl. Phys. Lett. **109**, 053505 (2016).

[3] H. Zheng, G. Chatzidrosos, A. Wickenbrock, L. Bougas, R. Lazda, A. Berzins, F. H. Gahbauer, M. Auzinsh, R. Ferber, and D. Budker, *Level anti-crossing magnetometry with color centers in diamond*, Proc. of SPIE **10119**, 101190X-1 (2017).

Flight Model Design of the Coupled Dark State Magnetometer for the China Seismo-Electromagnetic Satellite

Andreas Pollinger[1,2], Roland Lammegger[2], Werner Magnes[1], Irmgard Jernej[1], Christian Hagen[1], Michaela Ellmeier[1,2], Wolfgang Baumjohann[1]

1. Space Research Institute, Austrian Academy of Sciences, Schmiedlstraße 6, 8042 Graz, Austria
2. Institute of Experimental Physics, Graz University of Technology, Petersgasse 16, 8010 Graz, Austria

The Coupled Dark State Magnetometer (CDSM) is a scalar magnetometer based on two-photon spectroscopy of free alkali atoms. Coherent Population Trapping (CPT) leads to narrow optical resonance features, which enable a precise determination of the magnetic field-dependent Zeeman energy level shifts. Systematic errors, which usually degrade the accuracy of single CPT magnetometers, are cancelled or at least minimized by the use of several CPT resonances in parallel. CPT inherently allows omni-directional measurements. This leads to a moderately complex, all-optical sensor design without double cell units, excitation coils or electro-mechanical parts.

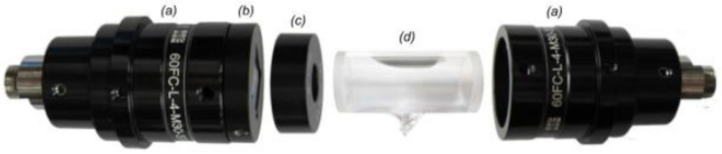

Fig. 1 The sensor consists of two fibre couplers (a), a polariser (b), a quarter-wave plate (c) and a ^{87}Rb-filled glass cell (d).

The measurement principle was discovered in 2008 [1] and since then the instrument has been developed by the two institutes involved for future space missions [2, 3]. The first demonstration in space will take place aboard the China Seismo-Electromagnetic Satellite (CSES) mission. The flight model will be launched into a low Earth orbit in August 2017. Furthermore, the CDSM is baseline instrument for the JUpiter ICy moons Explorer (JUICE) mission of the European Space Agency (ESA) to visit the Jovian system.

The presentation includes an introduction of the measurement principle, the instrument design for the CSES mission and performance characteristics such as accuracy, sensor heading and temperature dependencies as well as noise.

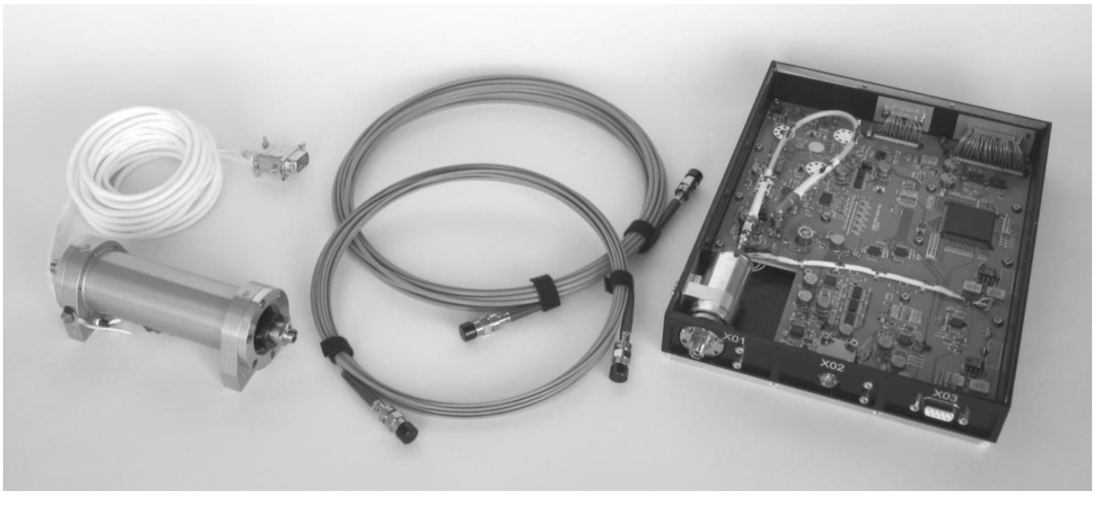

Fig. 2 Flight model for the China Seismo-Electromagnetic Satellite (CSES) mission.

References

[1] R. Lammegger, *Method and device for measuring magnetic fields*, WIPO, Patent WO/2008/151344 (2008).

[2] A. Pollinger, M. Ellmeier, W. Magnes, C. Hagen, W. Baumjohann, E. Leitgeb, R. Lammegger, *Enable the inherent omni-directionality of an absolute coupled dark state magnetometer for e.g. scientific space applications*, IEEE Instrumentation and Measurement Technology Conference (I2MTC) Proceedings, 33 (2012).

[3] A. Pollinger, *Development and Evaluation of a Control Unit for the Coupled Dark State Magnetometer*, PhD Thesis, Graz University of Technology (2013).

Combination of Atomic Magnetometry with Solid State Samples

Daniel Arnold[1], Jörg Wrachtrup[1,2], Ilja Gerhardt[1,2]

1. 3. Institute of Physics, University of Stuttgart and Center for Integrated Quantum Science and Technology, IQST, Pfaffenwaldring 57, D-70569 Stuttgart, Germany

2. Max Planck Institute for Solid State Research, Heisenbergstraße 1, D-70569 Stuttgart, Germany

Sensitive magnetometry implemented in atomic vapors has been established in the past decades. It has mastered the transition from the lab to a variety of field applications. The key parameters are the achievable line-width and the associated signal-to-noise ratio [1]. In parallel, the research on solid-state and spin-active samples formed a growing field to optical sciences as well. The latter sensor system, such as nitrogen vacancy centers in diamond [2], does generally not exhibit a good DC-sensitivity [3], but is well suitable for magnetometry on different frequency ranges and on nm-sized samples in their close proximity [4]. Defect centers can be singled out, single photon emission was detected, and the present research covers not only the field of optical magnetometry, but also quantum information [5] and nano-scale thermometry [6].

In the past two years, we have implemented a rubidium M_x-magnetometer [7]. The design is suitable for in-cooperating a small ($\approx$ 2 mm $\varnothing$) solid state experiment (see Fig. 1a and b). The design principles and the home-made cell design will be discussed in the presentation.

One of the first samples which is researched is a bulk sample of nitrogen-vacancy defect centers in a ppm-concentration diamond (see Fig. 1c). We will outline the specific strength of atomic vapors and nitrogen-vacancy centers and discuss options of combining both techniques.

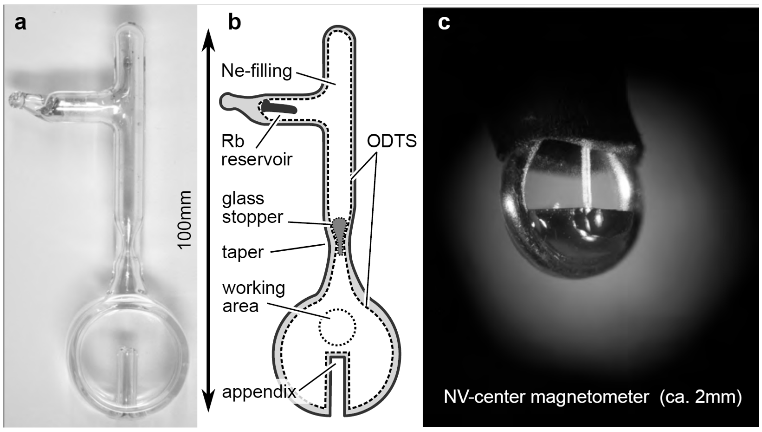

Fig. 1 a) Photograph from one of the rubidium cells, suitable for inserting a solid-state sample. **b)** The design combines buffer gas, anti-relaxation coating, and an appendix for the solid-state sample. **c)** The diamond NV-center magnetometer, multi-mode fiber coupled and with a rigid-waveguide antenna.

How and if a hybrid device can surpass the quality measures of a single sensor system alone is presently under research. Especially the difference frequency range poses challenging hurdles to their combination. On the other hand, our experiments originate from a more fundamental approach, namely to the questions if and how two optical magnetometers can influence each other. A few steps on other systems have been taken in the past [8,9]; we believe that a combination with solid-state samples might lead to a significant decrease in sensor size and might open the route to new samples which can be researched with atomic magnetometry.

References

[1] D. Budker and M. Romalis, *Optical magnetometry*, Nature Phys. **3**, 227 (2007).
[2] F. Jelezko and J. Wrachtrup, *Single defect centres in diamond: A review*, Phys. Status Solidi A **203**, 113, 3207 (2006).
[3] T. Wolf *et al.*, *Subpicotesla Diamond Magnetometry*, Phys. Rev. X **5**, 041001 (2015).
[4] T. Staudacher *et al.*, *Nuclear Magnetic Resonance Spectroscopy on a (5-Nanometer)^3 Sample Volume*, Science **339**(6119), 561 (2013).
[5] G. Waldherr *et al.*, *Quantum error correction in a solid-state hybrid spin register*, Nature **506**, 204 (2014).
[6] P. Neumann *et al.*, *High-Precision Nanoscale Temperature Sensing Using Single Defects in Diamond*, Nanoletters **13**(6), 2738 (2013).
[7] D. Arnold *et al.*, *A rubidium M_x-magnetometer for measurements on solid state spins*, Rev. Sci. Instrum. **88**, 023103 (2017).
[8] H.-C. Koch *et al.*, *Design and performance of an absolute ^{3}He/Cs magnetometer*, Eur. Phys. J. D **69**, 202 (2015).
[9] Y. Kubo *et al.*, *Strong Coupling of a Spin Ensemble to a Superconducting Resonator*, Phys. Rev. Lett. **105**(14), 140502 (2010).

A Simultaneous Multi-location Measurement Method Based on Pump-Beam Modulation of Atomic Magnetometers by Electro-optic Modulation

Yosuke Ito, Yuki Mamishin, Tetsuo Kobayashi

Graduate School of Engineering, Kyoto University, Kyotodaigaku-Katsura, Nishikyo-ku, Kyoto, Japan

Simultaneous multi-location measurements are essential to apply optically pumped atomic magnetometers (OPAMs) to biomagnetic applications such as magnetoencephalograms (MEGs) and magnetocardiograms (MCGs). For multi-location measurements, it is commonly used to align many OPAMs, each of which consists of a set of a cell, a pump beam and a probe beam [1, 2]. However, it is difficult to calibrate sensor properties of each OPAM because each sensor cell has different alkali-metal densities, pressure of buffer gases and so on. Therefore, we have been investigating the multi-channel OPAM with multiple pump and probe beams irradiating a large sensor cell containing K and Rb atoms [3]. In this method, however, we can only obtain the signals integrated along the probe beam passing through. To obtain the magnetic field distribution along the probe beam direction, we proposed the pump beam modulation method with optical choppers [4].

In this study, we carried out simultaneous magnetic field measurements at two locations using a pump beam modulation method with electro-optic modulators (EOMs), which can realize the sinusoidal modulation. The experimental setup was similar to the reference [4]. As a test signal, we applied measured magnetic field of 48 pT and 11 Hz. The pump beam was divided into two beams whose intensities were sinusoidally modulated with the modulation frequencies of 31 Hz and 43 Hz aiming at measuring spontaneous cortical rhythmic activities such as alpha rhythm (8-13 Hz). The probe beam passing through the two pump beams was detected with a polarimeter and synchronously demodulated with 31 Hz and 43 Hz to distinguish the two signals at different positions.

Figure 1 shows the experimental results. The sinusoidal modulation could suppress the peaks of higher harmonics. The frequency accuracy of the EOMs was much higher than that of the optical choppers, in consequence the noise level at low frequency was lower. The noise levels were 352 $\mathrm{fT_{rms}/Hz^{1/2}}$ and 800 $\mathrm{fT_{rms}/Hz^{1/2}}$ with modulation frequencies of 31 Hz and 43 Hz, respectively. As seen in Fig. 1 right, there is a peak at 8 Hz, which is the second-order harmonic wave of 31-Hz modulation. Therefore, we have to select the proper modulation frequency for each measurement object. The sensitivity reached 160 $\mathrm{fT_{rms}/Hz^{1/2}}$ by increasing the pump beam intensity.

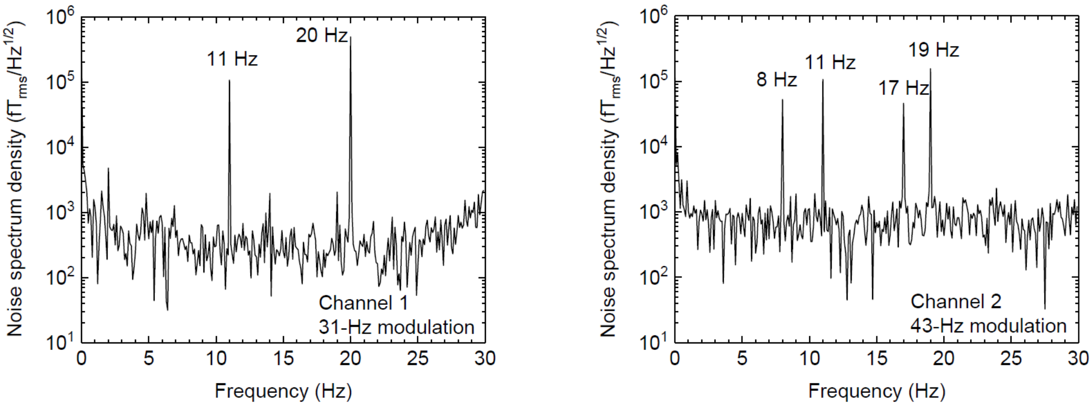

Fig. 1 Noise spectrum densities obtained with modulation frequencies of 31 Hz and 43 Hz.

We demonstrated simultaneous multi-location measurements with modulated pump beams using EOMs towards biomagnetic applications. The experimental results indicate the feasibility of the presented method to biomagnetic applications. In future, we plan to measure MCGs and MEGs by this technique.

References

[1] G. Bison, N. Castagna, A. Hofer, P. Knowles, J.-L. Schenker, M. Kasprzak, H. Saudan, and A. Weis, *A room temperature 19-channel magnetic field mapping device for cardiac signals*, Appl. Phys. Lett. **95**, 173701 (2009).

[2] R. Wyllie, M. Kauer, G. S. Smetana, R. T. Wakai, and T. G. Walker, *Magnetocardiography with a modular spin-exchange relaxation-free atomic magnetometer array*, Phys. Med. Biol. **57**, 2619 (2012).

[3] Y. Ito, D. Sato, K. Kamada, and T. Kobayashi, *Measurements of Magnetic Field Distributions With an Optically Pumped K-Rb Hybrid Atomic Magnetometer*, IEEE Trans. Magn. **50**, 4006903 (2014).

[4] Y. Mamishin, Y. Ito, and T. Kobayashi, *A Novel Method to Accomplish Simultaneous Multilocation Magnetic Field Measurements Based on Pump-Beam Modulation of an Atomic Magnetometer*, IEEE Trans. Magn. **53**, 4001606 (2017).

Towards a Practical Pulsed Magnetometer

Thomas Kornack, Elizabeth Foley

Twinleaf LLC, Princeton, New Jersey 08540 USA

We discuss progress towards a practical total field optical magnetometer based on the free induction decay of alkali metal atoms. Our work is inspired by the record-breaking scalar sensitivity achieved by Sheng *et al.* [1], but here our focus is on making a system that is centimeter-scale and practical for real-world use. We identify several advantages to the pulsed approach in sensitivity, bandwidth, and accuracy. The Larmor frequency is obtained by directly counting the signal from the sensor without the need for any feedback loop. The lack of a feedback loop permits higher bandwidth measurements in the few-kHz regime and higher accuracy near the bandwidth limit. We will discuss the accuracy of the magnetometer and how heading errors may be suppressed. High sensitivity is obtained by pumping the atoms into the end state and operating at higher atom density; in this regime very high optical rotations are obtained, as shown in Fig. 1.

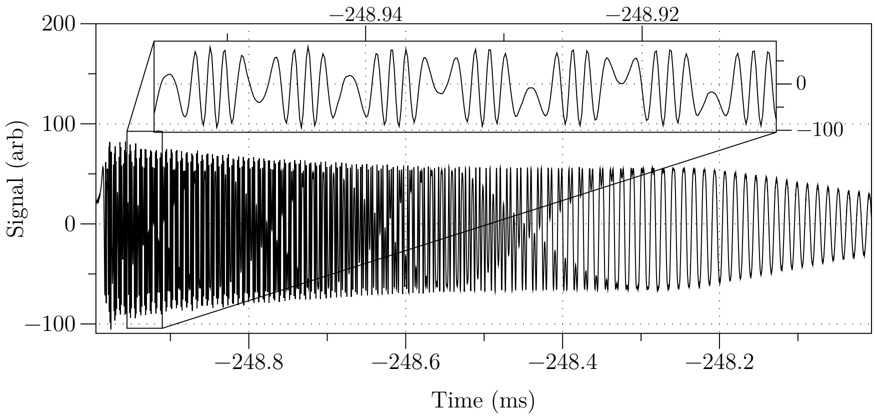

Fig. 1 Very high optical rotation signals provide multiple zero crossings per Larmor precession period.

We obtain multiple zero crossings per Larmor precession period, thereby significantly increasing potential readout sensitivity. We explore some of the compelling challenges in the analysis of these timeseries.

The development of a practical pulsed magnetometer depends on the development of a suitable pump laser with high peak power. We have demonstrated a pump laser with 10 mW average power with efficiency far exceeding the efficiencies of typical VCSELs. Since the pump laser is off for the duration of the measurement, the sensor lacks any of the familiar pump lightshifts and pump noise contributions to sensor noise. Existing VCSEL technology provides an effective probe beam for this system, resulting in a compact, low-power and high performance sensor.

References

[1] D. Sheng *et al.*, *Subfemtotesla Scalar Atomic Magnetometry Using Multipass Cells*, Phys. Rev. Lett. **110**, 160802 (2013).

Suppression of nonlinear Zeeman effect and heading error in earth-field alkali-vapor magnetometers

Guzhi Bao[1,2], **Arne Wickenbrock**[1,3], **Dmitry Budker**[1,3,4,5]

1. Johannes Gutenberg-Universität Mainz, 55128 Mainz, Germany
2. Department of Physics, East China Normal University, Dongchuan Road 500, 200241 Shanghai, China
3. Helmholtz Institut Mainz, 55099 Mainz, Germany
4. Department of Physics, University of California, Berkeley, CA 94720-7300, USA
5. Nuclear Science Division, Lawrence Berkeley National Laboratory, Berkeley, CA 94720, USA

High-sensitivity magnetometers are used in a wide variety of applications ranging from geophysics [1] to fundamental physics [2] and medicine [3]. Alkali-metal-vapor atomic magnetometers have seen tremendous progress in recent years improving their sensitivities to below the $\mathrm{fT}/\sqrt{\mathrm{Hz}}$ level [1,4] at submicrotesla fields. However, when it comes to the geophysical field range (up to 100 μT), one has to contend with the nonlinear Zeeman (NLZ) effect [5], which causes splitting of different components of the magnetic resonances as well as lineshape asymmetries. This leads to signal dilution and spurious dependence of the readings of a scalar sensor on the relative orientation of the sensor and the field, the heading error [6], particularly troublesome in airborne and marine systems. Here we introduce a technique where atomic spins are locked by a radio-frequency field to suppress the NLZ effect and heading error.

Spin locking is often used in Nuclear Magnetic Resonance (NMR) experiments to prevent precession or decay of nuclear magnetization [7]. By applying a continuous-wave rf field or composite pulses, the magnetization is spin locked in the effective field and decays to equilibrium with relaxation time $T_{2,\mathrm{eff}}$, which can be much longer than typical spin-relaxation time T_2. In atomic system, rf field can also lock the different spin subgroups. This prevents splitting, shifts and lineshape asymmetries. Different from other schemes, spin locked magnetometer is more flexible when magnetic field's amplitude and orientation angle keep changing.

References

[1] H. B. Dang, A. C. Maloof, and M. V. Romalis, *Ultrahigh sensitivity magnetic field and magnetization measurements with an atomic magnetometer*, Appl. Phys. Lett. **97**, 151110 (2010).

[2] G. Vasilakis, J. M. Brown, T. W. Kornack, and M. V.Romalis, *Limits on New Long Range Nuclear Spin-Dependent Forces Set with a K-^{3}He Comagnetometer*, Phys. Rev. Lett. **103**, 261801 (2009).

[3] G. Bison, N. Castagna, A. Hofer, P. Knowles, J.-L.Schenker, M. Kasprzak, H. Saudan, and A. Weis, *A room temperature 19-channel magnetic field mapping device for cardiac signals*, Appl. Phys. Lett. **95**, 173701 (2009).

[4] M. P. Ledbetter, I. M. Savukov, V. M. Acosta, D. Budker, and M. V. Romalis, *Spin-exchange-relaxation-free magnetometry with Cs vapor*, Phys. Rev. A **77**, 033408 (2008).

[5] S. J. Seltzer, P. J. Meares, and M. V. Romalis, *Synchronous optical pumping of quantum revival beats for atomic magnetometry*, Phys. Rev. A **75**, 051407R (2007).

[6] E. B. Alexandrov, *Recent progress in optically pumped magnetometers*, Phys. Scr. **T105**, 27 (2003).

[7] A. J. Vega, *Relaxation in spin-echo and spin-lock experiments*, J. Magn. Res. (1969), **65**(2), 252 (1985).

T14

Double Resonance Magnetometry in Arbitrarily Oriented Static Fields

Stuart J. Ingleby, Carolyn O'Dwyer, Iain Chalmers, Paul F. Griffin, Aidan S. Arnold, Erling Riis

Department of Physics, SUPA, University of Strathclyde, 107 Rottenrow East, Glasgow, UK

Our magnetometry development is focussed on compact, portable sensors for geophysical field measurements. In order to develop practical sensors with minimised size and power requirements, single beam double-resonance magnetometry is used, avoiding any requirement for extensive optical hardware or full-field compensation. Magnetic resonance in atomic polarisation is detected using a polarimeter to measure optical rotation in transmitted pump light, allowing rejection of common-mode optical noise. The application of this technique to unshielded geophysical field measurements requires detailed understanding of systematic effects arising in arbitrary orientations of the static field B_0.

We report the development and calibration of a test system for double resonance measurements in generated static fields of well-controlled magnitude and orientation, including systems for automated B_0 control and software generated modulation/demodulation [1]. The sensitivity of these devices depends on signal amplitude, phase and RF broadening, all of which vary with B_0 orientation. By working in a low-field, weak-pumping regime, we obtain experimental measurements of anisotropy in these parameters, in agreement with theoretically derived distributions [2]. We comment on the importance of measurement mode and signal demodulation in optimising double-resonance sensitivity and bandwidth, and the suitability of these techniques for compact, portable magnetometers.

This work is supported by the UK Quantum Technology Hub in Sensors and Metrology [3].

References

[1] S. J. Ingleby, P. F. Griffin, A. S. Arnold, M. Chouliara, and E. Riis, *High-precision control of static magnetic field magnitude, orientation, and gradient using optically pumped vapour cell magnetometry*, Rev. Sci. Instrum. **88**, 043109 (2017).

[2] S. J. Ingleby, C. O'Dwyer, P. F. Griffin, A. S. Arnold, and E. Riis, *Orientational Effects on the Amplitude and Phase of Optical Rotation Signals in Double Resonance Atomic Magnetometry*, submitted for publication.

[3] www.quantumsensors.org

Realising the advantages of OPM-MEG: Scanner casts and data modelling

Tim M. Tierney

Wellcome Trust Centre for Neuroimaging, University College London, London, WC1N 3BG, UK

Human brain imaging using MEG requires models of how neuronal current flows through the head and models of the sensor geometry. As we begin to measure with higher signal to noise than ever before, these models need to become increasingly accurate. I will describe how we perform OPM measurements using scanner-casts (individualised helmets containing sensor arrays). I will describe how we can test from which brain structures we are actually measuring by comparing different anatomical models of the brain and how we can also use this knowledge (of human brain anatomy) to refine our estimates of sensor geometry. I will go on to show empirical examples of how we can use the known functional organisation of the human cortex to verify our modelling assumptions.

T16

OPM MEG with field nulling technology: Towards real world neuroimaging

Elena Boto

Sir Peter Mansfield Imaging Centre, School of Physics and Astronomy, University of Nottingham, Nottingham, UK

Current MEG systems are built around superconducting sensors that are fixed in position in a cumbersome, 'one-size-fits-all' cryogenic dewar. The subject's head must be fixed to this dewar to prevent motion. These characteristics make participation in MEG studies challenging for many subjects (including patients, and children). In this talk I will describe a new type of MEG system, which is built using OPMs and worn on the head as a helmet. When used in conjunction with field-nulling technology subjects can move freely without compromising data quality. Measurements generated with this system compare well to the current state-of-the-art, even when the subject makes large head movements. This work opens new possibilities, not only for new patient cohorts, but for a new generation of neuroscientific investigation allowing, for the first time, mapping of human brain function during real world interactions.

Magnetoencephalography with a 20-Channel Optically Pumped Magnetometer Array

Peter D. D. Schwindt[1],Amir Borna[1], Tony R. Carter[1], Anthony P. Colombo[1], Yuan-Yu Jau[1], Jim McKay[2], Julia Stephen[3], Michael Weisend[4,5]

1. Sandia National Laboratories, PO Box 5800, Albuquerque, NM 87185-1082, USA
2. Candoo Systems Inc., 2991 Thacker Avenue, Coquitlam BC Canada V3C 4N6
3. The Mind Research Network and Lovelace Biomedical and Environmental Research Institute, Albuquerque, NM 87106, USA
4. Rio Grande Neurosciences, Inc., 6401 Richards Avenue, Santa Fe, NM 87508, USA
5. Department of Neurosurgery, University of New Mexico, Albuquerque, NM 87131, USA

The primary magnetic sensor used for magnetoencephalography (MEG) is the super conducting quantum interference device (SQUID). Low-Tc SQUIDs must be operated within a liquid helium Dewar, and this cryogenic infrastructure adds significant size, expense, and complexity to SQUID-based MEG systems. In recent years, optically pumped magnetometers (OPMs) have demonstrated sub-femtotesla sensitivities and have emerged as potential replacements for SQUIDs in MEG applications. We have been working to develop a complete MEG system including a person-sized magnetic shield and a 20-channel array of OPMs. Each channel of this array is able to measure two components of the magnetic field in a sequential manner with both components being measured transverse to the scalp [1]. With this array we have been able to measure three human subjects, using auditory and median nerve stimulation to evoke responses in the auditory and somatosensory cortices respectively. As an example of our data, in Fig. 1(a), we show the response from the brain to a 1 kHz tone averaged over approximately 300 trials. In Fig. 1(b), a several picoTesla response is observed from the median nerve stimulation, and this response is observed in single trials with only band pass filtering (0.5 Hz to 150 Hz). No other data processing is required. In this talk I will present the development of our OPM-based MEG system, the performance our OPM array in the person-sized shield, and the results of preliminary studies with human subjects, including preliminary localization results of magnetic sources. Additionally, I will discuss our initial measurements on the stability of our system in terms of the gain of the sensors and the angle of the sensed magnetic field vector; both must be well known and stable for accurate magnetic source localization.

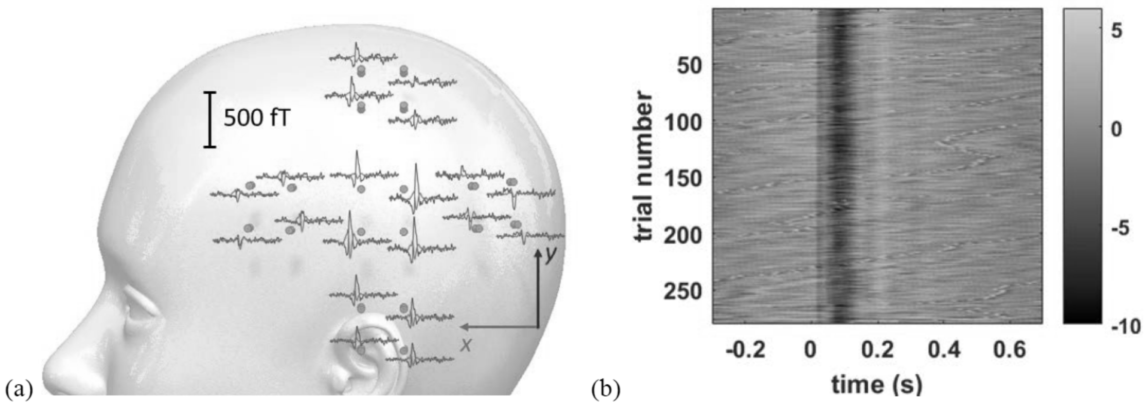

Fig. 1 (a) Spatial distribution of the auditory evoked fields across the OPM array. (b) Single-trial somatosensory evoked magnetic fields. The color bar has units of picoTesla.

References

[1] A. P. Colombo, T. R. Carter, A. Borna, Y.-Y. Jau, C. N. Johnson, A. L. Dagel, and P. D. D. Schwindt, *Four-channel optically pumped atomic magnetometer for magnetoencephalography*, Opt. Express, **24**(14), 15403 (2016).

T18

Quality of Visual Gamma-band Responses Measured with an Optically-pumped Magnetometer

Joonas Iivanainen[1], **Rasmus Zetter**[1], **Lauri Parkkonen**[1,2]

1. Department of Neuroscience and Biomedical Engineering, Aalto University, Espoo, Finland
2. Aalto NeuroImaging, Aalto University, Espoo, Finland

Neural oscillations are ubiquitous in a living brain. These oscillations are observable in the so-called local field potentials in the cortex and in electric potential (EEG) and magnetic field (MEG) on the head surface. Gamma-band (30–100 Hz) oscillations are of considerable interest because they appear to reflect local neural processing and because of their hypothesized role as a fundamental mechanism for neural communication. Here, we measured human visual gamma-band activity with an optically-pumped magnetometer (OPM) using a visual stimulus that has been shown to elicit a strong gamma-band response with MEG [1]. We compared the signal quality of the OPM response to those measured with a commercial SQUID-based MEG system.

We measured three subjects (S1–S3) twice in a three-layer magnetically shielded room: first with a commercial OPM (QuSpin Inc., Louisville, CO, USA) and then with a 306-channel MEG system (Elekta Oy, Helsinki, Finland). To evoke visual gamma-band responses, we used 100 trials of contracting sine wave gratings with a task (see Ref. 1 for details). The OPM was placed on the scalp above the left occipital lobe and was set to measure the magnetic field component normal to the scalp. The acquired data were high-pass filtered at 1 Hz to remove slow drifts. From the SQUID measurement, 26 parieto–occipital magnetometers with a strong gamma-band response in the time–frequency representation were selected for further analysis.

The empty-room noise floor for the OPM was about 15 fT/Hz$^{1/2}$ while the average noise floor for the 26 SQUID magnetometers was 4 fT/Hz$^{1/2}$. Fig. 1. summarizes the results for S1 who had a particularly strong response. The gamma-band response around 60 Hz and the alpha/beta-band suppression around 13 Hz are clearly visible in the spectra of both OPM and SQUID magnetometers and also in the time–frequency representations. The t-values for the power difference between baseline and stimulation show that the OPM can measure the response with a high SNR; for other subjects, the relation between t-values of OPM and SQUIDs were similar. The mean (and range) ratios (OPM vs. SQUIDs that showed the response) of the peak gamma-amplitudes were 4.6 (3.0–6.2), 3.0 (1.7–4.4) and 2.4 (1.7–3.5) for S1, S2 and S3, respectively.

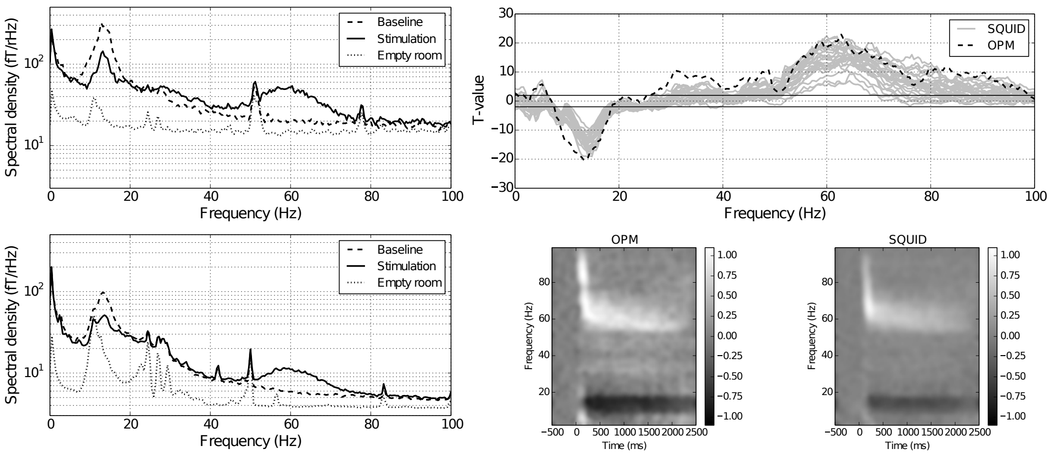

Fig. 1 Spectral characteristics of the induced response for the OPM and 26 parieto–occipital SQUID magnetometers. **Left:** Spectra of OPM (top) and average spectra of SQUIDs (bottom). **Right top:** t-values for the power difference between baseline and stimulation. Significance level ($p < 0.05$) for OPM is indicated with vertical lines. **Right bottom:** Time–frequency representations of the OPM and of those SQUIDs (averaged) with the strongest response.

We have shown that OPM can detect gamma-band responses with a SNR comparable (or better) to SQUIDs despite the higher sensor noise and 'brain noise'. We expect the SNR of the OPM to be even better when the position of the sensor can be optimized. In the future, gamma-band responses could be measured with a dense array of OPMs for optimal spatial sampling of the field and for an experimental verification of the improvement in spatial resolution provided by the on-scalp array [2].

References

[1] N. Hoogenboom *et al.*, *Localizing human visual gamma-band activity in frequency, time and space*, NeuroImage **29**, 764 (2006).
[2] J. Iivanainen *et al.*, *Measuring MEG closer to the brain: Performance of on-scalp sensor arrays*, NeuroImage **147**, 542 (2017).

Development of a microfabricated optically-pumped magnetic gradiometer array for integration with a transcranial magnetic stimulation array

S. P. Krzyzewski, A. R. Perry, D. Sheng, B. Korenko, N. V. Nardelli, S. Knappe

Department of Mechanical Engineering, University of Colorado, 1111 Engineering Dr., 80309 Boulder, USA

We report on the progress towards developing a 24-channel chip-scale atomic gradiometer array coupled to a multichannel transcranial magnetic stimulation (TMS) system. The combination of the two systems will provide a novel approach for brain imaging. The microfabricated magnetic field sensors do not require cryogenic cooling and can be placed closed to the scalp. The requirement is that the sensors record data from the brain within 10 ms after a 1 T strong magnetic field pulse is switched off. The magnetometers operate in the spin-exchange free regime for higher sensitivity [1,2] by use of the zero-field level crossing resonance [3] to reduce the effects of low frequency noise on the measurement. The sensor (Fig. 1) is constructed on an optical bench printed with stereolithography. The rubidium vapor cells are constructed by anodically bonding Pyrex to a silicon shell of inner dimensions 3 mm x 3 mm x 2 mm, and filling with roughly 1 amagat of N_2 and a droplet of rubidium. The sensor uses a single laser split between the two cells for both optical pumping and probing of the atoms. The cells are separated by 2 cm. A laser at 1550 nm strikes the surface of each cell, and is absorbed to heat the cell to roughly 150 °C. We perform phase-sensitive detection of the absorption signal by modulating a pair of Helmholtz coils on each cell, and demodulate using a lock-in amplifier. The dispersive signal from the lock-in amplifier is sent to a PID, which feeds back onto the Helmholtz coils. The spectral density of the feedback signal is measured to determine the sensitivity of the sensor.

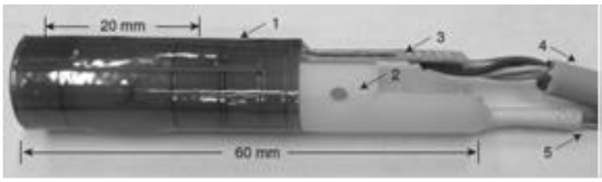

Fig. 1 Photograph of the magnetic gradiometer. 1. Kapton flexible coil, 2. Optical bench, 3. PCB, 4. CAT5e cable, 5. Optical fibers. Taken from [4].

The sensitivities of individual magnetometers are between 13 and 26 $\mathrm{fT/Hz^{1/2}}$, with gradiometer sensitivities as low as 10 $\mathrm{fT/Hz^{1/2}}$ or 5 $\mathrm{fT/Hz^{1/2}}$ at frequencies above 20 Hz (Fig. 2). The gradiometer has a common-mode rejection ratio between 100 and 1000 depending on PID controller settings and sensor bandwidth.

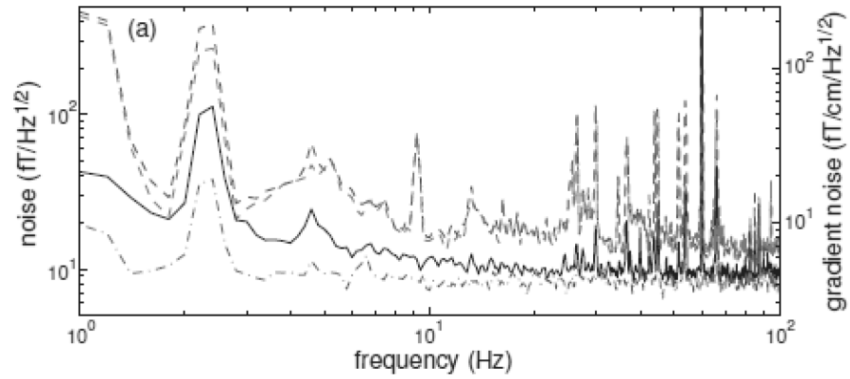

Fig. 2 Measured magnetic field and gradient field sensitivity of the sensor. The top two dashed lines correspond to the individual magnetometers, the black solid line is the noise of the difference between them. The lowest dashed line is the subtraction of the lock-in amplifier quadrature outputs. Taken from [4].

References

[1] W. Happer and H. Tang, *Spin-exchange shift and narrowing of magnetic resonance lines in optically pumped alkali vapors*, Phys. Rev. Lett. **31**(5), 1877 (1973).

[2] J.C. Allred, R.N. Lyman, T.W. Kornack, and M.V. Romalis, *High sensitivity atomic magnetometer unaffected by spin-exchange relaxation*, Phys. Rev. Lett. **89**(13), 130801 (2002).

[3] C. Cohen-Tannoudji, J. Dupont-Roc, S. Haroche, and F. Laloe, *Diverses résonances de croisement de niveaux sur des atomes pompés optiquement en champ nul. I. Théorie*, Rev. Phys. Appl. **5**, 95 (1970).

[4] D. Sheng, A.R. Perry, S.P. Krzyzewski, S. Geller, J. Kitching, and S. Knappe, *A microfabricated optically-pumped magnetic gradiometer*, Appl. Phys. Lett. **110**, 031106 (2017).

Magnetoencephalography with a Cs-Based High-Sensitivity Compact Atomic Magnetometer

Jingwei Sheng[1,a)], Shuangai Wan[2,a)], Yifan Sun[1], Rongshe Dou[2], Yuhao Guo[2], Kequan Wei[2], Kaiyan He[1], Jie Qin[2], Jia-Hong Gao[1]

1. Center for MRI Research, Peking University, Yiheyuan Road 5, Beijing, China
2. Beijing Automation Control Equipment Institute, Quantum Technology R&D Center of China Aerospace Science and Industry Corporation, Feihanglu, Beijing, China
a) Jingwei Sheng and Shuangai Wan contributed equally to this work

In recent years, substantial progress has been made in developing atomic magnetometer (AM) or optically pumped magnetometer (OPM) as the new generation of MEG [1]. While most proposed compact AMs are K- or Rb-based with single beam configurations, we proposed a Cs-based two beam compact AM (Cs-AM) designing. The feasibility of Cs-based magnetometer has been verified by previous study [2], and a theoretical optimization indicates that the ultimate sensitivity will be 0.2 $\mathrm{fT/Hz^{1/2}}$, which is sufficient enough to detect human brain activities. The main advantage for employing Cs is that it has the highest saturated vapor pressure of all the stable alkali metals, yielding a much lower operating temperature (100 - 120°C) compared with K and Rb. Such lower temperature will benefit Cs-AM with potentially thinner thermal insulating layer and less electric heating noise. In the present study, the noise power spectrum density of the current Cs-AM was measured, and its performance was verified on human auditory evoked response by comparing with SQUID magnetometer. Our preliminary results demonstrate a promising potential of such OPM for future realizations of the multi-channel and compact designs.

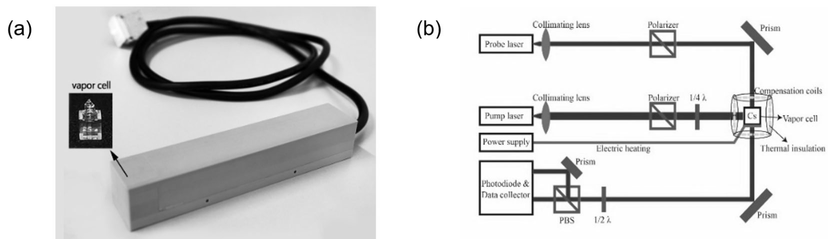

Fig. 1 (a) Current compact Cs-AM detector with small Cs vapor cell; (b) Schematic diagram of the two-beam configuration system employed in the current compact Cs-AM.

As Figure 1(a) shows, the outer size of current sensor is 2.5x2.7x15 $\mathrm{cm^3}$, with a 4x4x4 $\mathrm{cm^3}$ vapor cell in front of the sensor, the distance between the center of the vapor cell and the outside of the sensor is less than 6 mm. Figure 1(b) shows the two-beam-laser configuration with the probe light perpendicular to the pump laser in the cell. A cube glass cell containing both Cs mental and 700 torr of He and 50 Torr N_2 buffering gas. A thin non-magnetic heating element was attached on the vapor to keep the cell in high temperature and a thermal insulation was added to ensure that the temperature outside the detector was below 40°C.

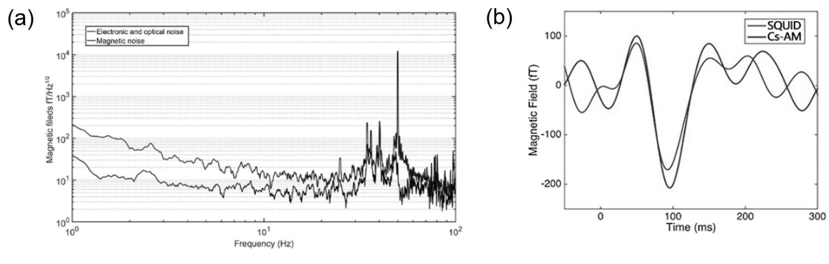

Fig. 2 (a) Noise spectrum density of the current Cs-AM; (b) Comparison of event related human auditory response field of both Cs-AM and corresponding SQUID channel.

Figure 2(a) shows the noise power spectral density of the current single sensor magnetometer (blue line) as well as the electronic and optical noise in the absence of pump beam (black line). It is shown that the noise level is approximately 10 $\mathrm{fT/Hz^{1/2}}$ between 10 to 30 Hz. Figure 2(b) shows the comparison of OPM measurements and corresponding SQUID magnetometer results of human auditory response. The classic M100 peak was obviously found in both Cs-AM and the corresponding SQUID channel, and it is seen that these two time series share a similar temporal profile. The results indicate the possibility of using compact Cs-AM for MEG recordings, and the current Cs-AM has the potential to be designed for multi-sensor arrays and gradiometers for future neuroscience studies.

References

[1] I. K. Kominis, T. W. Kornack, J. C. Allred, and M. V. Romalis, *A subfemtotesla multichannel atomic magnetometer*, Nature **422**, 596 (2003).
[2] I. M. Savukov, M. Ledbetter, V. Acosta, D. Budker, and M. Romalis, *Cesium Spin-Exchange-Relaxation-Free Magnetometer*, Phys. Rev. A **77**, 033408 (2008).

Towards Second-Generation Commercial OPMs for BioMagnetism

Orang Alem, Svenja Knappe, Vishal Shah

QuSpin, Inc., 2011 Cherry St., Unit 112, 80027 Louisville, Colorado

In 2016, we launched our first-generation commercial zero-field OPMs (QZFM) for BioMagnetism. The QZFM sensors were designed to enable wide scale adoption of Magnetoencephalography and fetal Magnetocardiography type applications. The primary goal of the first-generation sensors was to introduce clinical researchers around the world to OPM technology. With the experience gained from manufacturing over 200 sensors, and with invaluable inputs from the user community, we will soon begin the development of our second-generation sensors. In this presentation, we will discuss the status of our technology, the performance and current limitations, and the objectives for the second-generation sensors. We will also briefly describe our progress towards clinical grade systems development.

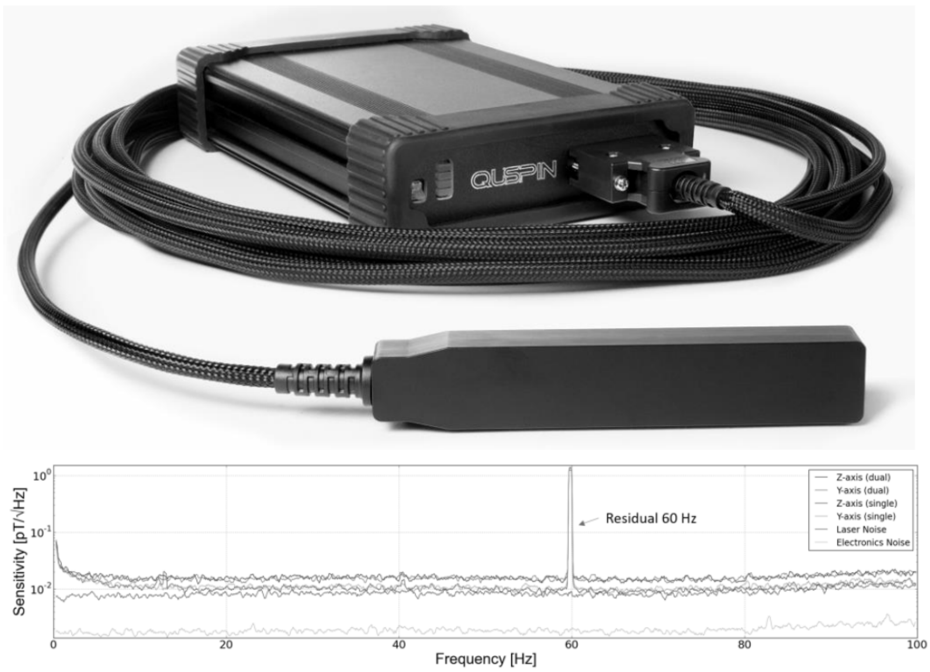

Figure 1 shows a photograph of the QZFM sensor head (front) and the stand-alone electronic controller (back). The sensors can operate in single sensitive axis mode, or dual sensitive axes mode (simultaneous Y and Z). A typical sensor noise floor spectrum is shown in the bottom of Figure 1.

Quantum Optical Magnetometry for Biomedical Applications

Kasper Jensen[1], Hans Christian Stærkind[1], Jens Arnbak[1], Bo Hjorth Bentzen[2], Eugene S. Polzik[1]

1. Niels Bohr Institute, University of Copenhagen, Blegdamsvej 17, 2100 Copenhagen, Denmark
2. Department of Biomedical Sciences, University of Copenhagen, Blegdamsvej 3, 2200 Copenhagen N, Denmark

We have developed highly sensitive miniature optical magnetometers based on cesium vapor. Using such magnetometers, we have detected biological signals from an isolated animal nerve and an isolated animal heart. The main component of our optical magnetometer is a miniature cesium vapor cell which is coated on the inside with paraffin. The cell is kept at room- or human body temperature and can be placed at sub-mm distance to a biological object. Those features together with high sensitivity make our magnetometer perfect for detecting magnetic fields from biological objects with high spatial resolution. Our magnetometer utilizes optical pumping with circular polarized light, which polarizes the cesium atoms along the direction of an applied static magnetic field. Any biomagnetic field which is present will drive the atomic polarization away from this direction. The atomic polarization, and thereby the bio-magnetic field, is measured using the Faraday rotation of linearly polarized probe light.

We have detected animal nerve impulses with a miniature (1 mm x 1 mm x 7.7 mm) cesium magnetometer [1]. In that experiment, the nerve was stimulated electrically in one end, which triggered an action potential that propagated to the other end. Our magnetometer is capable of detecting a nerve impulse at several mm distance (Fig. 1a-c), corresponding to the distance between the skin and nerves in medical studies. Possible applications of our magnetometer include diagnostics of multiple sclerosis, myotonia and intoxication in patients. Magnetometers can also be used for detecting the fetal heartbeat [2]. We have measured the magnetocardiogram (MCG) of an isolated guinea-pig heart (Fig. 1d,e). The size of a guinea-pig heart is comparable to the size of the heart of a fetus of 20 week gestational age. For the MCG-measurements, we used a 5 mm x 5 mm x 5 mm vapor cell. We can resolve the P, QRS and T features consistent with what is seen in a standard electrocardiogram (ECG).

High sensitivity is a requirement for detecting tiny biomagnetic signals. The sensitivity of optical magnetometers is fundamentally limited by the quantum noise originating from the Heisenberg uncertainty principle. In the past, we have reached quantum-limited sensitivity when detecting radio-frequency magnetic fields [3]. Our magnetometer optimized for detection of nerve impulses (which have frequency components in the DC-1 kHz range) has a sensitivity which is within a factor of two from the quantum limit. The magnetometer optimized for MCG (which has frequency components in the DC-100 Hz range) has currently a sensitivity of 200 $\mathrm{fT}/\sqrt{\mathrm{Hz}}$ (Fig. 2f). We are working on mitigating low-frequency noise, for instance by gradiometry, in order to obtain a quantum-limited sensitivity also for detection of the MCG. This will allow us to perform fetal-MCG and to detect individual P, QRS and T features (without averaging) which is important for early diagnosis of fetal heart diseases.

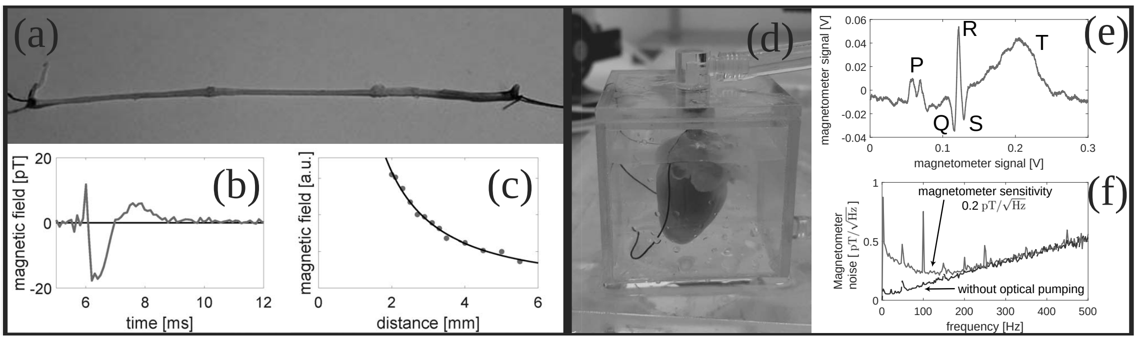

Fig. 1 (a) Frog sciatic nerve. (b) Magnetic field from a nerve impulse. (c) Magnetic field as a function of distance from the nerve. (d) Isolated guinea-pig heart. (e) Magnetic field from the heart (average of 10 heartbeats). (f) Sensitivity for the magnetometer optimized for MCG.

References

[1] K. Jensen *et al.*, *Non-invasive Detection of Animal Nerve Impulses with an Atomic Magnetometer Operating Near Quantum Limited Sensitivity*, Sci. Rep. **6**, 29638 (2016).
[2] O. Alem *et al.*, *Fetal magnetocardiography measurements with an array of microfabricated optically pumped magnetometers*, Phys. Med. Biol. **60**, 4797 (2015).
[3] W. Wasilewski *et al.*, *Quantum Noise Limited and Entanglement-Assisted Magnetometry*, Phys. Rev. Lett. **104**, 133601 (2010).

The Global Network of Optical Magnetometers for Exotic Physics searches

Theo Scholtes[1] **for the GNOME collaboration**

1. Physics Department, University of Fribourg, Chemin du Musee 3, CH-1700 Fribourg, Switzerland

The Global Network of Optical Magnetometers (GNOME [1]) is an international effort searching for exotic physics beyond the Standard Model by looking for atomic spin perturbations induced by the Earth's motion through the cosmic background.

The network consists of a set of magnetically shielded optical magnetometer stations distributed over the globe streaming time-stamped local magnetic field readings to a common server which processes data for website display [2] and off-line data analysis. The detection of space-time correlated signals of the individual magnetometer nodes of the network would be a signature of transient dark-matter structure composed of exotic fields predicted by a class of dark- matter theories. A distributed multi-station detector network will not only discriminate real sought-for transient events from local magnetic perturbations (false positives), but will yield furthermore directional and temporal information on possible dark-matter interaction events.

Fig. 1 Screenshot taken from the publicly accessible GNOME website [2] showing the live status of the GNOME nodes. The website allows visitors to display measured time series data sets and their corresponding frequency spectra.

Currently, GNOME consists of six operational magnetometer nodes and efforts to extend the network by additional stations, mainly located in Eastern-Asia are on-going (Fig. 1). The first long-term data-taking run of the network is foreseen to start in the middle of 2017 and is expected to set new constraints on the properties of hypothetical dark-matter candidates.

While the motivation and promising science cases to be covered by the GNOME effort as well as data analysis methods will be covered by other presentations at this workshop, this talk will focus on the experimental realization of the network. We will present the configurations and features of the individual GNOME magnetometer stations, and present insights into technical aspects and possible future extensions of the network.

References

[1] S. Pustelny, D. F. Jackson Kimball, C. Pankow, M. P. Ledbetter, P. Wlodarczyk, P. Wcislo, M. Pospelov, J. R. Smith, J. Read, W. Gawlik, D. Budker, *The Global Network of Optical Magnetometers for Exotic physics (GNOME): A novel scheme to search for physics beyond the Standard Model*, Ann. Phys. **525**, 659 (2013).

[2] https://budker.uni-mainz.de/gnome/

Constraints on the coupling of the proton spin to gravity

Derek F. Jackson Kimball, Jordan Dudley, Yan Li, Dilan Patel, Julian Valdez

Department of Physics, California State University – East Bay, Hayward, California 94542-3084, USA

Results of a search for a long-range coupling between the mass of the Earth and Rb nuclear spins will be reported. The experiment simultaneously measures the spin precession frequencies for overlapping gaseous ensembles of ^{85}Rb and ^{87}Rb atoms contained within an evacuated, antirelaxation-coated vapor cell [1]. Rubidium atoms are spin-polarized in the presence of an applied magnetic field by synchronous optical pumping with circularly polarized laser light. Spin precession is probed by measuring optical rotation of far-off-resonant, linearly polarized laser light. Simultaneous measurement of ^{85}Rb and ^{87}Rb spin precession frequencies enables suppression of magnetic-field-related systematic effects. The nuclear structure of the Rb isotopes makes the experiment particularly sensitive to anomalous spin-dependent interactions of the proton [2]. Our experiment improves constraints on spin-gravity interactions of the proton by approximately five orders of magnitude.

Light spin-0 fields with scalar and pseudoscalar couplings to matter lead to long-range spin-dependent potentials [3-5]. If the new field is considered to be an additional component of gravity, as suggested by certain scalar-tensor extensions of general relativity that include torsion [6], there would be coupling of spins to gravitational fields, causing particles to acquire a gravitational dipole moment (GDM). The dominant gravitational field in a laboratory setting is that due to the Earth, which generates a spin-dependent Hamiltonian with the nonrelativistic form [5,7]:

$$H_g = k\frac{\hbar}{c}\boldsymbol{\sigma}\cdot\mathbf{g} \tag{1}$$

where k is a dimensionless parameter setting the scale of the new interaction, $\hbar$ is Planck's constant, σ is the intrinsic spin of the particle in units of $\hbar$, $\mathbf{g}$ is the Earth's gravitational field, and c is the speed of light. If the strength of the pseudoscalar coupling is the same as that of the tensor component of gravity, $k \approx 1$ [5].

During the course of the experiment, we have studied a number of important systematic effects related to vector and tensor light shifts, optical pumping effects, the ac and nonlinear Zeeman effects, and magnetic field gradients. These systematic errors and strategies used to mitigate their effects will be discussed.

References

[1] D. F. Jackson Kimball, I. Lacey, J. Valdez, J. Swiatlowski, C. Rios, R. Peregrina-Ramirez, C. Montcrieffe, J. Kremer, J. Dudley, and C. Sanchez, *A dual-isotope rubidium comagnetometer to search for anomalous long-range spin-mass (spin-gravity) couplings of the proton*, Ann. Phys. **525**, 514 (2013).

[2] D. F. Jackson Kimball, *Nuclear spin content and constraints on exotic spin-dependent couplings*, New J. Phys. **17**, 073008 (2015).

[3] J. E. Moody and F. Wilczek, *New macroscopic forces?*, Phys. Rev. D **30**, 130 (1984).

[4] B. A. Dobrescu and I. Mocioiu, *Spin-dependent macroscopic forces from new particle exchange*, J. High Energy Phys. **11**, 005 (2006).

[5] V. Flambaum, S. Lambert, and M. Pospelov, *Scalar-tensor theories with pseudoscalar couplings*, Phys. Rev. D **80**, 105021 (2009).

[6] F. W. Hehl, P. von der Heyde, G. D. Kerlick, and J. M. Nester, *General relativity with spin and torsion: Foundations and prospects*, Rev. Mod. Phys. **48**, 393 (1976).

[4] J. Leitner and S. Okubo, *Parity, Charge Conjugation, and Time Reversal in the Gravitational Interaction*, Phys. Rev. **136**, B1542 (1964).

Optical magnetometers for a next-generation neutron EDM experiment

Georg Bison[1] **for the nEDM collaboration**

1. Paul Scherrer Institut, 5232 Villigen, Switzerland

Experiments searching for the electric dipole moment (EDM) of the neutron require a stable and homogeneous magnetic field. Statistical and systematic uncertainties in such experiments depend on magnetic field gradients and fluctuations of those gradients and the field itself [1]. In order to monitor the different aspects of the magnetic field we developed a variety of special magnetometer systems based on optically-pumped Cs, ^{199}Hg, or ^{3}He. The used magnetometer techniques included variometers, multibeam vectior readout [2], accurate all-optical field readings [3], and the readout of precessing ^{3}He spins with Cs OPM [4,5]. We will present an overview of magnetometer systems in our current neutron EDM experiment as well as plans for a next-generation upgrade (n2EDM). The n2EDM experiment at PSI requires a large number of Cs sensors similar to arrays previously designed for bio-magnetometry [6, 7].

References

[1] J.M. Pendlebury *et al.*, *Revised Experimental Upper Limit on the Electric Dipole Moment of the Neutron*, Phys. Rev. D **92**, 092003 (2015).

[2] S. Afach, G. Ban, G. Bison *et al.*, *A highly stable atomic vector magnetometer based on free spin precession*, Opt. Express **23**(17), 22108 (2015).

[3] Z. D. Grujić, P. A. Koss, G. Bison, and A. Weis, *A sensitive and accurate atomic magnetometer based on free spin precession*, Eur. Phys. J. D **69**(5), 135 (2015).

[4] H.-C. Koch, G. Bison, Z. D. Grujić, W. Heil, M. Kasprzak, P. Knowles, A. Kraft, A. Pazgalev, A. Schnabel, J. Voigt, and A. Weis, *Design and performance of an absolute ^{3}He/Cs magnetometer*, Eur. Phys. J. D **69**(8), 202 (2015).

[5] H.-C. Koch, G. Bison, Z.D. Grujić, W. Heil, M. Kasprzak, P. Knowles, A. Kraft, A. Pazgalev, A. Schnabel, J Voigt, and A. Weis, *Investigation of the intrinsic sensitivity of a ^{3}He/Cs magnetometer*, Eur. Phys. J. D **69**(11), 262 (2015).

[6] G. Lembke, S. N. Erné, H. Nowak, B. Menhorn, A. Pasquarelli, and G. Bison, *Optical multichannel room temperature magnetic field imaging system for clinical application,* Biomed. Opt. Express **5**(3), 62 (2014).

[7] G. Bison, N. Castagna, A. Hofer, P. Knowles, J.-L. Schenker, M. Kasprzak, H. Saudan, and A. Weis, *A room temperature 19-channel magnetic field mapping device for cardiac signals*, Appl. Phys. Lett. **95**(17), 173701 (2009).

^{3}He Optical Magnetometer for the Absolute Calibration of Muon g-2 Magnetic Field Measurement

Midhat Farooq[1,2], **Tim Chupp**[1,2]

1. University of Michigan, 450 Church St., Ann Arbor, MI 48109 United States
2. Fermilab, Road A-1, Batavia, IL 60510, United States

The muon g-2 experiment at Fermilab (E989) investigates the $> 3\sigma$ discrepancy between the standard model prediction and the current experimental measurement of the muon magnetic moment anomaly, $a_\mu = (g-2)/2$. The effort requires a precise measurement of the 1.45 T magnetic field of the muon storage ring to 70 ppb. The final measurement will employ multiple absolute calibration probes: two water probes and a ^{3}He probe, which is an optical magnetometer and the subject of this abstract. The ^{3}He probe offers a cross-check of the water probes with different systematic corrections, adding a level of confidence to the measurement.

A low-field ^{3}He probe was developed at the University of Michigan by employing a widely used method called Metastability Exchange Optical Pumping (MEOP) for the hyper-polarization of ^{3}He gas [1], followed by NMR to determine the frequency proportional to the magnetic field in which the probe is placed. The current probe is successfully measuring at low magnetic fields of ~30 G (Figure 1). In the next three months, a modified probe design for operation under high fields will be tested at Argonne National Lab using an MRI magnet. The MRI magnet was re-purposed at Argonne so it can be used for testing and calibrating the muon g-2 probes at the relevant field of 1.45 T. Future development involves the study of the systematic uncertainties to attain the error budget of less than 30 ppb for the absolute probes. Next, the calibration from the probes will be transferred to g-2 through several steps of a calibration chain ending in the final step of calibrating the NMR probes which measure the field in the muon storage ring at Fermilab.

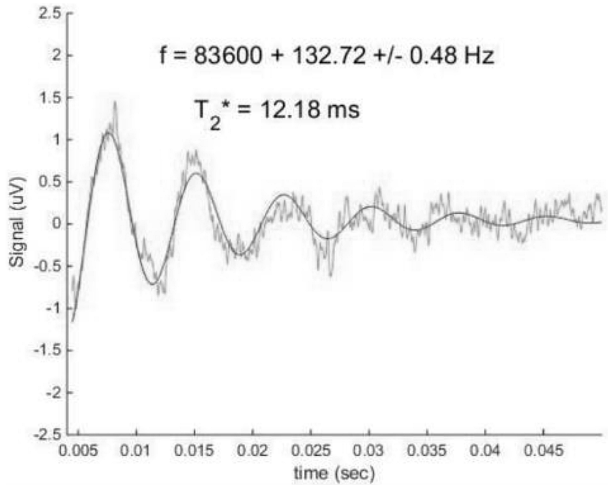

Fig. 1 Free Induction Decay signal from probe at low field (~30 G) at University of Michigan.

References

[1] F. Colegrove, L Schearer, and G. Walters, *Polarization of He^3 Gas by Optical Pumping*, Phys. Rev. Lett. **132**, 2561 (1963).

Atomic Magnetometry Based Magnetic Particle Imaging (MPI)

Simone Colombo[1], **Victor Lebedev**[1], **Alexey Tonyushkin**[2], **Vladimir Dolgovskiy**[1], **Theo Scholtes**[1], **Zoran D. Grujić**[1], **Antoine Weis**[1]

1. Physics Department, University of Fribourg, Chemin du Musée 3, CH-1700 Fribourg, Switzerland
2. Physics Department, University of Massachusetts, 100 Morrissey Blvd., Boston, MA 02125-3393, USA

We have built a Magnetic Particle Imaging (MPI) scanner based on atomic magnetometer detection. MPI is a patented method [1] for imaging spatial distributions of magnetic nanoparticles (MNPs) in view of biomedical applications. MNPs have a superparamagnetic behavior, i.e., they saturate when exposed to relatively small fields of a few mT and do not show a remnant magnetization. The detection of the *nonlinear* $B_{\mathrm{MNP}}(H) \propto M(H)$ response of the flux density B_{MNP} produced by the MNPs exposed to an external driving field H_{drive} allows the discrimination of signals from such particles against the *linear* (para–/diamagnetic) background response of biological tissues.

Consider a spatially extended MNP sample exposed to an inhomogeneous magnetic field that has a field–free line (FFL) or field–free point (FFP). The field gradient will then saturate all MNPs, except those located near the FFL/FFP. Only the magnetization of these unsaturated MNPs will respond to an external modulation field $H_{\mathrm{mod}}(t)$ showing a non–zero AC–susceptibility $\chi_{\mathrm{AC}}(t) \propto \mathrm{d}M/\mathrm{d}H$ that will induce a modulation of the flux density of amplitude $\delta B_{\chi_{\mathrm{AC}}}$ at the location of a nearby–placed magnetometer. The MNP spatial distribution can then be inferred by scanning the position of the FFL/FFP through the sample and recording simultaneously the AC-susceptibility induced signal $\delta B_{\chi_{\mathrm{AC}}}$. In practice this scan is performed by superposing a homogeneous magnetic field of varying amplitude onto the gradient field. Conversely, the sample may be moved by mechanical means through the FFL/FFP.

We describe a coil system which, together with a pump–probe M_x–magnetometer using a heated Cs vapor + buffer gas cell [2], has allowed us to produce magnetic fields and gradients up to ≈10 mT and ≈2 T/m, respectively at the MNP sample location, while maintaining the atomic magnetometer sensitivity in the one–digit pT/Hz range.

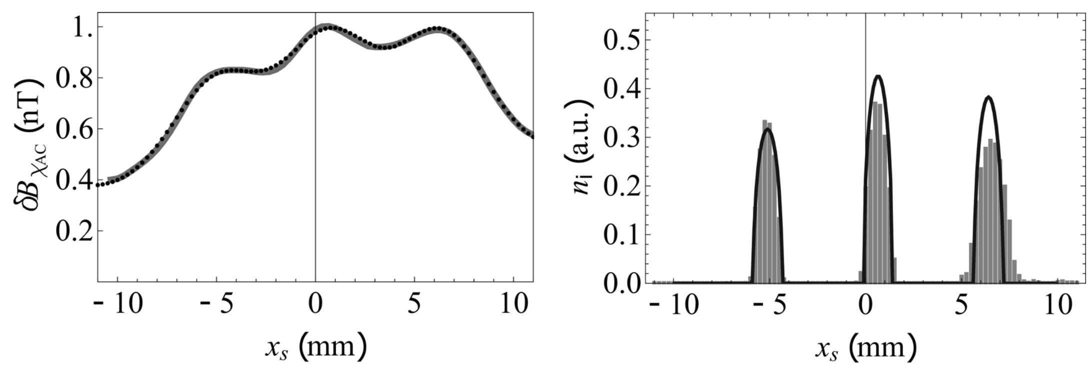

Fig. 1 Left: AC–susceptibility signal produced by 3 capillaries filled with MNP supensions. The detected atomic magnetometer signal (solid gray line) is shown together with a fit (black dots) obtained from an inverse model solution. Right: The histograms show the MNP distributions obtained from the data on the left by source reconstruction (inverse problem), the solid lines represent the ideal distributions from three capillaries.

We have realized 1D scanners with sub–mm spatial resolution by moving either the sample mechanically across the FFL (Fig. 1), or by moving the FFL magnetically through the sample. We have also demonstrated a hybrid 2D scanner, in which one dimension is scanned mechanically and the other one magnetically. Work towards a mechanical 3D scanner is in progress.

References

[1] B. Gleich and J. Weizenecker, *Tomographic imaging using the nonlinear response of magnetic particles*, Nature **435**, 1214 (2005).
[2] S. Colombo, V. Lebedev, A. Tonyushkin, Z. D. Grujić, V. Dolgovskiy, and A. Weis, *Towards a mechanical MPI scanner based on atomic magnetometry*, International Journal On Magnetic Particle Imaging **3**, 1 (2017).

Applications of Miniature Scalar Atomic Magnetometers

Rahul Mhaskar
Geometrics, Inc., 2190 Fortune Dr., San Jose, CA 95131, USA

Scalar atomic magnetometers have been the instrument of choice for geomagnetic surveys for nearly half a century, with applications in mineral exploration, unexploded ordnance detection, archaeological expeditions, and Geology research [1]. The development of low power Vertical Cavity Surface-Emitting Lasers (VCSELs) has enabled miniaturization of the atomic magnetometer with corresponding reduction in weight and power consumption. The Chip-Scale Atomic Clock (CSAC) program, funded by the US Government, demonstrated the use of Micro-Electro-Mechanical Systems (MEMS) processes to fabricate atomic devices on a large scale [3], thus making it possible to produce alkali-vapour-based atomic devices, such as atomic magnetometers, economically in large volume.

Miniature atomic magnetomers with very low size, weight and power (SWaP) are now becoming commercially available. These magnetomers, with their very low payload signature, are ideally suited for deployment from autonomous platforms. Thus, a geophysical survey that might have required a few days to complete can now be conducted in a matter of hours, and at a much lower mobilization penalty, thus significantly reducing the survey cost. With a high sample rate, the spatial density of the recorded data can be very high, thus producing high-resolution maps of the geomagnetic field. We present the first such aerial survey performed using a UAS-mounted miniature magnetometer in Pennsylvania locating a capped oil-well-head.

Highly sensitive atomic magnetometers operating on the Bell-Bloom [4] principle do not require radio frequency magnetic field for their operation. Consequently, two of these sensors can be placed right next to each other forming a very short baseline gradiometer. Combined with a very high sensitivity of the sensors of less than $1\mathrm{pT}/\sqrt{\mathrm{Hz}}$, such a gradiometer has been used to measure the magnetocardiography (MCG) signal in a commercial, unshielded environment.

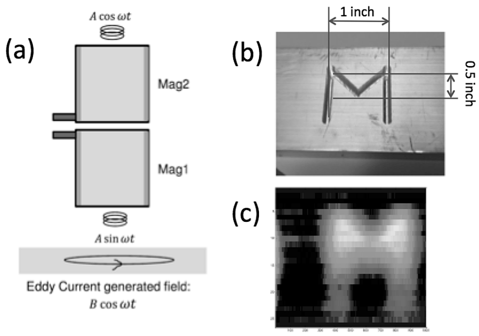

Fig. 1 (a) The schematic shows the placement of the sensors, the excitation coil and the conducting material being inspected for defect using the eddy current technique. (b) shows the "M"-shaped 3 mm deep channel carved in a 6 mm thick aluminium block. (c) shows the measurement from the backside of the conductive block using the eddy current technique.

A high sample rate enables the use of this gradiometer in a balanced eddy current measurement [5]. In such a measurement, two coils driven in series with low frequency currents excite the two magnetometers placed adjacently. One of the magnetometers is scanned over a conductor containing defects such as a void or a crack. The output of the magnetometer is demodulated in reference with the output of the second magnetometer to obtain the difference in the phase of the two readouts at the excitation frequency. A deviation in the phase difference indicates the presence of a defect. While such a measurement is routinely performed with pick-up coils, the depth of interrogation is limited to at most a millimetre due to the high frequencies involved required for high sensitivity. Using a magnetometer as described that is sensitive to DC magnetic fields, a very low excitation frequency can be used, thus vastly increasing the depth of interrogation within the conductor. Using this technique, the magnetometer was used to image a void in an aluminium block.

A number of applications of magnetometers such as medical instrumentation, NMR, security, non-destructive testing and broad-area magnetic imaging have been stymied because of the lack of a suitable sensor. With low power miniature atomic sensors becoming commercially available and new technologies being developed that promise vastly improved sensitivity, bandwidth, and most importantly, usability in the field, the number of applications is poised to increase considerably.

References

[1] J. Milsom and A. Eriksen, *Field Geophysics*, 4th Edition, Wiley Press (2011).
[2] P. D. D. Schwindt, S. Knappe, V. Shah, L. Hollberg, and J. Kitching, *Chip-scale atomic magnetometer*, Appl. Phys. Lett. **85**, 6409 (2005).
[3] S. Knappe, V. Shah, P.D.D. Schwindt, L. Hollberg, and J. Kitching, *A microfabricated atomic clock*, Appl. Phys. Lett. **85**, 1460 (2004).
[4] W. E. Bell and A. L. Bloom, *Optically driven spin precession*, Phys. Rev. Lett. **6**, 280 (1961).
[5] R. Guilizzoni, J. C. Watson, P. Bartlett, and F. Renzoni, *Penetrating power of resonant electromagnetic induction imaging*, AIP Advances **6**, 095017 (2016).

Zero-to-Ultralow-Field-NMR spectroscopy with an atomic magnetometer in unshielded environment

V. Biancalana[1], G. Bevilacqua[1], Y. Dancheva[2], E. Mariotti[2], C. Rossi[3], A. Vigilante[2]

1. Dept. of Engineering and Mathematics (DIISM), University of Siena, Via Roma 56, 53100 Siena, Italy
2. Dept of Physics Science Earth and Environment (DSFTA), University of Siena, Via Roma 56, 53100 Siena, Italy
3. Dept of Biotechnology Chemistry and Pharmacy (DBCF), University of Siena, Via A. Moro 2, 53100 Siena, Italy

We have developed an optical scalar magnetometer operating in an unshielded environment based on D1 synchronous pumping and D2 polarimetry of Cs vapour [1] in a Bell & Bloom scheme. The main scope of this experimental research is to build a robust, user friendly and cost effective device with negligible maintenance costs. High sensitivity magnetic field / magnetic field gradients measurements are performed thanks to a multisensor arrangement and a system for magnetic field / field gradients compensation [2]. The sensors (Cs buffered glass cells of few cm^3 in volume) work at nearly room temperature and samples can be placed in their proximity.

The operation principle is based on optical pumping of an atomic sample positioned in an orthogonal magnetic field and measurement of the atomic precession. Optical pumping and precession probing are performed using a dual wavelength fiber coupled system. The ultimate sensitivity, in differential regime, is better than $100\mathrm{fT}/\sqrt{\mathrm{Hz}}$. The magnetometer operates in a bias magnetic field ranging from 100nT up to tens of μT, which can be actively stabilized.

Zero-to-ultra-low field (ZULF) NMR spectroscopy [3] has been performed in various kinds of samples. To this purpose remote prepolarization technique is exploited. A fast pneumatic shuttling system transports samples (a few ml in volume) from a prepolarizing Halbach assembly (nearly 1T field strength) to the magnetometer head, where a coil system is used to manipulate the nuclear spins.

Nuclear spin precession or relaxation can be measured with multiple shots recording. The robustness of the magnetometer and the implementation of various procedures for automatic good-shot recognition enable to perform long lasting measurements and averaging for signal-to-noise improvement. ZULF NMR spectroscopy has been applied in several molecules. We will present the case of trimethyl-phosphate tested at intermediate field strengths, i.e. in the condition where the $^3J[H,P]$ coupling and the spin-field interaction are of the same order of magnitude.

References

[1] G. Bevilacqua, V. Biancalana, Y. Dancheva, *Atomic orientation driven by broadly frequency-modulated radiation: Theory and experiment*, Phys. Rev. A **94**, 012501 (2016).
[2] G. Bevilacqua, V. Biancalana, P. Chessa, Y. Dancheva, *Multichannel optical atomic magnetometer operating in unshielded environment*, Appl. Phys. B **122**, 103 (2016).
[3] G. Bevilacqua, V. Biancalana, A. Ben-Amar Baranga, Y. Dancheva, C. Rossi, *Microtesla NMR J-coupling spectroscopy with an unshielded atomic magnetometer*, J. Magn. Res. **263**, 65 (2016).

Poster presentations

Optically Pumped Magnetometry at USTC

Dong Sheng

Department of Precision Machinary and Precision Instrumentation, University of Science and Technology of China, Hefei, P. R. China

We recently set up a new lab dedicated for optically pumped magnetometry at University of Science and Technology of China (USTC). We have built a K-Rb hybridly pumped system working in the spin-exchange-relaxation-free (SERF) regime. By optically pumping the K atoms and probing the Rb atoms, the sensor has reached a magnetic field sensitivity of 10 fT/Hz$^{1/2}$ with a 35 Hz bandwidth as shown in Fig. 1. We are working to update this system by adding nuclear spin gases into the cell for a compensated co-magnetometer. This will work as a node in a precision measurement network.

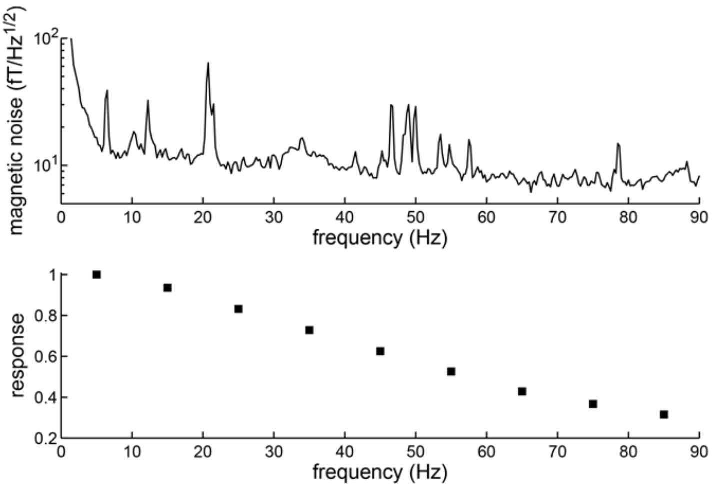

Fig. 1 Sensitivity and bandwidth of the K-Rb SERF magnetometer.

Another project of our lab is the nuclear spin co-magnetometer. We focus on suppressing the systematic error in the Xenon isotope-Rb system, such as the frequency shift due to the polarized Rb atoms and Bloch-Siegert shift due to the nuclear spin cross-talk. By resolving the quadrupole splitting of ^{131}Xe atoms and probing the Rb atoms with a modulation scheme, we aim to reach a 5 nHz systematic error. This system will apply to many precision measurements that require accuracy of the co-magnetometer signal.

Study of the Directional Dependence of Magnetic Resonance Signals in Orientation-Based Atomic M_x-Magnetometers

Victor Lebedev, Simone Colombo, Vladimir Dolgovskiy, Theo Scholtes, Zoran D. Grujić, Antoine Weis

Physics Department, University of Fribourg, Chemin du Musée 3, CH-1700 Fribourg, Switzerland

We present a study of the dependence of lock-in-demodulated signals of M_x-type *orientation*-based single beam laser-pumped cesium vapor magnetometers on the direction of the static magnetic field $\vec{B}_0=\omega_L/\gamma_F$, and compare experimental results to the theoretical model predictions [1]. We have studied in particular two distinct magnetometer configurations, viz., one in which the RF-field, $\vec{B}_1 \cos\omega_{\mathrm{RF}}t$, is parallel to the light beam direction $\vec{k}$, and one in which it is perpendicular to the latter. Using an automated steering and DAQ system we have systematically recorded magnetic resonance spectra for 2'400 orientations of the static field $\vec{B}_0$, spanning the complete 4π solid angle. At each field orientation a magnetic resonance spectrum was recorded using a dual-channel lock-in amplifier. Each spectrum was then analysed by fitting an algebraic magnetic resonance lineshape function [1], from which the lineshape parameters (resonance center frequency, resonance linewidth, on-resonance amplitude $R(\omega_{\mathrm{RF}}=\omega_L)$, and on-resonance phase $R(\omega_{\mathrm{RF}}=\omega_L)$) have been extracted, allowing the study of these parameters as a function of $\hat{B}_0$.

We have made a detailed account for sources of experimental imprecisions and discussed the applicability of the approximations made in the theoretical model. Our experiments accurately confirm (within measurement uncertainties) the algebraic model predictions [1] for the directional dependence of optically detected magnetic resonances [2]. We will further report on an ongoing related study of the directional dependencies of *alignment*-based magnetometers, of which much less known in the literature.

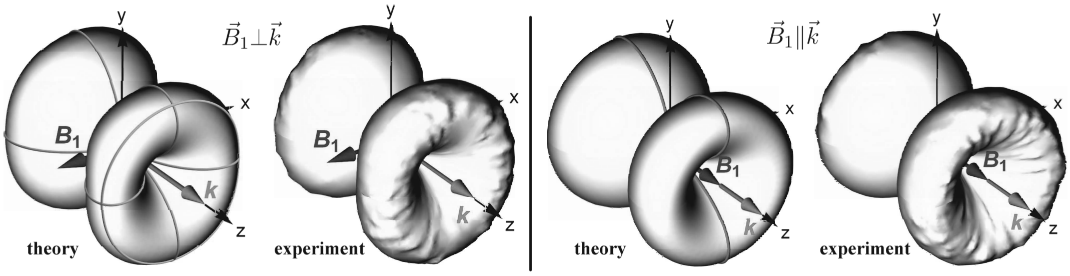

Fig. 1 Theoretical and experimental directional dependencies of the on-resonance R-signals in the $\vec{B}_1 \perp \vec{k}$ (left) and $\vec{B}_1 \| \vec{k}$ (right) magnetometer geometries.

References

[1] A. Weis, G. Bison, and Z. D. Grujić, *Magnetic Resonance Based Atomic Magnetometers*, in *High Sensitivity Magnetometers*, ed. by A. Grosz, M. J. Haji-Sheikh, S. C. Mukhopadhyay (Springer, 2017).

[2] S. Colombo, V. Dolgovskiy, T. Scholtes, Z. D. Grujić, V. Lebedev, and A. Weis, *Orientational Dependence of Optically Detected Magnetic Resonance Signals in Laser-Driven Atomic Magnetometers*, Appl. Phys. B **123**, 35 (2017).

Accurate Cesium Magnetometer Based on Free Alignment Precession

Zoran D. Grujić[1], Jari Piller[2], Victor Lebedev[1], Yongqi Shi[1,2], Vladimir Dolgovskiy[1], Theo Scholtes[1], Simone Colombo[1], Antoine Weis[1]

1. Physics Department, University of Fribourg, Chemin du Musée 3, CH-1700 Fribourg, Switzerland
2. Institute of Electronics, Chinese Academy of Sciences, Beijing 100190, China

Our team participates in an international collaborative effort searching for a permanent electric dipole moment of the neutron (nEDM experiment) [1]. In the ongoing nEDM experiment an array of 16 Cs magnetometers monitors spatial and temporal variations of the 1 μT magnetic field applied to the ultracold neutrons. This application requires both sensitivity and accuracy. Currently, each Cs magnetometer in the array is operated in the so-called M_x-geometry, in which the frequency of a weak magnetic resonance driving AC magnetic field is phase-locked to the Larmor precession frequency, ω_L, of the atomic spin polarization. Despite the fact that frequency measurements are very precise, this method suffers from unpredictable systematic shifts because of imprecisions of the reference phase settings.

Recently, we have investigated a Cs magnetometer based on *free spin precession (FSP)*, in which spin orientation (vector polarization) is produced by amplitude-modulated circularly-polarized light [2]. The FSP magnetometer has shown satisfactory sensitivity and improved accuracy with respect to the M_x magnetometer, but suffers from an (as yet not explained) systematic heading error limiting its accuracy. Here we present an alternative principle of operation of a magnetometer based on *free alignment precession (FAP)*. A single FAP measurement cycle consists of two phases: a pumping phase and a readout phase. Atomic alignment (tensor polarization) of the cesium vapor is produced by pumping with linearly-polarized light that is amplitude-modulated at $2\omega_L$, see Fig. **??**. After pumping, the FAP signal is detected in a readout phase by the same light beam, set to a constant (low) intensity. When the field of interest is orthogonal to the light polarization, an oscillation at $2\omega_L$ is imprinted onto the transmitted light power. The photocurrent is amplified and digitized and an off-line analysis is used to infer the magnetic field magnitude $\vec{B}{=}\omega_L/\gamma_F$, where $\gamma_F{\approx}3.5$ Hz/nT. We will present our current results, problems and prospects of the FAP magnetometer.

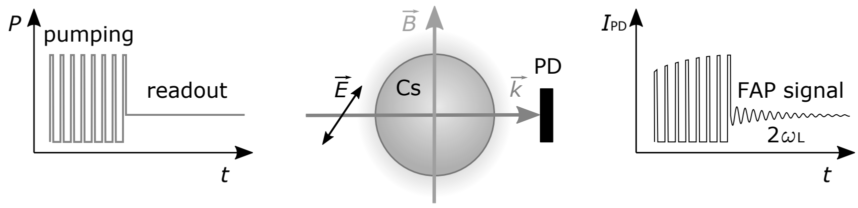

Fig. 1 Left: Input light power P as function of time during the first phase of a FAP-cycle. Center: Deployed FAP geometry. Right: Photocurrent I_{PD} generated by transmitted light on the photodiode PD. During the pump phase the linearly-polarized amplitude-modulated light produces a precessing steady-state alignment, as evidenced by the increasing vapor transmission. During the readout phase, the precessing alignment's decay is detected by the PD.

References

[1] J. M. Pendlebury *et al.*, *Revised experimental upper limit on the electric dipole moment of the neutron*, Phys. Rev. D **92**, 092003 (2015).
[2] Z. D. Grujić, P. A. Koss, G. Bison, and A. Weis, *A sensitive and accurate atomic magnetometer based on free spin precession*, Eur. Phys. J. D **69**, 135 (2015).

P04

On the statistical sensitivity and quantum limits of spin noise spectroscopy

Morgan W. Mitchell[1,2], Vito Giovanni Lucivero[1], Ricardo Jiménez-Martínez[1], Aleksandra Dimic[3], Charikleia Troullinou[1], Jia Kong[1] and Janek Kolodynski[1]

1. ICFO-Institut de Ciencies Fotoniques, The Barcelona Institute of Science and Technology, 08860 Castelldefels (Barcelona), Spain
2. ICREA – Institució Catalana de Recerca i Estudis Avançats, 08015 Barcelona, Spain
3. Faculty of Physics, University of Belgrade, Studentski Trg 12-16, 11000 Belgrade, Serbia

Precise knowledge of the spin orientation of atomic ensembles is demanded in a wide range of scenarios, from further progress in best-in-class atomic clocks and magnetometers to the preparation of non-classical states of matter and memories. Implementing quantum-limited detection schemes is challenging, however. Shot-noise in the detectors can mask the motion of the spins limiting the precision of estimations. Here we describe our recent work and results aimed at overcoming this challenge in alkali-based sensors. We will describe versatile instrumentation to optically prepare and detect alkali vapors using coherent and polarization-squeezed light and optimal estimation techniques [1]. We have studied the fundamental limits in the optimal estimation of system properties of atomic ensembles in thermal equilibrium via spin noise spectroscopy [2]. Our experimental results agree with spectral estimation theory, which predicts that shot noise imposes "local" standard quantum limits for any given probe power and atom number, and also "global" standard quantum limits when probe power and atom number are taken as free parameters. Using squeezed-light we show sensitivity beyond the atom and photon-number-optimized global standard quantum limit. We will report our progress in the development and verification of these techniques in the time domain as required for real-time sensing and control applications, e.g. magnetometry.

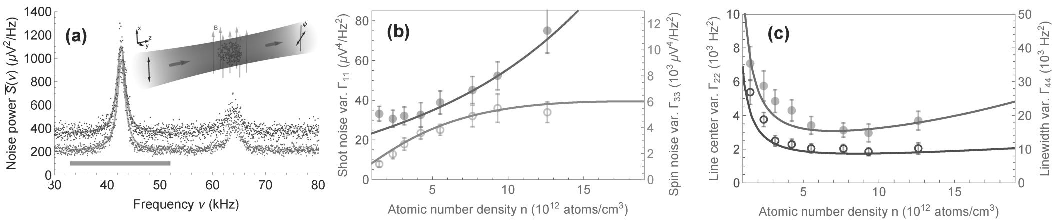

Fig. 1 (a) Spin noise spectra. Representative noise spectra showing spin noise resonances of Rb vapor, upper spectrum with coherent-state probing, lower spectrum with polarization-squeezed probe light. The bar below spectra shows fit region for ^{85}Rb spectra, the curves show fits to the data based on a model consisting of a Lorentzian ,with resonance at the Larmor frequency, and frequency-independent background due to shot noise [1,2] for both coherent and squeezed spectra, respectively. Inset: principle of spin noise measurement. Polarized light experiences Faraday rotation by an angle ϕ proportional to the on-axis magnetization of the atomic ensemble, and is detected with a polarimeter (not shown). (b) - (c) Spin noise sensitivity. Sensitivity of spin noise spectroscopy versus atomic density in theory and experiment. Optical power is $P = 2$ mW throughout. (b) Lower curve shows Γ_{22}, the variance of the Larmor frequency estimate, computed by theory and from experiment (hollow circles), on left axis. Upper curve shows Γ_{44}, the variance of the resonance linewidth estimate, and observed variance (filled circles), on right axis. (c) Upper curve shows Γ_{11}, the variance of the shot noise estimate, from theory and from experiment (filled circles), on left axis. Lower curve shows Γ_{33}, the variance of the resonance amplitude, due spin noise, estimate, and observed variance (hollow circles), on right axis. Error bars show plus/minus one standard error.

References

[1] V. G. Lucivero, R. Jiménez-Martínez, J. Kong, and M. W. Mitchell, *Squeezed-light spin noise spectroscopy*, Phys. Rev. A **93**, 053802 (2016).
[2] V. G. Lucivero, A. Dimic, J. Kong, R. Jiménez-Martínez, and M. W. Mitchell, *Sensitivity, quantum limits, and quantum enhancement of noise spectroscopies*, Phys. Rev. A **95**, 041803(R) (2017).

The Ground State Hanle Effect with Linearly-Polarized and Unpolarized Light

Yongqi Shi[1,2], Zoran D. Grujić[1], Theo Scholtes[1], Simone Colombo[1], Vladimir Dolgovskiy[1], Victor Lebedev[1], Antoine Weis[1]

1. Physics Department, University of Fribourg, Chemin du Musée 3, CH-1700 Fribourg, Switzerland
2. Institute of Electronics, Chinese Academy of Sciences, Beijing 100190, China

In a previous study [1] we have explored the Ground State Hanle effect (GSHE) of Cs atoms that were optically-pumped with **linearly-polarized laser light**. In that case the GSHE is the result of the destruction of the initial atomic alignment (tensor polarization) oriented along the light polarization by a (scanned) transverse magnetic field. Here we present a related experiment in which an initial alignment along the light propagation direction $\vec{k}$ is produced by optical pumping with **unpolarized laser light**, and make a quantitative comparison of the two experiments.

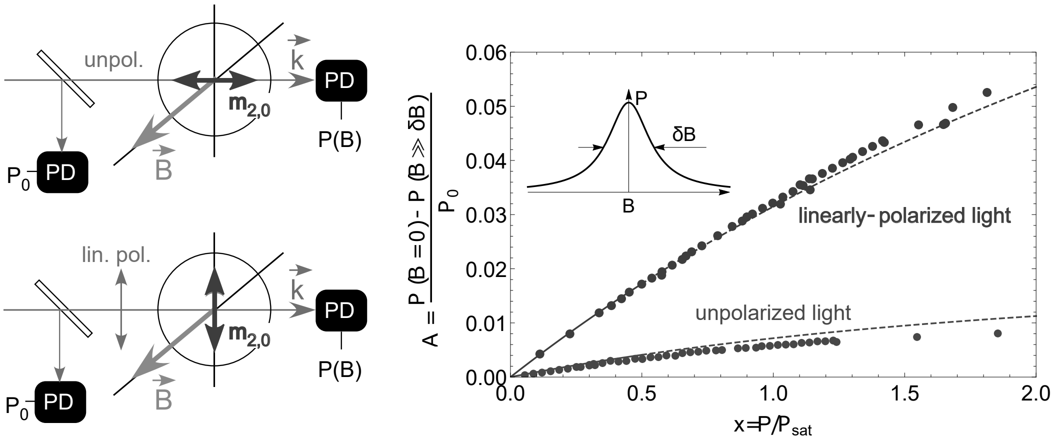

Fig. 1 Left: The two investigated GSHE geometries. Right: Experimental power-normalized Hanle amplitudes (dots), together with results of scaled model calculations (solid lines).

The experiments were done in a paraffin-coated Cs vapour cell at room temperature using laser radiation resonant with the 4→3 component of the Cs D_1 transition.We scrambled the laser beam's polarization by sending it through a multimode fiber wound as 20 (10 cm diameter) loops on a support structure, resulting in a residual degree of polarization <5%. We record the change of transmitted power when scanning a magnetic field, perpendicular to the alignment in both cases, yielding the well known Lorentzian-shaped GSHE resonances [1].

The amplitudes of the Hanle resonances are inferred from off-line fits by algebraic model functions, assuming equivalence of the three alignment relaxation rates. The dependence of the Hanle amplitudes on laser power is shown on the right graph, together with the predictions of (scaled) algebraic model calculations that are — in principle — valid only for $x \ll 1$, i.e., for $P \ll P_{\mathrm{sat}}$.

References

[1] E. Breschi and A. Weis, *Ground-state Hanle effect based on atomic alignment*, Phys. Rev. A **86**, 053427 (2012).

P06

Towards a high-density squeezed-light magnetometer

Charikleia Troullinou[1], Ricardo Jiménez-Martínez[1] , Jia Kong[1], and Morgan W. Mitchell[1,2]

1. ICFO-Institut de Ciencies Fotoniques, The Barcelona Institute of Science and Technology, 08860 Castelldefels (Barcelona), Spain
2. ICREA – Institució Catalana de Recerca i Estudis Avançats, 08015 Barcelona, Spain

Increasing the sensitivity limits of alkali-based magnetometers is an active area of interest [1-3]. A promising approach to reach this goal relies on quantum-non-demolition (QND) measurements and squeezed-light, which have enabled magnetic field sensitivities beyond the spin projection noise limit [4,5] and photon shot-noise limit [6-8]. To date, however, these techniques have been used to improve the performance of optical magnetometers independently but not within the same device. Their simultaneous use remains an open challenge. Furthermore it is not clear if squeezed-light can improve the performance of magnetometers operating at high alkali densities [7], such as required to operate micro-fabricated [9] and SERF magnetometers [10], and at which spin noise is more prominent.

Previously our group implemented a squeezed-light magnetometer but only reached sensitivities at the $\mathrm{nT}/\sqrt{\mathrm{Hz}}$ level [6]. In collaboration with Prof. W. Gawlik, a better sensitivity ($70\mathrm{fT}/\sqrt{\mathrm{Hz}}$) [3] was reached but in a magnetometer configuration not amenable for squeezed-light probing and QND measurements. Our recent work aims at implementing a magnetometer limited by both spin and photon shot noise in the high-density regime for which QND measurements and squeezed light can be beneficial. Contrary to previous squeezed-light magnetometers based on spin-alignment [6-8] we use a magnetometer architecture based on spin-orientation of the atoms and use phase-sensitive detection to extract the magnetometer signal. This approach will allow us to implement a number of features not found in previous squeezed light magnetometers. Particularly we probe the spin orientation of the atomic ensemble via the optical Faraday effect, which is an efficient technique to implement QND measurements. The Bell-Bloom magnetometer allows us to work at high frequencies where our detectors and squeezed-light source are photon shot-noise limited. Finally, through power-spectral analysis of the phase-sensitive recorded signal we identify the different contributions due to spin noise and photon shot-noise. This fundamental noise as well as technical noise, such as magnetic noise are evident in the magnetometer output and set the effective bandwidth of the device [9]. This magnetometer architecture is simple and it is applied in a wide variety of current magnetometer implementations. Furthermore, our analytical techniques are based on standard power-spectral analysis [10], which can be deployed in existing magnetometers with little effort.

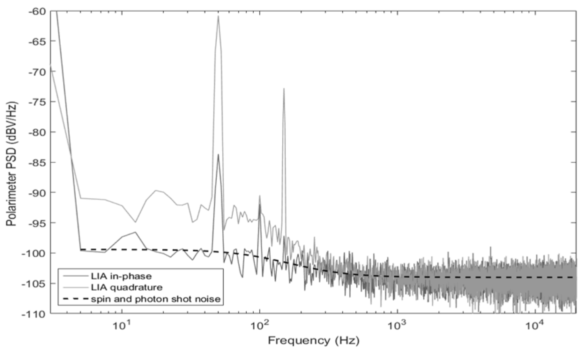

Fig. 1 Power spectral analysis of the Lock in Amplifiers output for signal obtained with probe power at 500μW and pump power 40μW. The spin and photon shot noise is estimated by fitting the signal of Spin Noise Spectroscopy for the same power and density conditions.

References

[1] D. Sheng, S. Li, N. Dural, and M. V. Romalis, *Subfemtotesla Scalar Atomic Magnetometry Using Multipass cells*, Phys. Rev. Lett. **110**, 160802 (2013).
[2] Z. D. Grujić, P. A. Koss, G. Bison, and A. Weis, *A sensitive and accurate atomic magnetometer based on free spin precession*, Eur. Phys. J. D **69**, 135 (2015).
[3] V. G. Lucivero, P. Anielski, W. Gawlik, and M. W. Mitchell, *Shot-noise-limited magnetometer with sub-picotesla sensitivity at room temperature*, Rev. Sc. Instr. **85**, 113108 (2014).
[4] K. Jensen *et al.*, *Quantum Noise Limited and Entanglement-Assisted Magnetometry*, Phys. Rev. Lett. **104**, 133601 (2010).
[5] R. J. Sewell *et al.*, *Magnetic Sensitivity Beyond the Projection Noise Limit by Spin Squeezing*, Phys. Rev. Lett. **109**, 253605 (2012).
[6] F. Wolfgramm *et al.*, *Squeezed-Light Optical Magnetometry*, Phys. Rev. Lett. **105**, 053601 (2010).
[7] T. Horrom, R. Singh, J. P. Dowling, and E. E. Mikhailov, *Quantum-enhanced magnetometer with low-frequency squeezing*, Phys. Rev. A **86**, 023803 (2012).
[8] N. Otterstrom, R. C. Pooser, and B. J. Lawrie, *Nonlinear optical magnetometry with accessible in situ optical squeezing*, Opt. Lett. **39**, 6533 (2014).
[9] V. Shah, G. Vasilakis, and M. V. Romalis, *High Bandwidth Atomic Magnetometery with Continuous Quantum Nondemolition Measurements*, Phys. Rev. Lett. **104**, 013601 (2010).
[10] V. G. Lucivero *et al.*, *Sensitivity, quantum limits, and quantum enhancement of noise spectroscopies*, Phys. Rev. A **95**, 041803(R) (2017).

Test System for Investigation of Geometry Dependent Systematic Effects in Double Resonance Magnetometry

Carolyn O'Dwyer, Stuart J. Ingleby, Paul F. Griffin, Iain Chalmers, Aidan Arnold, Erling Riis

Department of Physics, University of Strathclyde, 107 Rottenrow East, Glasgow, UK

Double resonance magnetometry can be used to measure magnetic fields with high precision [1] in a range of applications. We aim to build magnetic sensors which can operate unshielded in the geophysical range, with a focus on portable and compact magnetometers. We have begun by minimising our hardware in all iterations of our system. We employ a single laser to pump the atomic medium while perturbing the field with an RF coil. First we aim to understand the geometry dependent systematic effects inherent to this type of sensor.

We have built a test system to develop techniques for controlling the field amplitude and gradient. Here we will discuss the field control we have achieved through calibration and optimisation of our double resonance technique in this controlled, shielded environment [2]. Arbitrary fields may be applied in any orientation in order to simulate the type of fields we aim to detect. By exploiting iterative optimisation routines and software controlled current sources we have achieved field magnitude tolerances of 0.94 nT and orientation tolerances of 5.9 mrad. This automated, self-calibrating test system will enable us to address the geometry dependent effects and develop deadzone free, compact magnetometers.

This work is supported by the UK Quantum Technology Hub in Sensors and Metrology.

References

[1] S. Groeger, G. Bison, J.-L. Schenker, R. Wynands, and A. Weis, *A high-sensitivity laser-pumped M_x magnetometer*, Eur. Phys. J. D **38**, 239 (2006).

[2] S. J. Ingleby, P. F. Griffin, A. S. Arnold, M. Chouliara, and E. Riis, *High-precision control of static magnetic field magnitude, orientation, and gradient using optically pumped vapour cell magnetometry*, Rev. Sci. Instrum. **88**, 043109 (2017).

P08

On the Heading Error of Various OPM Types

Rob IJsselsteijn[1,2], **Volkmar Schultze**[2], **Gregor Oelsner**[2], **Florian Wittkämper**[2], **Ronny Stolz**[2]

1. Supracon AG, An der Lehmgrube 11, D-07751 Jena, Germany
2. Leibniz Institute of Photonic Technologies, Albert-Einstein-Straße 9, D-07745 Jena, Germany

The heading error of OPM, viz. deviations of the measured magnetic field from the real magnitude B_0 in dependence on the magnetometer orientation, originates from three classes of sources: the nonlinear Zeeman effect getting remarkably already at Earth's magnetic-field strength, self-made operation-mode inherent magnetic fields, and magnetic uncleanliness of the measurement setup. In order to get rid of the latter, we installed the OPM sensor head on a specially prepared plastic rotary table, shown in Fig. 1, inside our magnetic-field shielding barrel [1]. The magnetic field generated by the Helmholtz coil system inside the barrel was kept constant in size and direction for each series of measurements.

The quality of the measurement setup was evaluated with glass-blown buffer-gas free Cesium vapor cells from Fribourg [2], working in the conventional M_x mode. With careful tuning to the $F = 4 \rightarrow F' = 3$ hyperfine transition of the Cs-D1 line, the sole action of the non-linear Zeeman effect at $B_0 = 50\ \mu$T is visible, which can be eliminated by the combination of two vapor cells pumped with circular polarization of opposite helicity – a well-known method [3].

Staying with the M_x operational mode we investigated the heading error of our integrated buffer-gas cells [4]. Since the absorption lines of neighboring hyperfine transitions overlap in our setup, a fine-tuning of the laser frequency is needed in order to cancel light-shift effects.

Such suppression of the light-shift is not possible for the operation in the light-narrowing (LN) mode, where strong detuned pumping near the (broadened) $F = 3 \rightarrow F' = 3;4$ transition is used to get improved magnetic-field sensitivity [5]. However, by taking the mean value obtained with two cells pumped with opposite circular polarization, the light-shift error can be suppressed significantly. The remaining heading error is determined by the vectorial addition of B_0 and the light-shift in pump direction k.

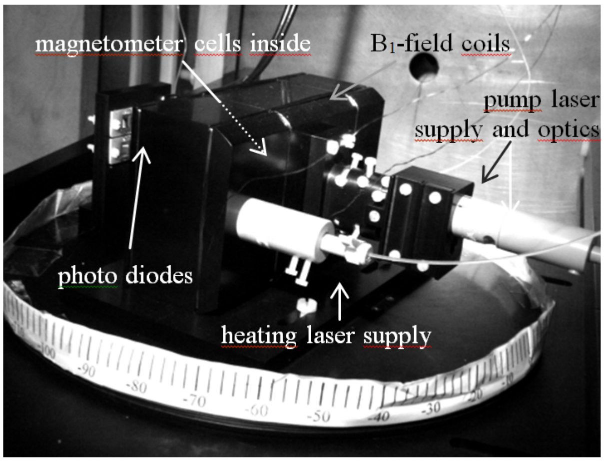

Fig. 1 Rotary table with OPM measurement setup.

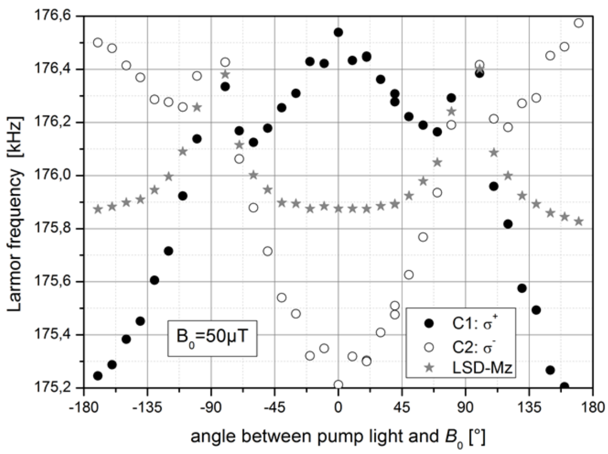

Fig. 2 Heading error in LSD-Mz mode for the two single cells and the LSD-Mz configuration.

In the light-shift dispersed M_z (LSD-Mz) mode [6] the best sensitivity is obtained for parallel orientation of k and B_0. This gives the opportunity to suppress strongly the afore-mentioned action of the vectorial addition of light-shift and B_0 by taking the mean value of the LSD-Mz signal (Fig. 2). However, the dependence of the heading error on the operational parameters is more complex than for the other regarded OPM types. These dependencies as well as special features of the other OPM types will be presented and discussed.

References

[1] V. Schultze, R. IJsselsteijn, and H.-G. Meyer. *Noise reduction in optically pumped magnetometer assemblies*, Appl. Phys. B **100**, 717 (2010).

[2] N. Castagna, G. Bison, G. Domenico, A. Hofer, P. Knowles, C. Macchione, H. Saudan, and A. Weis, *A large sample study of spin relaxation and magnetometric sensitivity of paraffin-coated Cs vapor cells*, Appl. Phys. B **96**, 763 (2009).

[3] T. Yabuzaki and T. Ogawa, *Frequency shifts of self-oscillating magnetometer with cesium vapor*, J. Appl. Phys. **45**, 1342 (1974).

[4] S. Woetzel, V. Schultze, R. IJsselsteijn, T. Schulz, S. Anders, R. Stolz, and H.-G. Meyer, *Microfabricated atomic vapor cell arrays for magnetic field measurements*, Rev. Sci. Instrum. **82**, 033111 (2011).

[5] T. Scholtes, V. Schultze, R. IJsselsteijn, S. Woetzel, and H.-G. Meyer, *Light-narrowed optically pumped M_x magnetometer with a miniaturized Cs cell*, Phys. Rev. A **84**, 043416 (2011); Erratum **86**, 059904(E) (2012).

[6] V. Schultze, B. Schillig, R. IJsselsteijn, T. Scholtes, S. Woetzel, and R. Stolz, *An Optically Pumped Magnetometer Working in the Light-Shift Dispersed M_z Mode*, Sensors **17**, 561 (2017).

Sensitive and stable Hanle-type 2D magnetometer

G. Bison[1], V. Bondar[3], P. A. Koss[3], A. Schnabel[2], N. Severijns[3], J. Voigt[2], E. Wursten[3]

1. Paul Scherrer Institut, Villigen PSI, Switzerland
2. Physikalisch Technische Bundesanstalt, Berlin, Germany
3. Institute for nuclear and radiation physics, KU Leuven, Belgium

We report on a Hanle-type magnetometer that uses the same system as the free spin precession magnetometer published in [1]. The magnetometer is most sensitive at zero magnetic field. It uses four laser beams to measure the magnetic field vector components along two orthogonal directions. The influence of the common mode power fluctuations in the laser beams is greatly suppressed due to a differential detection scheme. This leads to high magnetometric sensitivity even at low detection frequencies.

Sensitivities of better than 60 $\mathrm{fT}/\sqrt{\mathrm{Hz}}$ could be demonstrated simultaneously for both measurement channels in a well shielded environment. A minimum Allan deviation, limited by residual field fluctuations, of better than 40 fT was observed for integration times of 2s. The magnetometer is ideal for sensitive low-frequency field measurements in offset fields and close to zero field. Among the possible applications for this system is the determination of quasi-static shielding factors of passive magnetic shields. It can also be used to search for undesired magnetic field correlations in fundamental physics experiments such as EDM searches.

References

[1] S. Afach *et al.*, *Highly stable atomic vector magnetometer based on free spin precession*, Opt. Express **23**, 22108 (2015).

Chip-scale Atomic Magnetometer Based on Free Induction Decay for Ultra-low Magnetic Field Detection

Dominic Hunter, Savino Piccolomo, Erling Riis

Dept.of Physics, University of Strathclyde, 107 Rottenrow East, G4 0NG Glasgow, Scotland

Sensitive and accurate detection of ultra-low magnetic fields is of prime importance in numerous applications including biomedical science, such as magnetocardiography and magnetoencephalography [1, 2], geophysical surveying [3], and fundamental science [4]. In particular, chip-scale atomic magnetometers offer significant advantages in power dissipation, cost of fabrication, and size whilst maintaining sub-pT level sensitivities.

Here we describe an optically pumped ^{133}Cs magnetometer containing a $1.5\,mm$ thick sensor head of volume $25\,mm^3$. The vapour cell contains N_2 buffer gas to impede atomic diffusion to the cell walls, resulting in a broadened and shifted optical spectrum, and is operated at a temperature of $\sim 85\,°C$ to ensure an optimized atomic density. Many atomic magnetometer schemes operate in a cw regime were the spin preparation (pump) and detection (probe) stages are performed simultaneously with a single laser beam [5]. Here we discuss a pump-probe approach that separates these distinct phases in the time-domain, allowing the prepared atomic polarization to precess freely at the Larmor frequency whilst decaying exponentially as a consequence of various relaxation processes inherent to the vapour cell.

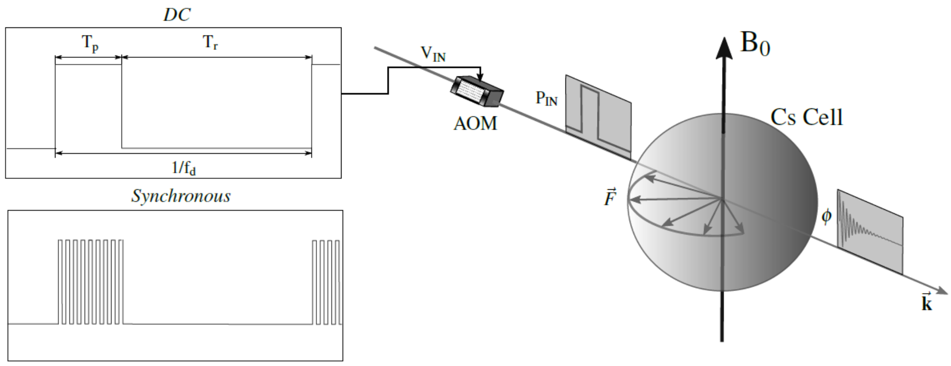

Fig. 1 Experimental model conveying the mechanisms behind a FID magnetometer. A high power light pulse builds up spin polarization during the pump phase. The left-most graphs depict two possible voltage inputs (DC or synchronous) that can be applied to the acousto-optic modulator. Precession in the transverse field is observed during a weak probe stage along with spin relaxation.

Depending on the proportionality between the bias field of interest and the damping rate; DC or synchronous modulation at the Larmor frequency, or one of its sub-harmonics, can be implemented to maximize the optical pumping efficiency. Modulation in the dispersive properties of the sample are observed during the readout phase as an oscillation in the polarization rotation angle at the Larmor frequency. Magnetic field information can be easily extracted from truncated FID signals epitomizing the high bandwidth capability. This technique also provides significant advantages in accuracy over driven magnetometers as the precession is monitored directly and not subject to systematic frequency shifts imposed by phase errors in the feedback signal [6], however careful consideration of potential AC stark shifts is required at elevated probe intensities. An optimal sensitivity of $\sim 1\,pT/\sqrt{Hz}$ has been measured in a shielded environment which is ultimately limited by depolarizing collisions with the vapour cell walls due to the smallest cavity dimension.

References

[1] S. Groeger, G. Bison, P. E. Knowles, R. Wynands, and A. Weis, *Laser-pumped cesium magnetometers for high resolution medical and fundamental research*, Sens. Actuat. A. Phys. **129**, 1 (2006).
[2] H. Xia, A. Ben-Amar Baranga, D. Hoffman, and M. Romalis, *Magnetoencephalography with an atomic magnetometer*, Appl. Phys. Lett. **89**, 211104 (2006).
[3] W. Stuart, *Earth's field magnetometry*, Rep. Prog. Phys. **35**, 803 (1972).
[4] C. Baker, D. Doyle, P. Geltenbort, K. Green, M. van der Grinten, P. Harris, P. Iaydjiev, S. Ivanov, D. May, J. Pendlebury, J. D. Richardson, D. Shiers, and K. F. Smith, *Improved Experimental Limit on the Electric Dipole Moment of the Neutron*, Phys. Rev. Lett. **97**, 131801 (2006).
[5] S. Groeger, G. Bison, J.-L. Schenker, R. Wynands, and A. Weis, *A high-sensitivity laser-pumped mx magnetometer*, Eur. Phys. J. D **38**, 239 (2006).
[6] Z. D. Grujić, P. A. Koss, G. Bison, and A. Weis, *A sensitive and accurate atomic magnetometer based on free spin precession*, Eur. Phys. J. D **69**, 135 (2015).

Comparison of Two Sensor Designs for the Coupled Dark State Magnetometer

Michaela Ellmeier[1,2], Christoph Amtmann[1], Andreas Pollinger[2], Werner Magnes[2], Christian Hagen[2], Irmgard Jernej[2], Roland Lammegger[1]

1. Institute of Experimental Physics, Graz University of Technology, Petersgasse 16, 8010 Graz, Austria
2. Space Research Institute, Austrian Academy of Sciences, Schmiedlstraße 6, 8042 Graz, Austria

The measurement principle of the Coupled Dark State Magnetometer (CDSM) is based on the differential measurement of two dark state resonances [1]. The dark states are established by Coherent Population Trapping (CPT) [2]. The CPT effect is a quantum interference effect which we experimentally realize in the ^{87}Rb hyperfine structure of the D1 line by a high frequency modulated light field. For the excitation of the coupled dark state resonances we use a so called Λ-shaped excitation scheme consisting of two ground states and one excited state. The two ground states are coherently coupled to the excited state by the two components of the high frequency modulated laser light field. The interaction of the light fields with the atomic level structure causes a destructive interference of the transitions from the ground states to the excited state. As a result, the atomic population gets trapped in a so called dark state where it is decoupled from the light fields which causes a reduction of the absorption and in consequence a decrease of the fluorescence. The benefit of this effect is that very narrow (sub Doppler) resonance line widths of about 30 Hz can be achieved [3]. For this reason, it is used for precision measurements like in compact atomic clocks [4] and magnetometers.

These magnetometers measure the magnetic field depend shift of the ground state transition frequency according to the Zeeman effect. However, the transition frequency is additionally shifted by other parameters like laser intensity or sensor cell temperature and buffer gas pressure. These shifts cannot be distinguished from a magnetic field induced shift at first glance. For this reason, the measurement principle of the CDSM uses a differential measurement of two dark state resonances which are almost equally influenced by the mentioned experimental parameters and thus cancels the disturbing influences. The CDSM prototype was developed for an application in space in a cooperation between the Institute of Experimental Physics of Graz University of Technology and the Space Research Institute of the Austrian Academy of Sciences. The prototype consists of a compact electronics unit inside of the spacecraft and a sensor unit outside of the spacecraft which are connected by optical fibres. The benefits of the CDSM magnetometer are its compact and robust design, a high dynamic magnetic field measurement range ($\sim$50-100,000 nT) and its omnidirectional measurement principle. The omnidirectionality is achieved by switching between two coupled dark state resonances which have even and odd CPT resonance quantum numbers and therefore an opposite angular dependence on the external magnetic field [5]. The first demonstration of the CDSM in space will be in summer 2017 in the course of the China Seismo-Electromagnetic Satellite mission.

For the further upcoming Jupiter Icy Moon Explorer (JUICE) mission, a new sensor configuration is currently developed. The new sensor design aims at a reduction of the optical pumping effect across the Zeeman manifold. The optical pumping effect is caused by the interaction of the polarized light with the atomic ensemble and results in a changed ground state population distribution. The changed population distribution influences the line shape of each single CPT resonance depending on the used ground states and thus can have an impact on the compensation effect of the coupled dark state resonances. The new sensor, which is based on a dual transition of the laser light through the sensor cell, will be presented and a comparison between the original and the new sensor design is drawn. With this new design we were able to reduce the influence of the optical pumping effect and obtain a balancing of the CPT resonance spectrum. We present first performance measurements with both sensors and discuss the magnetic field measurement accuracy of the CDSM compared to an Overhauser magnetometer.

References

[1] R. Lammegger, *Method and device for measuring magnetic fields*, WIPO, Patent WO 2008/151344 A3 (2008).
[2] E. Arimondo, *Coherent Population Trapping in Laser Spectroscopy*, Prog. Opt. **35**, 257 (1996).
[3] M. Erhard and H. Helm, *Buffer-gas effects on dark resonances: Theory and experiment*, Phys. Rev. A **63**, 043813 (2001).
[4] W. Zhong, *Review of chip-scale atomic clocks based on coherent population trapping*, Chin. Phys. B **23**, 030601 (2014).
[5] A. Pollinger, M. Ellmeier, W. Magnes, C. Hagen, W. Baumjohann, E. Leitgeb, R. Lammegger, *Enable the inherent omni-directionality of an absolute coupled dark state magnetometer for e.g. scientific space applications*, 2012 IEEE International Instrumentation and Measurement Technology Conference (I2MTC 2012) Proceedings, 33 (2012).

P12

Laser frequency locking using a transversal magnetic field for helium-based magnetometers

François Beato

CEA Leti, 17 Avenue des Martyrs, Grenoble, France

Our team has been working for several decades on ^{4}He Optically Pumped Magnetometers. After the development of a scalar magnetometer for ESA's SWARM satellites, we made proof of concept of heart and brain activity recordings with room temperature sensors. My PhD compares several schemes for probing helium atoms for improving magnetometer sensitivity. Some of those require a very stable laser tuning. An interesting laser locking method is based on the circular dichroism of the metastable helium gas subject to a milliTesla transverse magnetic field. I will present both the theoretical analysis and the experimental results achieved with this stabilization method.

Theory of Nonlinear Optical Wave Mixing Magnetometry

L. Deng[1], C. Zhu[2], E. W. Hagley[1]

1. National Institute of Standards and Technology, Gaithersburg, Maryland USA 20899
2. School of Physical and Engineering Sciences, Tongji University, Shanghai, China 200092

Single-beam atomic magnetometers relying on the nonlinear magneto-optical rotation (NMOR) effect have been thoroughly studied using a simple three-state Λ-scheme in both electromagnetically-induced transparency mode and Raman mode [1,2]. Recently, a cross-polarization optical wave mixing scheme has been introduced where more than 500-fold optical NMOR SNR enhancement has been observed [3]. Here, we present a nonlinear optics framework to explain the observed SRN enhancement, explaining the physics of the Zeeman-coherence nonlinear optical wave mixing scheme.

In a Zeeman-coherence optical wave mixing (WM) scheme the WM field creates a second excitation pathway via the mutually-influencing Zeeman coherence building up in the intermediate states, resulting in parametric propagation dependent dispersion amplification that leads to observed large enhancement of the NMOR SNR.

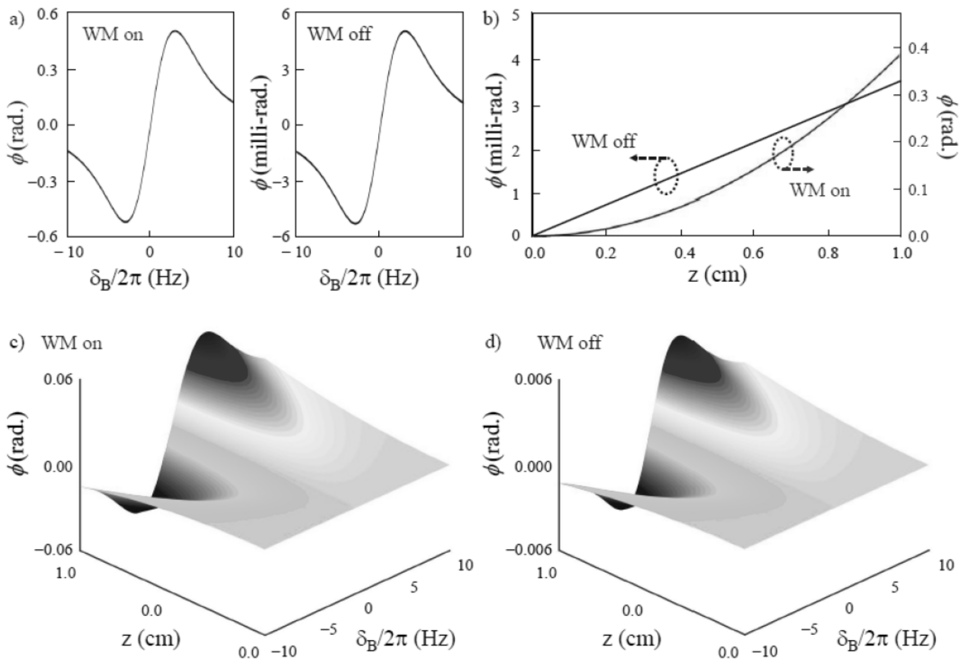

Fig. 1 (a) NMOR effect of the optical WM scheme (red trace, left) and the single-probe Λ-scheme (blue trace, right) as a function of δ_B at z = 1 cm. Parameters are chosen to show a representative 110-fold NMOR signal enhancement. If the blue trace is rescaled vertically by a factor of 110 the resonance line shape is non-distinguishable from that of the red trace, attesting the fact that the WM scheme does not alter the magnetic resonance line shape. (b) NMOR as a function of propagation distance z for the single-probe Λ-scheme (blue) and the WM scheme (red) at $\delta_B/2\pi = 5$ Hz. (c) and (d): NMOR as a function of z and δ_B with (c), and without (d), the WM field. Parameters: $\Omega p(0)/2\pi = 300$ kHz, $\Omega_{\mathrm{WM}}(0)/2\pi = 200$ kHz, $\delta_B/2\pi = 1$ GHz, $\delta_4/2\pi = 0.5$ GHz, $\Gamma/2\pi = 300$ MHz, $\gamma_0/2\pi = 10$ Hz, $\kappa = 10^9$/(cm.s), $\rho_{11}/(0) = \rho_{33}/(0) = 0.5$. Simulation uses a generic four level atomic system.

We note that the observed NMOR SNR enhancements have been verified by full numerical calculations using both nonlinear optics formulism [4] and the standard ellipsometry formulism [5]. With our parameters, these two mathematics treatments yield identical results.

References

[1] D. Budker and M. Romalis, *Optical Magnetometry*, Nature Phys. **3**, 227 (2007).
[2] V.A. Sautenkov *et al.*, *Enhancement of magneto-optic effects via large atomic coherence in optically dense media*, Phys. Rev. A **62**, 023810 (2000).
[3] F. Zhou, C. Zhu, E. W. Hagley, and L. Deng, *Symmetry-breaking Zeeman-coherence Optical Wave Mixing Magnetometry*, arXiv:1609.00431 (2016).
[4] Y.R. Shen, *The Principles of Nonlinear Optics*, Chapters 13 - 16, John Wiley & Sons (1984).
[5] M. Auzinsh, D. Budker, S. Rochester, *Optically Polarized Atoms*, Oxford University Press (2010).

P14

A Potassium Magnetometry Based Current Source for the n2EDM Experiment at PSI

Peter A. Koss[1], Georg Bison[2], Vira Bondar[1], Christopher Crawford[3], Elise Wursten[1], Nathal Severijns[1]

1. Institute for Nuclear and Radiation Physics, KU Leuven, 3001 Heverlee, Belgium
2. Paul Scherrer Institute, 5232 Villigen, Switzerland
3. Department of Physics, University of Kentucky, Lexington, KY 40506, USA

The search for new physics is a very active topic in today's fundamental research. Until now no direct observation of physics beyond the standard model (BSM) has been made. The neutron electric dipole moment (nEDM) is an observable which could hint to a certain class of BSM theories. The nEDM experiment at the Paul Scherrer Institute (PSI) is currently running with the best sensitivity ever [1]. A follow up of the present setup is planned and will be called n2EDM. This setup will have much improved capabilities in terms of nEDM statistics, magnetic field monitoring, magnetic field uniformity and stability.

The stability of the B_0 field of our nEDM experiment depends on many factors: shielding factor of the mu-metal, performance of the active field stabilization, local magnetic contaminations and temperature. However, the stability of B_0 will be limited fundamentally by the current source which feeds the B_0 coil. For the next generation nEDM experiment we are building an ultra-stable current source based on atomic magnetometry (see Fig.1).

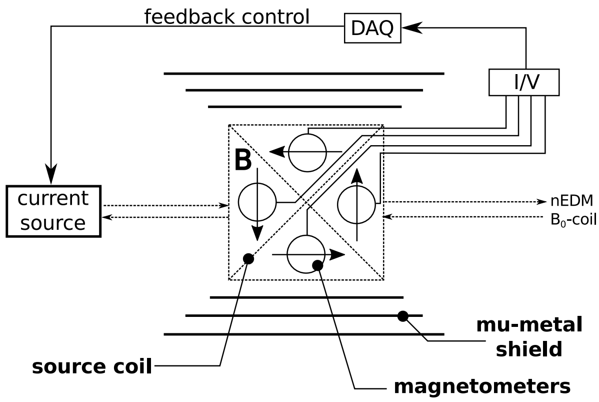

Fig. 1 ***Current source concept.*** A low noise current source is connected in series with the nEDM B_0-coil and a dedicated "source coil" outside of the nEDM setup. The source coil is a field confining coil with four quadrants. Each quadrant holds a Potassium magnetometer, which monitors the local field. The feedback control uses the readout of the four magnetometers to compensate for a drift of the current.

We intend to exploit the high sensitivity of optically pumped magnetometers by converting a current drift into a magnetic field drift [2]. For this we have developed a magnetic field confining coil (see Fig.1), which is able to discriminate an external field perturbation from a current drift [3]. The latter changes the field modulus in all four quadrants of the coil by the same amount. An external field will affect each quadrant in a different way.

We intend to use Potassium magnetometers based on free spin precession (FSP) signals. This mode of operation has been shown to yield a high sensitivity as well as low systematics and long term stability [4]. The use of Potassium will allow us to work at higher fields than with Cesium. In this way we gain in relative sensitivity since the coil constant of the source coil can be tailored to the needs of our current source. With this concept we plan to achieve a 10^{-9} stability on a 20 mA current.

References

[1] C. Baker *et al.*, *The search for the neutron electric dipole moment at the Paul Scherrer Institute*, Phys. Procedia **17**, 159 (2011).
[2] V. Y. Shifrin, C. G. Kim, and P. G. Park, *Atomic magnetic resonance based current source*, Rev. Sci. Instrum. **67**, 833 (1996).
[3] P. A. Koss, C. Crawford, G. Bison, E. Wursten, M. Kasprzak, and N. Severijns, *PCB Coil Design Producing a Uniform Confined Magnetic Field*, IEEE Magn. Lett. **PP**, 1 (2017).
[4] Z. D. Grujić, P. A. Koss, G. Bison, and A. Weis, *A sensitive and accurate atomic magnetometer based on free spin precession*, Eur. Phys. J. D **69**, 135 (2015).

Cross-correlation analysis between Optically-Pumped Magnetometers for Dark Matter searches

Vincent Dumont

Department of Physics, University of California, Berkeley, California 94720-7300, USA

Recent works have demonstrated the possibility to detect the presence of Dark Matter fields using atomic magnetometers where the crossing through the Earth of domain walls generated by an axion-like field and coupled to the spins of standard-model particles can be identified [1]. In this presentation, we give a detailed overview of the theoretical background and introduce the **G**lobal **N**etwork of **O**ptical **M**agnetometers to search for **E**xotic physics (GNOME) [2].

We will describe the analysis approach that we follow to identify transient exotic spin couplings to domain walls from dark matter field. Such transient signal cannot however be directly associated to “exotic” physics for individual magnetometers and one must cross-correlate any putative transient signal with the other stations in the network in order to distinguish false positives to real transient signatures.

An important aspect of the transient signal that is worth noting is that its expected bandwidth and duration are not known as no theoretical constraints have been placed on those properties, making more difficult and complex the identification procedure of such transient signals.

We introduce two techniques which, in combination, provide a powerful tool to adequately identify coherent transient signals among optical magnetometer stations. The first technique is the so-called Excess Power search method [3] which consists of scanning the entire time-frequency space and look for possible trigger signals of different bandwidth and/or duration. Once a time-frequency trigger map has been produced for each station for a given chunk of time, a coincidence analysis can be used to cross-correlate the different triggers found for each magnetometer station.

We will wrap up the presentation by presenting the first coincidence analysis results over a full month of acquired magnetic field data.

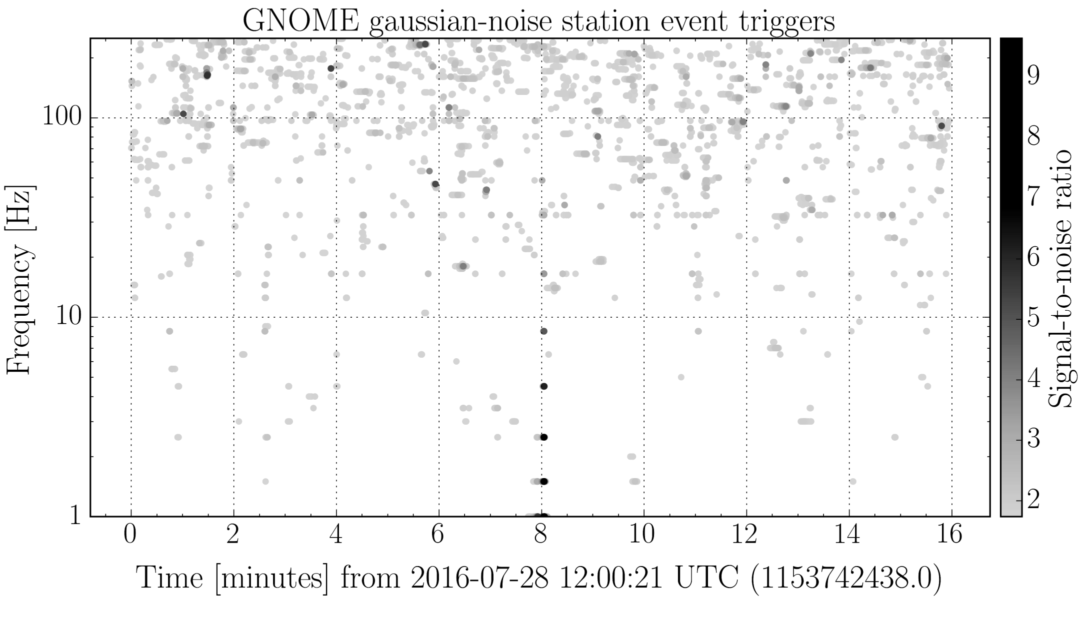

Fig. 1 Time-frequency trigger map from simulated magnetic field data where a gaussian burst signal has been injected in the data. The burst can be identified at minute 8 of the data chunk’s time period.

References

[1] M. Pospelov, S. Pustelny, M. P. Ledbetter, D. F. J. Kimball, W. Gawlik, and D. Budker, *Detecting Domain Walls of Axionlike Models Using Terrestrial Experiments*, Phys. Rev. Lett. **110**, 021803 (2013).

[2] S. Pustelny, D. F. Jackson Kimball, C. Pankow, M. P. Ledbetter, P. Wlodarczyk, P. Wcislo, M. Pospelov, J. R. Smith, J. Read, W. Gawlik, and D. Budker, *The Global Network of Optical Magnetometers for Exotic physics (GNOME): A novel scheme to search for physics beyond the Standard Model*, Ann. Phys. **525**, 659 (2013).

[3] W. G. Anderson, P. R. Brady, J. D. Creighton, and É. É. Flanagan, *Excess power statistic for detection of burst sources of gravitational radiation*, Phys. Rev. D **63**, 042003 (2000).

P16

Description and Characterization of the Optical Magnetometer in Mainz Dedicated to the Global Network of Optical Magnetometers for Exotic Physics Searches (GNOME)

Hector Masia-Roig[1], Arne Wickenbrock[1], Dmitry Budker[1,2,3] for the GNOME collaboration

1. Johannes Gutenberg-Universität Mainz, 55128 Mainz, Germany
2. Helmholtz-Institut Mainz, 55128 Mainz, Germany
3. Department of Physics, University of California, Berkeley, CA 94720-7300, USA

GNOME is a novel experimental scheme which enables the investigation of exotic spin couplings between nuclei and exotic fields generated by astrophysical sources measuring spin precession. It consists of a network of geographically separated (>100km), time synchronized, ultrasensitive optical magnetometers in a magnetically shielded environment. Such a configuration enables the study of global transient effects.

Currently, there are six magnetometer sensors placed around the world which are able to measure synchronously. Here the performance of the magnetometer built in Mainz for the GNOME collaboration is presented. Long term stability, bandwidth, and sensitivity of the sensor are carefully characterized. However, local perturbations of the sensor can fake axion signals. The implementation of a veto channel to disregard those effects is described. Even though the optimal operation of the magnetometer for GNOME is in phase-locked loop mode, the response of an open-loop mode magnetometer is studied for field changes higher than the resonance width. This response exhibits a beating between the atomic spins and the laser modulation frequency.

Self-compensating atomic magnetometer for searches of transient anomalous spin couplings

Mikhail Padniuk

Marian Smoluchowski Institute of Physics, Jagiellonian University, Łojasiewicza 11, 30-348 Krakow, Poland

Despite numerous sophisticated attempts, modern exotic physics still hides many unresolved mysterious. Questions such a: What does dark matter consist of? What is a dark energy? What is the source of bariogenesis? Is the universe isotropic? are just several examples of the most fundamental questions of contemporary science.

Many theoretical models try to address that fundamental questions by developing theories extending the Standard Model. A number of these theories predicts existence additional spin-dependent forces mediated by light particles outside of the Standard Model. These particles may interact with electrons or nucleons, leading to measurable effects on ordinary matter.

Despite experiments searching for such new particles/interactions, there is no direct evidence of such exotic forces. It leads to two possibilities. First - the theoretical models are not correct. Second - experiments lack of sensitivity or their methodology is wrong.

In the presentation, a new approach enabling observation of new spin-dependent interactions will be discussed. This approach is based on optical Rb-K-^{3}He co-magnetometer operated in self-compensated regime. The self-compensated regime is achieved in a following way: first nuclear polarization of ^{3}He is created by spin-exchange optical pumping. Then the compensation field is applied to null magnetic field experienced by Rb atoms. This allows ^{3}He magnetization, adiabatically changing with external magnetic fields (e.g.,induced due to residual field drift) effectively shield Rb atoms leaving them in zero magnetic field. To the contrary, the coupling due to non-magnetic (exotic) fields would have the effect on both spicies, inducing changes of polarization state of light. Thereby, the self-compansating magnetometer enables precise searches for exotic fields and particles. This makes the self-compensated magnetometer less sensitive the electromagnetic interactions.

I will discuss a setup of the self-compensated optical magnetometer. The first results of its operation will be reported and magnetometer to exotic spin-depended couplings will be analyzed. The optimization to the transient exotic coupling will be investigated. This is important due to the envisioned operation of the magnetometer as a part of the Global Network of Optical Magnetometers for Exotic physics (GNOME) [1]. The GNOME make possible correlated measurements of spin-depended forces at distant locations ($>$100 km). Such makes possible an approach suppression of noncorrelated noise and indicate correlated perturbations on measured signals.

References

[1] S. Pustelny, D. F. Jackson Kimball, C. Pankow, M. P. Ledbetter, P. Wlodarczyk, P. Wcislo, M. Pospelov, J. R. Smith, J. Read, W. Gawlik, and D. Budker, *The Global Network of Optical Magnetometers for Exotic physics (GNOME): A novel scheme to search for physics beyond the Standard Model*, Ann. Phys. **525**, 659 (2013).

P18

Detecting J-coupling in the gaseous molecule by spin-exchange optical pumping

Yunlan Ji[1], Min Jiang[1]

1. Department of Modern Physics, University of Science and Technology of China, Hefei, Anhui 230026, China

Spin-exchange optical pumping is a method to transfer polarization of optically pumped alkali metal atoms to another kind of atoms, which can be used to polarize the noble gas and investigate the fundamental process, such as the physical mechanism in the binary collision. The previous research mainly focus on the noble gas for its long spin depolarization time[1-3]. In this work, we extend the system to alkali-metal atoms and polyatomic molecules as demonstrated in Fig. 1. To achieve the distorted wave function of polarized alkali valence electron during a collision between the alkali metal atom and the molecule, the molecular orbital theory is applied. And through the acquired wave function, we can estimate the effect of spin exchange derived from the Fermi contact interaction[4]. Taking the gaseous methane as example, the enhancement factor for carbon is -2.7 and for hydrogen is 4.4, the effective magnetic field B_{eff} of the sample in a spherical vapor cell is on the scale of nT when the ^{87}Rb polarization is 87% with the number density $5 \times 10^{14}\mathrm{cm}^{-3}$.

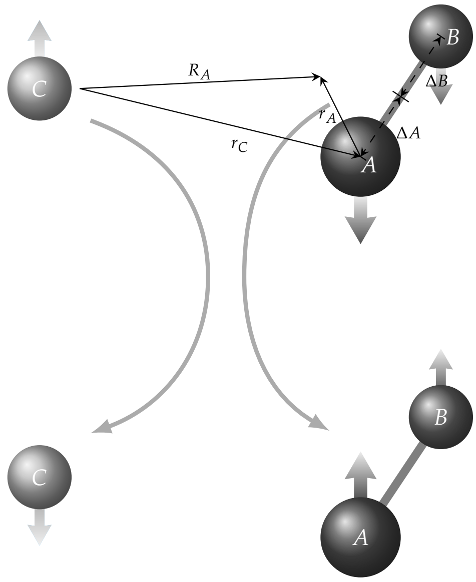

Fig. 1 The effect of the spin exchange between polarized electron spin and nuclear in a molecule. The polarization of different atoms in a molecule depends on the molecular configuration.

Since the SERF atomic magnetometer can achieve the sensitivity of several $\mathrm{fT}/\sqrt{\mathrm{Hz}}$, it is possible to use SERF atomic magnetometer to detect the signal in gaseous nuclear magnetic resonance. Based on our theoretical calculation, we design the scheme for the experiment as shown in Fig. 2. First gas molecule is polarized through optical pumping accompanied by the polarization of rubidium atoms. Then dc magnetic field pulses are applied to rotate the spins to the detection direction. Finally the magnetic signal with the precession frequency of J-coupling at zero field is detected.

Fig. 2 The sequence to detect the J-coupling by spin-exchange optical pumping.

The idea of gaseous nuclear magnetic resonance can be applied to detect various gaseous sample, and analyze the molecule structure by detecting the J-coupling, and it provides a promising step towards the research gaseous-state NMR.

References

[1] M. S. Albert, G. D. Cates, B. Driehuys, W. Happer, B. Saam, C. S. Springer Jr, and A. Wishnia, *Biological magnetic resonance imaging using laser-polarized ^{129}Xe*, Nature **370**, 199 (1994).

[2] E. Babcock, B. Chann, T. G. Walker, W. C. Chen, T. R. Gentile, *Limits to the Polarization for Spin-Exchange Optical Pumping of ^{3}He*, Phys. Rev. Lett. **96**, 083003 (2006).

[3] T. G. Walker and W. Happer, *Spin-exchange optical pumping of noble-gas nuclei*, Rev. Mod. Phys. **69**, 629 (1997).

[4] R. M. Herman, *Theory of Spin Exchange between Optically Pumped Rubidium and Foreign Gas Nuclei*, Phys. Rev. **137**, A1062 (1965).

An Optically-Pumped Magnetometer for Field Mapping and Reconstruction of Distributed Source Locations

Vladimir Dolgovskiy[1], Benoît Richard[1], Ilja Fescenko[1,2], Simone Colombo[1], Victor Lebedev[1], Naota Sekiguchi[1,3], Junhai Zhang[1,4], Antoine Weis[1]

1. Physics Department, University of Fribourg, Chemin du Musée 3, 1700 Fribourg, Switzerland
2. Institute of Atomic Physics and Spectroscopy, University of Latvia, 1050 Riga, Latvia
3. Department of Applied Physics, Tokyo University of Agriculture and Technology, Tokyo 184-8588, Japan
4. College of Science, Harbin Engineering University, 150001 Harbin, People's Republic of China

Recently we have demonstrated a magnetic camera which is capable of measuring spatially-resolved time-dependent signals from weak magnetic sources [1]. The current realization of this device is based on an M_z optically pumped magnetometer. A thin layer of caesium atoms contained as a vapour in a cubic glass cell and confined therein by a buffer gas is spin-polarized by a sheet of circularly-polarized resonant laser light. The degree and orientation of the atoms' (vector) polarization depends on the magnitude and orientation of the local magnetic field. The atoms are exposed to a homogeneous magnetic offset field $\boldsymbol{B}_0$ oriented along one of the cube's axes, and the fluorescence emitted by the polarized layer is imaged onto a CCD camera. When scanning the offset field from negative to positive values, each camera pixel detects a resonant change of intensity, centred at $B_0 = 0$ (ground state Hanle resonance, [2]). With the offset field set to the half-width point of the Hanle resonance any additional local field components $\delta\boldsymbol{B}$ along $\boldsymbol{B}_0$ will change the corresponding pixel signal by $\delta S \propto \delta B$. In this way the CCD image represents a map of δB's spatial distribution.

From the recorded magnetic field patterns one wishes to retrieve information on the spatial distribution of the magnetic sources producing the field pattern. Here we propose a method to infer 2D planar distributions from our MSIC recordings by inverse problem solving using a simulated annealing algorithm. Figure 1 shows the experimental setup together with the experimentally recorded magnetic field distribution in the laser sheet sensing plane. The magnetic field is produced by a coil made out of 3 rectangular current loops stacked to form an 'F'-shape equivalent distribution of magnetic dipoles that yields a smeared-out field pattern in the sensing plane. The corresponding distribution of point-like dipoles is superposed with the field-producing current loops in the object plane. Our primary interest is the localization of magnetized magnetic nanoparticles (MNPs). MNPs start to play an important role in biomedical screening and therapy and different approaches for localizing MNPs in biological tissues have been proposed.

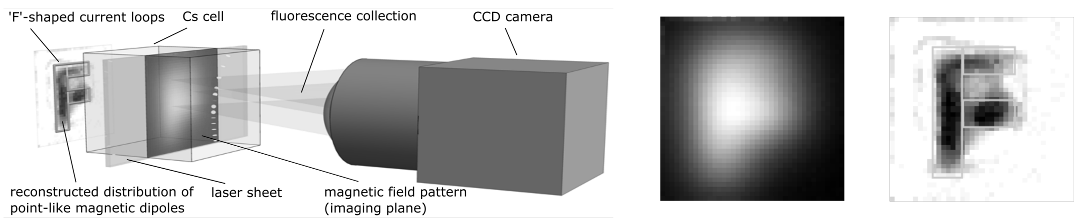

Fig. 1 Left: Experimental setup. Centre: Magnetic field map produced by an 'F'-shaped stack of 3 rectangular current loops. Right: Reconstructed distribution of point-like magnetic dipoles.

References

[1] V. Dolgovskiy, I. Fescenko, N. Sekiguchi, S. Colombo, V. Lebedev, J. Zhang, and A. Weis, *A Magnetic Source Imaging Camera*, Appl. Phys. Lett. **109**, 023505 (2016).

[2] N. Castagna and A. Weis, *Measurement of Longitudinal and Transverse Spin Relaxation Rates Using the Ground-State Hanle Effect*, Phys. Rev. A **84**, 053421 (2012).

P20

Multi-channel OPM-MEG during a visuo-motor task: induced responses and source localisation

Elena Boto[1], **Niall Holmes**[1], **George Roberts**[1], **James Leggett**[1], **Vishal Shah**[2], **Gareth R Barnes**[3], **Richard Bowtell**[1] **and Matthew J Brookes**[1]

1. Sir Peter Mansfield Imaging Centre, University of Nottingham, University Park, NG7 2RD Nottingham, UK
2. QuSpin Inc., 2011 Cherry Street, Unit 112, 80027 Louisville, CO, USA
3. Wellcome Trust Centre for Neuroimaging, Institute of Neurology, University College London, 12 Queen Square, WC1N 3BG London, UK

The excellent sensitivity and recent commercialisation (QuSpin Inc.) of optically-pumped magnetometers (OPMs) has inspired an interest in developing the next generation of Magnetoencephalography (MEG) systems. OPM-MEG would allow for a more flexible, user-friendly, less restrictive and non-cryogenic brain imaging tool as well as potentially higher signal-to-noise ratio (SNR) recordings.

Our previous work [1] focused on comparing the performance of a single OPM sensor against a state-of-the art SQUID-based system through repeating measurements. Here, a multi-channel array comprising 8 OPMs mounted in a 3D-printed, head-shaped scanner-cast [1] was used to perform OPM-MEG measurements.

A single subject performed a visuo-motor task: 45 trials of left index finger abduction during the presentation of a vertical grating shown for 2 s, followed by an 8 s fixation period. The experiment was performed three times: once in the CTF system (SQUID) and twice with the OPMs (once with the scanner-cast fixed relative to the room (OPM-restricted) and once where the subject was seated, but able to freely move their head (OPM-free-moving)). We used a time-frequency analysis of the radial magnetic field to evaluate the oscillatory (induced) response in sensor space in each experiment. We used a scalar beamformer (Synthetic Aperture Magnetometry – SAM [2]) to localise the neural networks responsible for beta frequency (13-30 Hz) power changes (decrease and post-movement rebound).

Panel A in Figure 1 shows the sensor-space induced response in the beta band, averaged across trials, for the three experiments. Only the channel which showed the largest response is shown for each experiment. As expected [3], we observe a decrease in amplitude during finger movement (0-2 s window) and a post-stimulus increase in amplitude (rebound) on movement cessation. Panel B shows the beamformer-reconstructed beta band time courses at the selected locations within the sensorimotor cortex. Note that locations selected include the peak decrease in power, the peak rebound, and a location with little task induced response.

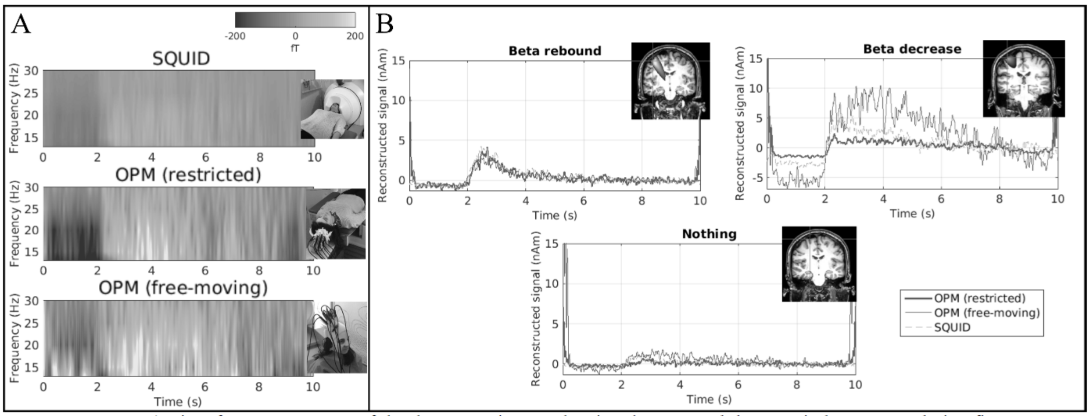

Fig. 1 A) Time-frequency spectra of the three experiments showing the expected decrease in beta power during finger abduction (0-2 s window) and the post-stimulus rebound. B) Beamformer-reconstructed time series at the peak locations of beta rebound and decrease, and also at a location displaying no brain activation.

We have shown the ability to beamform sources to the motor cortex using a multi-channel OPM array, even when the subject's head was unconstrained. Performance could be improved by nulling the ambient static (Earth's) magnetic field, which would potentially allow larger subject movements. OPM-MEG not only offers the advantage of bringing sensors closer to the brain, it also becomes a wearable device. This opens up a wealth of new paradigms and subject groups to investigate, potentially changing the scope of neuroscience experiments possible with MEG.

References

[1] E. Boto, S. S. Meyer *et al.*, *A new generation of magnetoencephalography: Room temperature measurements using optically-pumped magnetometers*, NeuroImage **149**, 404 (2017).

[2] S. E. Robinson and J. Vrba, *Functional neuroimaging by synthetic aperture magnetometry (SAM)*, In: T. Yoshimoto, M. Kotani, S. Kuriki, H. Karibe, N. Nakasato, editors. Recent Advances in Biomagnetism. Sendai, Japan: Tohoku University Press; 302 (1999).

[3] S. E. Robson, M. J. Brookes *et al.*, *Abnormal visuomotor processing in schizophrenia*, NeuroImage: Clinical **12**, 869 (2016).

Designing a cryogen-free MEG system for hippocampal recording

Sofie S. Meyer[1,2], **Andrew Levy**[2], **Matt Everatt**[3], **Mark Lim**[4], **Tim M. Tierney**[2], **James Bonaiuto**[2], **Yoshihito Shigihara**[2], **Elena Boto**[5], **Neil Burgess**[1,6], **Matthew J. Brookes**[5], **Richard Bowtell**[5], **Gareth R. Barnes**[2]

1. UCL Institute of Cognitive Neuroscience, University College London, London, WC1N 3AR, UK
2. Wellcome Trust Centre for Neuroimaging, Institute of Neurology, University College London, London, WC1N 3BG, UK
3. S4S (UK) Limited & Smilelign Ltd, 151 Rutland Road, Sheffield, S3 9PT, UK
4. Chalk Studios Ltd., 14 Windsor Street, London N1 8QG, UK
5. Sir Peter Mansfield Imaging Centre, School of Physics and Astronomy, University of Nottingham, Nottingham NG7 2RD, UK
6. UCL Institute of Neurology, University College London, London, WC1N 1PJ, UK

The hippocampus is critical for healthy brain function. It enables functions such as memory and navigation by co-ordinating neuronal activity across brain regions on a sub-second timescale. The hippocampus is also where many degenerative disorders such as dementia, as well as drug-resistant epilepsy, commonly strike. Currently, planning for surgical removal of drug-resistant epileptic foci includes a highly invasive additional surgical procedure where electrodes are placed inside the hippocampus for direct monitoring of electrophysiological activity. Therefore, a non-invasive and temporally resolved alternative method for recording from this deep structure (Fig. 1A) would be an attractive tool for both clinical and basic research.

To meet this goal, we propose building a wearable array of OPM sensors directly onto the subject, with the spatial configuration of sensors optimised to detect hippocampal signals. A key advantage of the new OPM sensors is that they do not necessarily have to be placed on the scalp surface. Here we investigate and quantify the extent to which sensors placed close to the roof of the mouth would be advantageous for OPM recording of hippocampal signals. To do this, we simulate hippocampal activity [1] to assess the possible field patterns at the scalp.

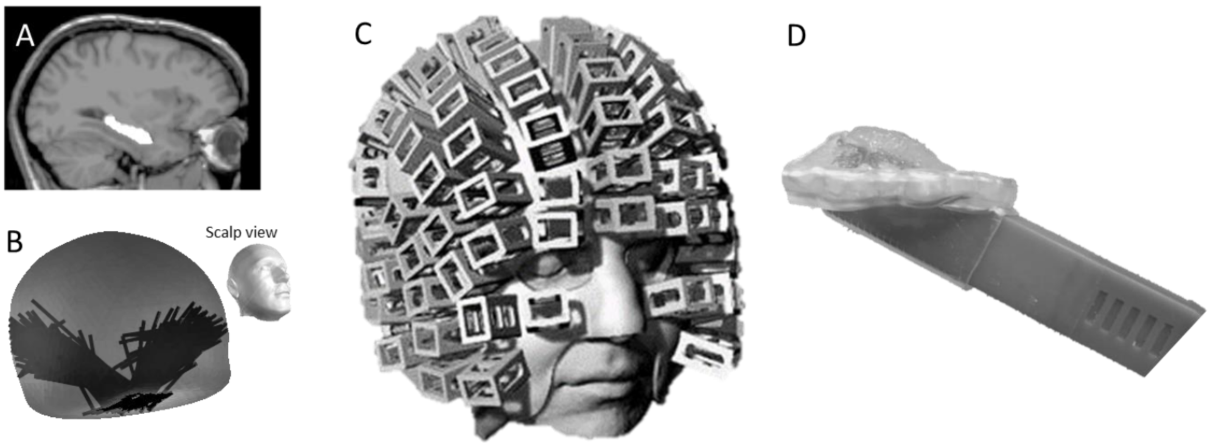

Fig. 1 OPM sensor configuration for hippocampal recording. **A)** Magnetic Resonance Image showing location of the hippocampus in white. **B)** For each hippocampal surface location, a sensitivity profile (lead-field) for the radial fields is calculated for an OPM sensor array placed 6.5 mm from a surface comprising the scalp and extending down over the roof of the mouth. For each hippocampal source, a line is drawn linking the field maxima and corresponding minima. Note that these pairings are almost exclusively temporal lobe-mouth pairs. **C)** Sample 3D printed scanner-cast for measuring hippocampal activity from the temporal lobes. The OPMs can hereby be stabilized with respect to one another and the brain's anatomy. **D)** 3D printed device for stabilizing and orienting OPM in the roof of the mouth.

Our modelling suggests that OPM arrays which can be worn can give a factor 4 signal detection advantage over conventional MEG due not only to the decreased stand-off, but also due to the flexibility in sensor placement. Fig. 1B shows the RMS lead-field profile across the scalp surface and extending down over the roof of the mouth with maxima and minima pairings (black lines) occurring almost exclusively between the mouth and sides of the head (Fig. 1B). We are now designing optimal wearable arrays for non-invasive hippocampal imaging ([2], Fig. 1C), including the placement of sensors inside the mouth (Fig. 1D).

References

[1] S.S. Meyer, H. Rossiter, M. J. Brookes, M. W. Woolrich, S. Bestmann, G. R. Barnes, *Using generative models to make probabilistic statements about hippocampal engagement in MEG*, Neuroimage **149**, 468 (2017).

[2] E. Boto*, S. Meyer*, V. Shah, O. Alem, S. Knappe, P. Kruger, M. Fromhold, M. Lim, P. G. Morris, R. Bowtell, G. R. Barnes, M. J. Brookes, *A New Generation of Magnetoencephalography: Room Temperature Measurements using Optically-Pumped Magnetometers*, Neuroimage **149**, 404 (2016).

P22

Estimating the geometry of OPM sensor arrays relative to the human brain

L. Duque-Muñoz[1], J. D. López[1], J. F. Vargas-Bonilla[1], T. M. Tierney[3], S. S. Meyer[3], E. Boto[2], R. Bowtell[2], M. J. Brookes[2], G. R. Barnes[3]

1. SISTEMIC, Department of Electronic Engineering, Universidad de Antioquia Medellín, Colombia
2. Sir Peter Mansfield Imaging Centre, University of Nottingham, University Park, NG7 2RD Nottingham, UK
3. Wellcome Trust Centre for Neuroimaging, University College London, London, WC1N 3BG, UK

Optically-pumped magnetometers (OPMs) have reached sensitivity levels that make them viable and wearable alternatives to traditional superconducting technology for magnetoencephalography (MEG). Here we address the problem of constructing accurate forward models that describe the expected sensor signal given activity in a particular brain region. One problem is the uncertainty in sensor position and orientation with respect to the brain. Previous work [1, 2, 3] has shown that these errors place a limit on the accuracy of any estimate of neuronal current flow. Here we used data based on OPM recordings using a scanner-cast – a 3D printed helmet based on a subject's MRI scan in which the sensor locations and orientations with respect to the cortical anatomy are known. We then perturb the sensor geometry (via simulation) and see if we can use analytic model comparison methods to estimate the true sensor geometry. The aim is to move towards wearable arrays that do not have to be contained within a rigid helmet.

We used single channel OPM data from a median nerve stimulation experiment [3]. First, we looked at the sensitivity of our models to random perturbations (of -20 to +20 degrees) in the orientation of each channel (Fig. 1a). Second, we moved the whole array in an arc around the head from -20 to 20 mm (Fig 1c). We scored each model using (negative variational) Free energy (a proxy for model evidence) as an objective function [4].

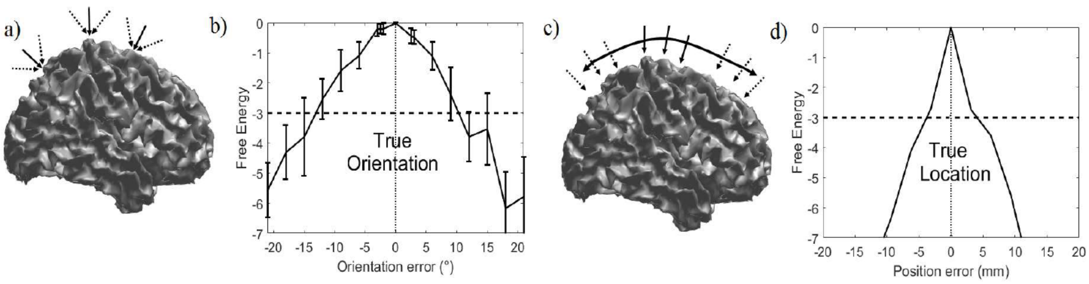

Fig. 1 a) Each individual OPM channel was randomly perturbed in orientation (dotted arrows). b) Free Energy vs orientation error, dotted line marks the significance threshold of -3 on a log scale, models below this line (with greater than +/-11 degrees of error) are significantly (20 times) less likely. c) Here the whole OPM array was moved relative to the brain. d) Free Energy vs change in array position, array location errors of greater than 5mm are significantly less likely and we have analytically estimated the true array location (at zero).

Results In Fig 1b) we show the sensitivity to individual channel orientation error. Note that the best model (as judged by the data fit) also accords with the true sensor orientations. In Fig 1d) we found that we are able to recover the true position of an OPM sensor array with respect to the brain and we are able to confidently (p¡0.05) reject array locations with more than 5mm of error.

We have shown that it is possible to accurately estimate sensor array geometry based on brain data without the need for fiducial markers or subject-specific helmets. This paves the way towards wearable and flexible array geometries which can be recovered through optimization post-hoc.

References

[1] A. Hillebrand and G. R. Barnes, *The use of anatomical constraints with MEG beamformers*, NeuroImage **20**, 2302 (2003).

[2] E. Boto, R. Bowtell, P. Krüger, T. M. Fromhold, P. G. Morris, S. S. Meyer, G. R. Barnes, and M. J. Brookes, *On the potential of a new generation of magnetometers for MEG: a beamformer simulation study*. PLoS One **11**, e0157655 (2016).

[3] E. Boto, S. S. Meyer, V. Shah, O. Alem, S. Knappe, P. Kruger, M. Fromhold, M. Lim, P. M. Glover, P. G. Morris, R. Bowtell, G. R. Barnes, and M. J. Brookes, *A new generation of magnetoencephalography: Room temperature measurements using optically-pumped magnetometers*, NeuroImage **149**, 404 (2017).

[4] K. Friston, J. Mattout, N. Trujillo-Barreto, J. Ashburner, and W. Penny, *Variational free energy and the Laplace approximation*, NeuroImage **34**, 220 (2000).

Towards wearable OPM-MEG: Using bi-planar field nulling coils to allow subject movement

Niall Holmes[1], Elena Boto[1], George Roberts[1], Vishal Shah[2], James Leggett[1], Matthew J Brookes[1], Gareth R Barnes[3] and Richard Bowtell[1]

1. Sir Peter Mansfield Imaging Centre, School of Physics and Astronomy, University of Nottingham, Nottingham, UK
2. QuSpin Inc., 2011 Cherry Street, Unit 112, Louisville, CO 80027, USA
3. Wellcome Trust Centre for Neuroimaging, Institute of Neurology, University College London, 12 Queen Square, London, UK

In conventional MEG measurements subjects are required to remain still in the MEG helmet (i.e. movement must be kept to less than 5mm over a scan that may take up to 30 minutes), this restricts subject groups which can be studied and the tasks that can be performed. OPM-based MEG [1], Fig 1a, could allow free movement of the subject during a recording. However, even inside a Magnetically Shielded Room (MSR) sensor movement induces large field variations which renders OPM data unusable, Fig 1b (solid line). Here large bi-planar coils were designed to produce homogenous fields that nulled the static field components ($\sim 20nT$) inside the MSR, thus allowing head movement during recordings. Coils on two planes placed either side of the subject were designed using methods adapted from MRI gradient coil design [2, 3]. The current distribution $\boldsymbol{J}$ is confined to two planar surfaces $|x|,|y| < L$ at $z = \pm a$ and described using the stream function, S defined as $\boldsymbol{J} = \nabla S \times \hat{z}$. S is parameterised as a two-dimensional Fourier series with symmetry defined by the target field as:

$$S = \sum_{n,m} \lambda_{n,m} \begin{cases} \sin\frac{m\pi x}{L}\cos\frac{(n-1/2)\pi y}{L} & \text{for } B_x \text{ coil} \\ \cos\frac{(n-1/2)\pi x}{L}\sin\frac{m\pi y}{L} & \text{for } B_y \text{ coil} \\ \cos\frac{(m-1/2)\pi x}{L}\cos\frac{(n-1/2)\pi y}{L} & \text{for } B_z \text{ coil} \end{cases} \tag{2}$$

Values of $\lambda_{n,m}$ are then chosen to minimise $\sum_t [B(r_t) - B_{targ}]^2 + \omega P$. Here $\boldsymbol{r}_t$ are the locations where a homogeneous field is required, B_{targ} is the target field and P is a tuneable power term. $\boldsymbol{B}$ is calculated from:

$$\mathbf{B} = \mu_0\{[ik_x\hat{\mathbf{x}} + ik_y\hat{\mathbf{y}}]^{sinh}_{cosh}(k_r z) - k_r\hat{\mathbf{z}}^{cosh}_{sinh}(k_r z)\}\tilde{S}e^{-k_r a} \tag{3}$$

$\tilde{\boldsymbol{B}}$ and $\tilde{S}$ are the two-dimensional Fourier transforms of the field and stream function with respect to x (k_x) and y (k_y) and $k_r = \sqrt{k_x^2 + k_y^2}$. The *sinh/cosh* terms correspond to the situation where S has the same/opposite sign on the two planes. The coil wire paths, Fig. 1c, are obtained from contours of S.

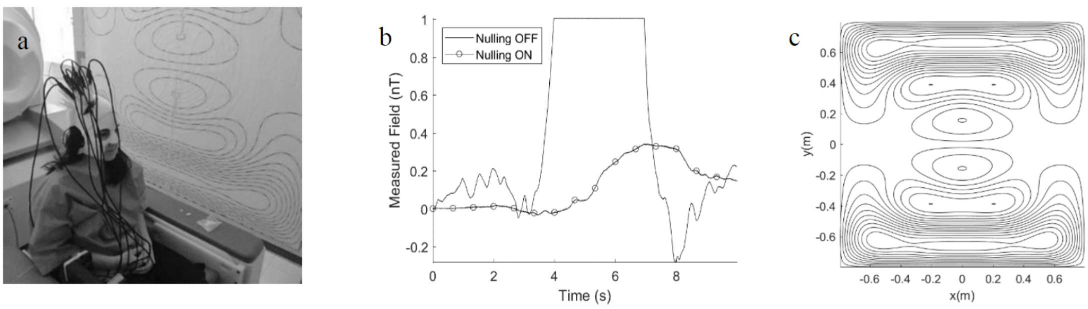

Fig. 1 (a) Subject seated between coil planes with OPMs worn in a 3D printed scanner-cast. (b) Magnetic field data recorded from a single sensor when the subject moves their head while taking a drink. Results shown with the nulling coils OFF and ON. Without nulling the OPMs go out of range. (c) Wire paths for the B_y coil. The B_x coil roughly corresponds to a 90° rotation of this coil about the z-axis.

The coils are 1.6 x 1.6 m^2 in size and produce homogeneous fields over a central 40 x 40 x 40 cm^3 volume. Coils were constructed by taping 0.56mm diameter copper wire onto sheets of MDF in layers. The coils are controlled with LabVIEW to null the vector field based on the signals from reference OPM sensors positioned around the subject's head. The resulting setup allows the subject to perform simple movements during a scan such as stretching, shaking the head or having a drink of water, Fig 1b (circled line). This work shows the potential for OPM-MEG experiments in subject groups that would have difficulty remaining still such as infants or individuals with movement disorders. Field gradient coils, which will allow a higher degree of field nulling over the sensor array, are now being constructed.

References

[1] E. Boto, S. Meyer *et al.*, *A new generation of magnetoencephalography: Room temperature measurements using optically-pumped magnetometers*, NeuroImage **149**, 404 (2017).
[2] K. Yoda, *Analytical design method of self shielded planar coils*, J. Appl. Phys. **67**, 191 (1990).
[3] J. W. Carlson *et al.*, *Design and evaluation of shielded gradient coils*, Magn. Res. Med. **26**, 4349 (1992).

P24

Exploring Crosstalk in an Optically Pumped Magnetometer Array for Magnetoencephalography – Simulation and Experiment

George Roberts[1], Elena Boto[1], Niall Holmes[1], James Leggett[1], Vishal Shah[3], Gareth R. Barnes[2], Richard Bowtell[1], Matthew J. Brookes[1]

1. Sir Peter Mansfield Imaging Centre, University of Nottingham, Building 18 University Park, Nottingham, UK
2. Wellcome Trust Centre for Neuroimaging, Institute of Neurology, University College London, 12 Queen Square, London
3. QuSpin Inc. 2011 Cherry Street, Unit 112 Louisville, CO 80027, USA

The recent development of integrated sensor packages ($\sim$1cm^2 cross section, 3x3x3mm sensing volume) for highly sensitive magnetometry (<15fT noise floor in 1-100 Hz frequency band, dynamic range of $\pm$5nT) has allowed fabrication of an OPM array for use in magnetoencephalography (MEG) [1]. Such an array necessarily brings the sensors into close proximity; since each sensor uses a set of on-board coils for reduction of the static field in the sensing volume and for the field modulation used in measurement, it is conceivable that the stray field from each sensor may produce interference in proximal sensors. We present theoretical and experimental evidence that these fields are small enough within our parameters of operation to be safely ignored for the purposes of MEG source reconstruction.

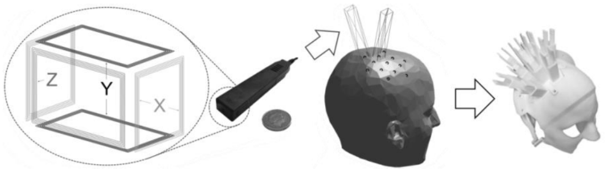

Fig. 1 Three pairs of coils (left) are found in the sensor head. Sensors are placed on a 3D printed scanner helmet, designed (using structural MRI) to fit a subjects scalp. Interference between sensors is then computed.

A discrete element Biot-Savart computation with 360 elements per current loop was used to calculate stray B-fields produced in the sensing volume of an adjacent sensor, for separations of 2-5cm. The known coil geometry and relative location of the sensing volumes was used to produce a physically accurate model. The coil current was chosen so that the maximum field produced by each coil at the cell centre (termed the base field) was 100pT. Relative strength is defined as the ratio of the absolute value of the perturbing coil's stray field to that of the base field. By calculating the vector sum of the base field $\mathbf{B}_{base}(\mathbf{r})$ and stray field $\mathbf{B}_{perturb}(\mathbf{r})$, the effective angle deflection from a proximal sensor can also be calculated:

$$\theta_{deflect} = \cos^{-1}\left(\frac{\mathbf{B}_{base}(\mathbf{r})\cdot\mathbf{B}_{sum}(\mathbf{r})}{||\mathbf{B}_{base}(\mathbf{r})||\cdot||\mathbf{B}_{sum}(\mathbf{r})||}\right) \text{ where } \mathbf{B}_{sum}(\mathbf{r}) = \mathbf{B}_{base}(\mathbf{r}) + \mathbf{B}_{perturb}(\mathbf{r}) \quad (4)$$

These quantities were determined over a variety of conditions: distance between sensors, all sets of interacting coil pairs (X-X, Y-X, Z-Y etc.), rotation around the long axis of the sensor, and accurate location in our MEG array. Simulations showed that the crosstalk from the modulation on the sensitive radial axis (Z) is small: 0.3° deflection, 2.5% relative strength at closest approach. Experimental validation was carried out using a 3D printed scanner cast, with locations corresponding to those in Fig.1. By driving the coils with a known frequency, the relative size of the field received in neighbouring sensors was determined from the ratio of the peaks; the mean was found to be 1.6$\pm$0.3 % and the maximum was 3% - approximately in line with simulations. The array will produce significantly higher crosstalk between the X, Y and Z coils which will need to be taken into account when using the OPMs in dual-axis mode (measuring two perpendicular field components).

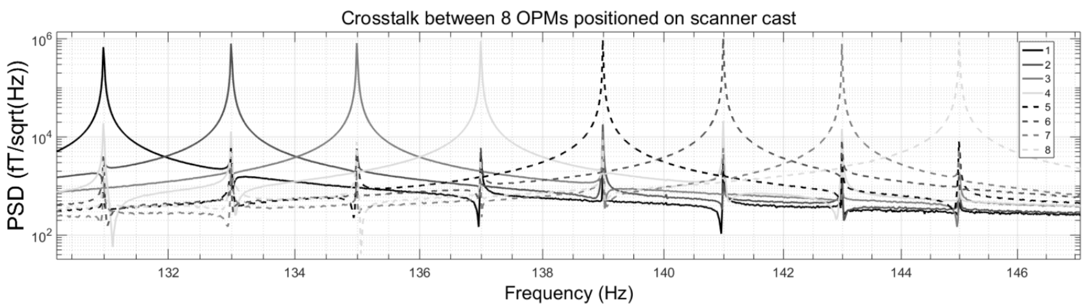

Fig. 2 Each of the 8 Z (radial) coils produces a field oscillating at a known frequency from 131-145Hz. The power spectra from 8 sensors shows crosstalk between sensors – the worst case relative interference size is 3%.

References

[1] E. Boto *et al.*, *A new generation of magnetoencephalography: Room temperature measurements using optically-pumped magnetometers*, NeuroImage **149**, 404 (2017).

Accuracy and Reliability of a multi-channel OPM MEG System for pre-surgical planning

Tim M. Tierney[1], Sofie Meyer[2], Leonardo Duque-Muñoz[3], Jose D. López[3], James Osbourne[4], Vishal Shah[4], Richard Bowtell[5], Matthew J. Brookes[5], Gareth R. Barnes[1]

1. Wellcome Trust Centre for Neuroimaging, University College London, London, UK, WC1N 3BG
2. Institute of Cognitive Neuroscience, University College London, London, UK, WC1N 3AZ
3. Departamento de Ingeniería Electrónica, Universidad de Antioquia, Medellín, Colombia
4. QuSpin Inc., 2011 Cherry Street, Unit 112, 80027 Louisville, CO, USA
5. Sir Peter Mansfield Imaging Centre, University of Nottingham, UK, NG7 2RD

Clinically, electrical stimulation of the median nerve is used to located primary sensory cortex during surgical planning [1]. Many of the patient groups (such as children) who would benefit from such surgical planning are however poorly served by conventional cryogenic MEG systems, built for adult head sizes. This is a barrier to the successful translation of MEG in this setting. Optically Pumped Magnetometers (OPMs) give us the possibility to not only position the sensors to fit any head size, but also offer increased signal amplitude relative to SQUIDs [2]. Here we present the first simultaneous multi-channel recordings of this median nerve response with a view to assessing accuracy and reliability in a clinical setting.

We recorded MEG data using OPMs housed in a 3D printed scanner-cast positioned over the subject's primary somatosensory cortex [2]. We made 13 simultaneous radial field measurements at 6.5mm offset from the scalp surface using QuSpin sensors within a mu-metal shielded room sited in central London with approximately 20nT residual static field. Data from 8 SQUID magnetometer channels were recorded simultaneously and used for reference noise cancellation. We used a non-linear optimization to explain the averaged recorded data using a single dipolar source. The localisation reliability was assessed using a bootstrapping procedure.

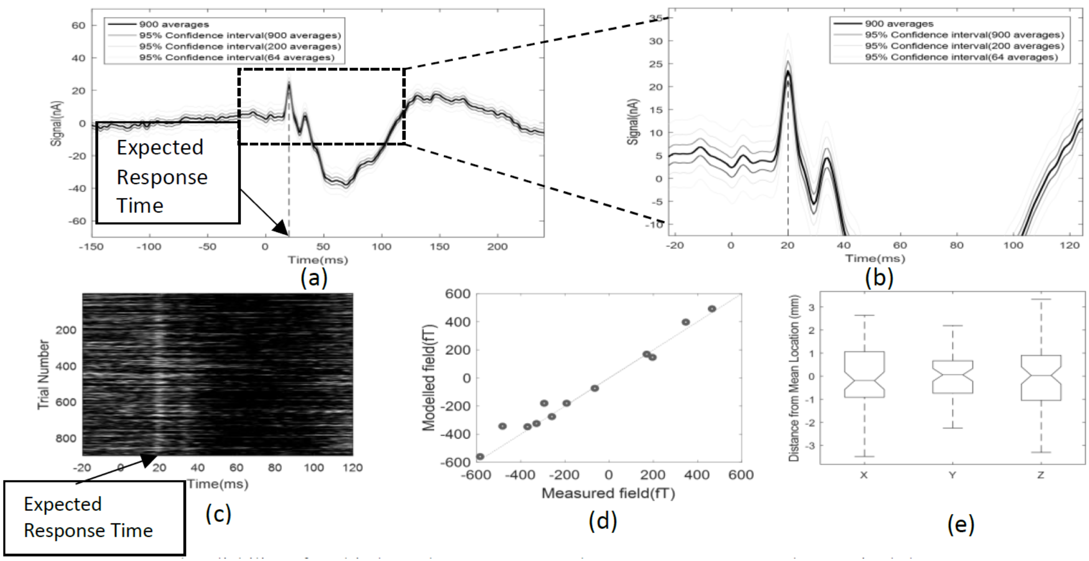

Fig. 1 Accuracy and Reliability of multi-channel OPM system. The OPM MEG system characterised the mean N20 response magnitude ($\sim$23 nAm) with $\sim$ 4nAm margin of error (a). The N20 response is expected to occur approximately 20ms post stimulation, which the OPM system accurately detects (b). The pattern is also visible at a single trial level (c). A single dipole fit is able to accurately model the observed magnetic field (d). The observed localisation of the dipole is reliable within $\sim$ 2-3mm (e).

Panels a, b shows the estimated dipole moment in primary sensory cortex as a function of time. With confidence intervals as a function of the number of averaged trials. Panel c shows the data at a single trial level. Panel d shows that a single dipole fit was able to accurately model the measured field with standard error of $\sim$7%. The mean location was estimated at coordinate (MNI): 50, -22, 46 with variability $\sim$ 2-3mm (Panel e) within primary sensory cortex. These results suggest that OPMs could provide accurate, reliable and cryogen-free clinically useful information.

References

[1] C. C. Wood, D. D. Spencer, T. Allison, G. McCarthy, P. D. Williamson, and W. R. Goff, *Localization of human sensorimotor cortex during surgery by cortical surface recording of somatosensory evoked potentials*, Journal of Neurosurgery **68** (1), 99 (1988).

[2] E. Boto *et al., A new generation of magnetoencephalography: Room temperature measurements using optically-pumped magnetometers*, NeuroImage **149**, 404 (2017).

P26

High subject throughput individualized OPM sensor array

T. H. Sander[1], T. Yang[2], J. Voigt[1], T. Middelmann[1], L. Trahms[1]

1. Physikalisch-Technische Bundesanstalt, Abbestraße 2-12, 10587 Berlin, Germany
2. Institute of Medical Psychology and Human Science Center, Ludwig-Maximilian Universität, 80336 München, Germany

Recently commercial single unit OPM magnetometer sensors became available [1] with a cross section of 13x19 mm and dual direction measurement capabilities. With these sensors, a MEG array can be tailored to a subject's or patients' individual anatomy as shown in [2]. A suitably segmented anatomical data set such as obtained from MRI or CT is used as input for the generative production (3D printing) of a high precision multichannel sensor holder.

Here we propose a rapid process to obtain medium precision individualized biomagnetic sensor arrays. Instead of relying on costly MRI or CT we use a 3D geometry scanner based on ultrasound technology [3]. A point cloud describing a surface is obtained by a manual operator placing a pen on successive surface points. Anatomical landmarks such as LPA, RPA, and Na are included as well. This point cloud is then input into a 3D design software (e.g. OPENSCAD [4]), a 3D printable surface is derived, and sleeves suitable for the sensors are added and the structure is printed. Printing of this structure takes up to 24 hours on a professional entry FDM printer. Therefore, subjects must come twice to the biomagnetic laboratory, but the costs for the sensor array holder are very low.

We show preliminary four channel data for MCG measured in a two layer magnetically shielded room (Ak3b, Vacuumschmelze, Hanau) at walk-in condition (door not closed) and auditory MEG data obtained in the seven layer magnetically shielded room BMSR2 of PTB. The Ak3b was demagnetized following established procedures [5] and the remnant field at the measurement position was (Bx, By, Bz) = (15, 12, 9) nT, the remnant field in the BMSR 2 was below 1 nT.

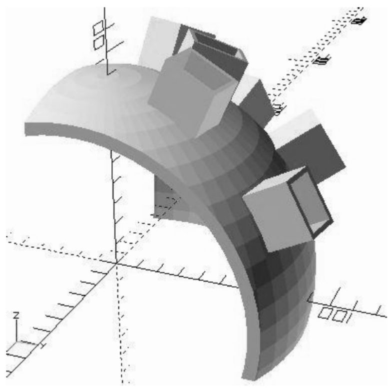

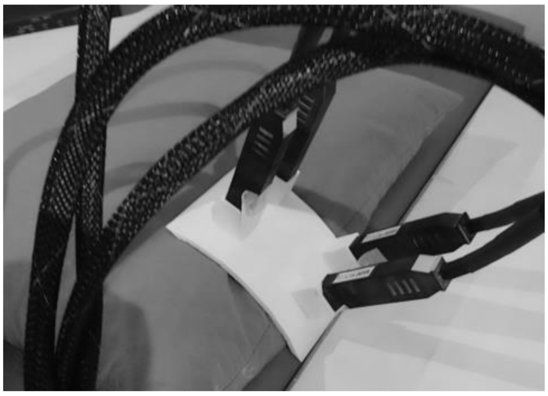

Fig. 1 (left) Schematic 3D design for the generative manufacture of an MEG OPM sensor array holder. (right) Picture of the four channel MCG holder.

Ease of measurement attributable to the cryogen free commercial OPM sensors is complemented by the ease of sensor holder design described here. We envisage this procedure mainly for exploratory cognitive research studies such as frequently performed in psychology and for screening of risk groups in cardiology. Clearly newer scanner technologies such as the Kinect [6] might replace the currently used device to obtain a 3D representation of the body surface.

Financial support from the European Metrology Research Programme (EMRP) and European Metrology Programme for Innovation and Research (EMPIR) is gratefully acknowledged. The EMRP and EMPIR are jointly funded by the participating countries within EURAMET and the European Union.

References

[1] QUSPIN: Zero-field magnetometer QZFM (https://quspin.com/products-zf-opm/) [accessed on 13.05.2017] (2017).

[2] E. Boto, S. S. Meyer, V. Shah, O. Alem, S. Knappe, P. Kruger, T. M. Fromhold, M. Lime, P. M. Glover, P. G. Morris, R. Bowtell, G. R. Barnes, M. J. Brookes, *A new generation of magnetoencephalography: Room temperature measurements using optically-pumped magnetometers*, NeuroImage **149**, 404 (2017).

[3] Zebris Medical: ELPOS system - discontinued (https://www.zebris.de/) [accessed on 13.05.2017] (2017).

[4] OPENSCAD (http://www.openscad.org/) [accessed on 13.05.2017] (2017).

[5] I. Altarev *et al.*, *A magnetically shielded room with ultra-low residual field and gradient*, Rev. Sci. Instrum. **85**, 075106 (2014).

[6] Kinect™ (http://www.xbox.com) (2017).

Multivariate statistical analysis of OPM sensor array data

T. H. Sander[1], O. Alem[2,3], J. Kitching[2], L. Trahms[1], S. Knappe[2,3]

1. Physikalisch Technische Bundesanstalt, Abbestrasse 2-12, 10587 Berlin, Germany
2. National Institute of Standards and Technology, 325 Broadway, Boulder, CO 80305 USA
3. University of Colorado, Boulder, CO 80309 USA

Recently prototype multichannel OPM magnetometer sensor arrays became available with 20 and more channels [1,2] consisting of individual sensor heads. With these arrays, multichannel data can be recorded allowing a combined analysis in the spatial and temporal domain to answer the basic questions of biomagnetism where and when a current was flowing in the body. Before such a result can be obtained, many signal processing steps are needed starting with an improvement of the signal-to-noise ratio (SNR). For evoked brain fields (Magnetoencephalography, MEG) or cardiac fields (Magnetocardiography, MCG) data epoch averaging is the most obvious method. But even before averaging statistical methods can be applied to the raw data to improve SNR and independent component analysis (ICA) is a well-established procedure for this. ICA is a family of many different algorithms and one approach [3,4] relies on decomposing signals into components with maximally different spectral signatures in the time domain.

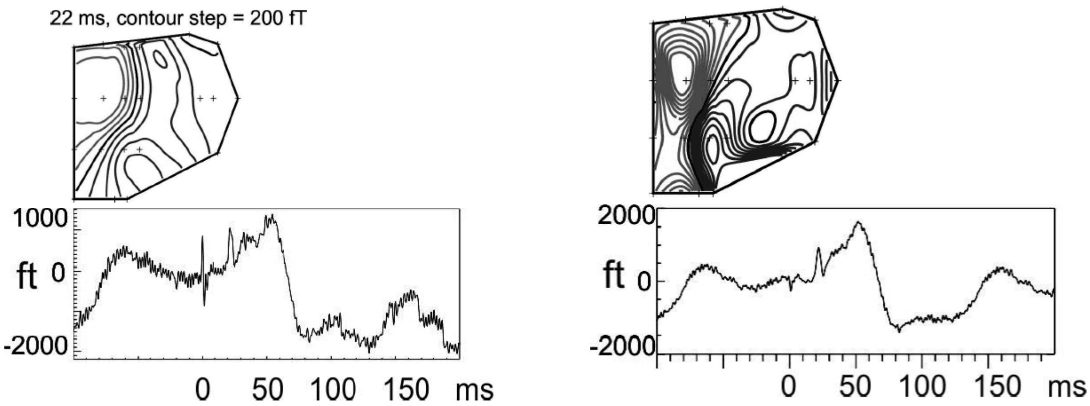

Fig. 1 (left) N20m map and time series obtained through averaging of 1300 responses. (right) N20m with improved SNR obtained from ICA de-noised raw data.

Here the ICA is applied to somatosensory MEG data obtained using the 21 channel OPM array described in [2]. Figure 1 (left) shows the averaged MEG response to somatosensory stimulation. An electrical pulse was applied at the wrist at 0 ms and at 20 ms the first brain response is visible as the second sharp peak in the time series. The map of the multichannel data at 22 ms ist shown above the time series. After application of ICA (Fig. 1, right) the averaged MEG response shows a much reduced noise ripple compared to the original result. The peak at 0 ms is much weaker, while the peak at 20 ms is preserved through selection of a brain response ICA component. The peak at 0 ms is a so called technical stimulus artefact and it is spatially not related to the brain response at 20 ms. The ICA field map (right) is more irregular compared to the averaged map (left), but it shows the overall dipolar structure. As ICA is a statistical method it is not informed of the structure of magnetic fields and often noisier maps result as a trade-off. The overall results are very similar to SQUID MEG obtained using somatosensory stimulation and ICA [5].

To summarize, statistical methods such as ICA introduced to SQUID signal processing have similar benefits when applied to multichannel OPM data. Besides the de-noising capabilities shown here ICA can help during the development of OPM array systems to assess signal quality.

References

[1] G. Bison, N. Castagna, A. Hofer, P. Knowles, J. L. Schenker, M. Kasprzak, H. Saudan, and A. Weis, *A room temperature 19-channel magnetic field mapping device for cardiac signals*, Appl. Phys. Lett. **95**, 173701 (2009).

[2] O. Alem, R. Mhaskar, R. Jiménez-Martínez, D. Sheng, J. LeBlanc, L. Trahms, T. Sander, J. Kitching, S. Knappe, *Magnetic field imaging with microfabricated optically-pumped magnetometers*, Opt. Express **25**, 7849 (2017).

[3] A. Ziehe, K.-R. Müller, *TDSEP - an efficient algorithm for blind separation using time structure*, In L. Niklasson *et al.* (eds.), Proceedings of the 8th ICANN, 675, Springer (1998).

[4] A. Belouchrani, K. Abed-Meraim, J.F. Cardoso, E. Moulines, *A blind source separation technique based on second-order statistics*, IEEE Trans. Sig. Proc. **45**, 434 (1997).

[5] T. H. Sander, M. Burghoff, G. Curio, L. Trahms, *Single evoked somatosensory MEG responses extracted by time delayed decorrelation*, IEEE Trans. on Signal Processing **53**, 3384 (2005).

P28

Exploiting Optically Pumped Magnetometer's Flexibility To Optimize The Problem Conditioning In Magnetorelaxometry Imaging

Aaron Jaufenthaler, Daniel Baumgarten

Institute of Electrical and Biomedical Engineering, University for Health Sciences, Medical Informatics and Technology, Eduard Wallnöfer-Zentrum 1, 6060 Hall in Tirol, Austria

Magnetic nanoparticles offer a large variety of promising applications in medicine thanks to their exciting physical properties. For most applications it is very important to know the quantitative spatial distribution of the particles. This distribution can be obtained by means of magnetorelaxometry (MRX) imaging [1]. Here, the response of the magnetization of the nanoparticles to sudden changes of an external magnetic field is measured and the distribution is reconstructed by solving an inverse problem. The particles are usually aligned by the magnetic field of excitation coils. After switching off this field, the magnetic relaxation field is measured. To date, SQUID sensors are predominantly used. Since the latest optically pumped magnetometers (OPMs) reach comparable sensitivities to SQUIDs in the order of 1 $\mathrm{fT}/\sqrt{\mathrm{Hz}}$ [1], OPMs may be used in relaxometry imaging. With respect to their flexible positioning, improvements in MRX imaging are expected. Imaging using magnetorelaxometry is typically an underdetermined inverse problem and can be written as $\mathbf{L} \cdot \mathbf{c} = \mathbf{B}$, where $\mathbf{L}$ is the lead-field matrix (which depends on geometrical and magnetical properties of the system), $\mathbf{c}$ is the vector of (unknown) particle concentrations and $\mathbf{B}$ is the vector of measurement data. When solving this problem the conditioning of the matrix $\mathbf{L}$ is essential, because good conditioning is a major factor of the obtained reconstruction quality. Recently, row dependency (RD) and column dependency (CD) have been proposed as novel figures of merit to evaluate and compare the condition of the matrix $\mathbf{L}$ [2]. RD is employed in case of a underdetermined system whereas CD is used in case of a overdetermined system, respectively. In contrast to other figures of merit, RD and CD are capable of comparing between different sensor arrays. It should be noted that the result is not affected by row or column scaling, respectively. RD is computed as follows where n denotes the number of rows of $\mathbf{L}$, $\mathbf{I}_i$ denotes the i-th row of $\mathbf{L}$ and $||\cdot||$ denotes the L_2 norm:

$$RD = \frac{\sum_{i=1}^{n-1} \sum_{j=i+1}^{n} \left| 90^\circ - \left| \cos^{-1}\left(\frac{\mathbf{I}_i \cdot \mathbf{I}_j}{||\mathbf{I}_i|| \cdot ||\mathbf{I}_j||} \right) \right| \right|}{\frac{n \cdot (n-1)}{2}}$$

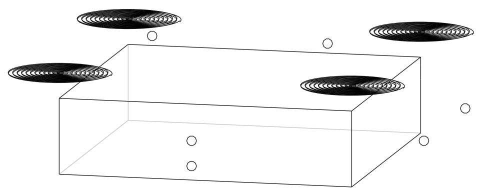

Fig. 1 exemplary target volume with activation coils and magnetic field sensors (dots) placed around the target.

In this work, we investigate the benefits of using OPMs in MRX imaging with respect to their flexible positioning by studying the condition of the underlying inverse problem. The simulation setup consists of a target volume, four activation coils and a variable, but defined number of magnetometers (304, 32, 16, 12, 8 or 4 magnetometers aligned in z-direction). It should be noted that for the simulations, we don't distinguish between SQUIDs and OPMs, since their parameters don't affect the lead field matrix $\mathbf{L}$. The four activation coils have a diameter of 170 mm and are modeled as Archimedean spirals with 864 segments each. Magnetization is done using sequential activation with a current of 1.2 A. Variations of the target volumes, the voxel size, position of the activation coils and the amount and position of the magnetometers were compared and investigated to optimize the reconstruction quality by computing the lead field matrix and the corresponding row dependency for each of the possible combinations mentioned. The parameters were selected to result in an overdetermined system in every case.

Our results show that the illness of the associated problem can be improved by placing the sensors at a minimum distance from the target volume. By comparing different sensor combinations we found, that using 12 sensors – where two sensors are located near each cube surface – results in a much lower (and thus better) row dependency, compared to the other setups, e. g. a RD of ≈ 24 by using 304 sensors and a RD of ≈ 7 using 12 sensors. Thus, the simulations demonstrate that exploiting OPM's position flexibility can be used to optimize the conditioning of the underlying problem and therefore the quantitative spatial reconstruction quality of the magnetic particle concentrations.

References

[1] M. Liebl *et al.*, *In-vivo quantification and characterization of magnetic nanoparticle distributions using magnetorelaxometry*, Biomedical Engineering / Biomedizinische Technik **60**(5), 427 (2015).

[2] B. Petković, *Assessment of Linear Inverse Problems in Magnetocardiography and Lorentz Force Eddy Current Testing*, Ph.D. dissertation, TU Ilmenau (2013).

Helium-based OPM for room-temperature bio-magnetic measurements

Gaëtan Lieb

High Performances Laboratory, CEA, MINATEC Campus, 17 rue des martyrs, 38054 Grenoble, France

Measuring the magnetic field generated by the electrical activity from the heart or from the brain requires a high sensitivity magnetometer. **Helium-based optically pumped magnetometers (OPM)** allow such a measurement to be performed at **room temperature**, without any thermal insulation. In this poster we will introduce the physical principles behind this sensor, which are based on parametric resonance in alignment. We will show recent proof of concept of heart and brain signal acquisition. We will also introduce ongoing developments for miniaturizing the device and operating it in an all-optical fashion in order to build sensor arrays.

P30

Can Optically Pumped Magnetometers (OPM) Capture Neuromagnetic Activity of Peripheral Nerves and the Spinal Coord?

Philip Broser[1], Diljit Singh Kajal[2,3], Adham Elshahabi[2,3,4], Christoph Braun[3,5,6]

1. Department of child neurology, Children's Hospital of Eastern Switzerland, Claudiusstrasse 6, 9006 St. Gallen, Switzerland
2. Graduate Training Center of Neuroscience, University of Tübingen, Österbergstr. 3, 72074 Tübingen, Germany
3. MEG-Center, University of Tübingen, Otfried-Müller-Str. 47, 72076 Tübingen, Germany
4. Department of Neurology, University of Tübingen, Hoppe-Seyler-Str. 3, 72076 Tübingen
5. CIMeC, Center for Mind/Brain Sciences, University of Trento, Corso Bettini 31, 38068 Rovereto, Italy
6. DIPSCO, Department of Psychology and Cognitive Science, University of Trento, Corso Bettini 84, 38068 Rovereto, Italy

Optically pumped magnetometers (OPM) are promising tools for the measurement of neuronal magnetic activity because their operation does not require cryogenic cooling with liquid helium and is thus much cheaper than the usage of SQUID-based magnetometers. Another advantage of OPMs is that they can be configured more freely in space and therefore allow for the measurement of various physiological signals. While successful measurements of neuromagnetic brain signals using OPMs have been already reported, the measurement of signal propagation in peripheral nerves and signal processing in the spine has not been explored intensively.

In our study, we have designed an experimental setup that enabled us to stimulate the median and tibial nerve in order to measure electrically evoked neuromagnetic activity from the 1st and 2nd neuron of the somatosensory pathway and to study the activity of the second motor neuron including the spinal reflex circuit.

First tests are promising and provide information about how a functioning measurement setup using OPMs should be established. If tests will reveal that neuronal acivity can be reliably recorded from peripheral nerves and the spinal coord, then the usage of OPMs has a great potential as an important tool for the diagnosis of neural degenration and nerve injuries in neurological praxis.

Co-registration in On-scalp Magnetoencephalography Based on Optically-pumped Magnetometers

Rasmus Zetter[1], **Joonas Iivanainen**[1], **Matti Stenroos**[1], **Lauri Parkkonen**[1,2]

1. Department of Neuroscience and Biomedical Engineering, Aalto University, Espoo, Finland
2. Aalto NeuroImaging, Aalto University, Espoo, Finland

Magnetoencephalography (MEG) is a non-invasive functional neuroimaging method for investigating neuronal activity in the living human brain [1]. MEG measures the magnetic field produced by neural currents in the brain using sensors positioned around the head. Zero-field optically-pumped magnetometers (OPMs) have recently reached sensitivity levels that enable their use in MEG [2, 3]. In contrast to the cryogenically cooled SQUID sensors used in conventional MEG systems, OPMs can be placed within millimetres from the scalp, enabling the construction of sensor arrays that conform to the shape of the head. Such *on-scalp* MEG systems have been shown [4, 5] to have considerable benefits over SQUID-based systems.

To properly estimate the location of neural sources within the brain, one must accurately know the position and orientation of all sensors in relation to the head. With adaptable on-scalp MEG sensor arrays, this co-registration becomes more challenging than in current SQUID-based MEG systems that use rigid sensor arrays, as the position and orientation of each sensor must be individually determined.

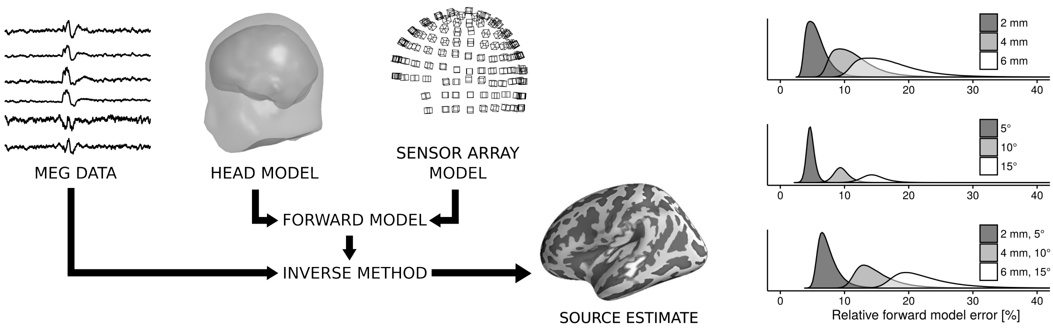

Fig. 1 Left: Illustration of the source estimation process in MEG. Right: Effects of different levels of RMS co-registration errors on the forward model. Top row: sensor position error, middle row: sensor orientation error, bottow row: both sensor position and orientation error.

We performed simulations to quantify how accurately one needs to know the position and orientation of sensors in an on-scalp MEG system. To this end, we created a hypothetical 184-channel OPM sensor array and applied it to three-shell (intracranial space, skull, scalp) head models acquired from 10 adult subjects, whereafter random co-registration errors were added to the sensor arrays. Additionally, a commercial 306-channel SQUID-based MEG system was included in the simulations as a comparison baseline. We applied metrics that quantify the effect of co-registration error on the forward models as well as metrics that quantify the performance of two common source estimation procedures, minimum-norm estimation and dipole fitting, in the presence of co-registration error.

We found that sensor position errors generally have a larger effect than orientation errors, and that these errors affect the localisation accuracy of superficial sources the most. Based on our results, we propose ¡ 4-mm RMS sensor position and ¡ 10° RMS sensor orientation error levels as a requirement for source estimation in on-scalp MEG. When fulfilling these criteria, source localisation accuracy of on-scalp MEG systems using currently available OPMs is similar to or higher than that of current SQUID-based MEG systems.

References

[1] M. S. Hämäläinen, R. Hari, R. J. Ilmoniemi, J. Knuutila, and O. V. Lounasmaa, *Magnetoencephalography–theory, instrumentation, and applications to noninvasive studies of the working human brain*, Rev. Mod. Phys. **65**, 413 (1993).

[2] H. Xia, A. Ben-Amar Baranga, D. Hoffman, and M. V. Romalis, *Magnetoencephalography with an atomic magnetometer*, Appl. Phys. Lett. **89**, 211104 (2006).

[3] V. K. Shah and R. T. Wakai, *A compact, high performance atomic magnetometer for biomedical applications*, Phys. Med. Biol. **58**, 8153 (2013).

[4] E. Boto, R. Bowtell, P. Krüger, T. M. Fromhold, P. G. Morris, S. S. Meyer, G. R. Barnes, and M. J. Brookes, *On the Potential of a New Generation of Magnetometers for MEG: A Beamformer Simulation Study*, PLoS One **11**, e0157655 (2016).

[5] J. Iivanainen, M. Stenroos, and L. Parkkonen, *Measuring MEG closer to the brain: Performance of on-scalp sensor arrays*, NeuroImage **147**, 542 (2017).

P32

Optically pumped magnetic field camera – A proposal

Christian B. Schmidt[1], **Gregor Oelsner**[1], **Rob IJsselsteijn**[2], **Volkmar Schultze**[1], **Ronny Stolz**[1]

1. Leibniz Institute of Photonic Technology, Albert-Einstein-Straße 9, D-07745 Jena, Germany
2. Supracon AG, An der Lehmgrube 11, D-07751 Jena, Germany

In this work, a new design for an optically pumped magnetic field camera (MC) is proposed which will be used to measure bio-magnetic fields. The MC is intended to be used as a non-invasive and absolute measuring tool in the neuroscientific research on epileptic activity and/or to monitor drug delivery in small animals. Therefore, the MC has to be able to monitor magnetic fields in the pico-Tesla range with a bandwidth of at least 100 Hz with a spatial resolution of a few millimetres. The last requirement leads to a working distance of a few millimetres as well as a thin gas cell and low spin diffusion with respect to the lateral resolution. These demands are met by the light-shift dispersed Mz (LSD-Mz) mode [1]. It furthermore disposes the need of a lock-in amplifier for each single pixel and the whole MC needs only one B_1-coil, due to the broad absorption peaks in the LSD-Mz mode of about 1kHz, which corresponds to 0.3μT magnetic field range for Cesium.

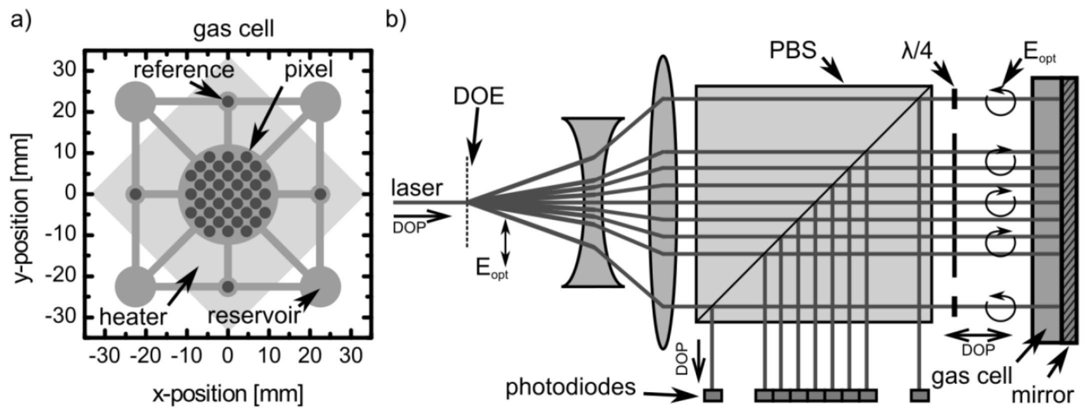

Fig. 1 (a) The centre of the gas cell (medium grey) contains the single pixels (dark grey) of the MC, which are pumped by σ^+-polarized light. The reference spots are pumped by σ^--polarized light. Pixels and references are covered by a heater (light grey) and are connected by channels to ensure identical conditions everywhere. Gas reservoirs are placed outside of the heater, making them cooler to prevent gas condensation in the optical beam paths. (b) A laser beam propagates through a diffractive optical element (DOE) to generate equally strong laser beams, while a following lens system collimates the laser beams. After a polarizing beam splitter (PBS) quarter wave plates generate the desired circular polarization of the beams needed at the gas cell. After the gas cell, the beams are reflected by a mirror, doubling the effective beam inside the gas cell. The PBS redirects the beams onto a photodiode array. (DOP: direction of propagation. E_{opt}: polarization of the optical electrical field.)

For the realization of the MC several problems have to be solved. First, the optical illumination of the MC has to be uniform for each pixel. Furthermore, the LSD-Mz mode needs a pixel and a reference pumped by different helicities of the laser light. A possible gas cell design with an appropriate illumination can be found in Fig. 1(a). For this structured illumination of the cell we intend to use a diffractive optical element (DOE). The resulting beam path of the MC is shown in Fig. 1(b), where the quarter wave plates have different orientation for pixel and reference beams. Secondly, the gas cells of the MC are quite large calling for a heating of the optical windows to prevent condensation of the alkali gas. Herein, we will use transparent semiconductors, like aluminium-doped ZnO (AZO) [2], for electrical heating via an off-resonant alternating current. Thirdly, due to the LSD-Mz principle, analogue balanced detectors will be used for each pixel-reference pair prior to analogue-digital conversion for data analyses. Based on this proposal, the MC setup is in preparation. First results will be presented.

References

[1] V. Schultze, B. Schillig, R. IJsselsteijn, T. Scholtes, S. Woetzel, and R. Stolz, *An Optically Pumped Magnetometer Working in the Light-Shift Dispersed M_z Mode*, Sensors **17** (3), 561 (2017).

[2] P. Banerjee, W.-J. Lee, K.-R. Bae, S. B. Lee, and G. W. Rubloff, *Structural, electrical, and optical properties of atomic layer deposition Al-doped ZnO films*, J. Appl. Phys. **108** (4), 043504 (2010).

OPM versus SQUID Arrays in MEG Functional Connectivity Estimation: A Simulation Study

Dmitrii Altukhov[1,4]**, Joonas Iivanainen**[2]**, Matti Stenroos**[2] **, Lauri Parkkonen**[2]**, Alexei Ossadtchi**[1,3]

1. Higher School of Economics, Artificial Intelligence and Data Analysis Department, Moscow, Russian Federation
2. Aalto University, Department of Neuroscience and Biomedical Engineering, Espoo, Finland
3. Higher School of Economics, Center for Cognition and Decision Making, Moscow, Russian Federation
4. Moscow State University of Pedagogics and Education, MEG Center, Moscow, Russian Federation

Magnetoencephalography (MEG) refers to measuring electric brain activity through the associated magnetic field outside the head. Here, we performed simulations to assess the performance of an MEG array of optically-pumped magnetometers (OPM) for detecting and localizing functional brain networks formed by linearly-coupled sources. We simulated OPM probe arrays that had 102 OPMs measuring either the tangential (tOPM) or normal component (nOMP) of the magnetic field, and compared them against two standard SQUID-based arrays that had 102 SQUIDs measuring the normal component of the magnetic field (nSQUID) or 204 SQUIDs measuring the planar gradient of the normal magnetic field (gSQUID). Given the superior spatial resolution delivered by the OPM arrays [1] we separately studied networks whose nodes are less vs. more than 3 cm apart.

We employed FreeSurfer software to segment the cortical mantle from MRIs of 10 adult subjects, decimated the resulting surfaces to 15 000 source points and calculated the corresponding forward matrix $\mathbf{G}$ using a three-compartment boundary element model. We simulated induced activity of a pair of coupled cortical sources as two 10-Hz sinusoidal oscillators with a random phase with respect to the trial onset but probabilistically connected via a mutual phase difference $\phi = \phi_0 + \delta\phi$ with $\delta\phi$ sampled from a uniform random distribution $[-\pi/4, \pi/4]$ and mean phase difference between the activity of the coupled sources set to $\phi_0 = \pi/2$ to rule out the spatial leakage effect. Each simulated dataset contained 100 epochs.

We performed N = 500 Monte-Carlo (MC) iterations. During each iteration the two coupled sources were chosen randomly from the 15 000 source points. For network detection, we decimated the cortical surface further keeping a subset of 1503 points. We performed separate simulations for spatially white (covariance $\mathbf{R}_\mathrm{w} = \sigma^2\mathbf{I}$) and spatially correlated ($\mathbf{R}_\mathrm{c} = \sigma^2\mathbf{G}\mathbf{G}^\mathrm{T}$) noise. For source-space connectivity analysis, we used iDICS obtained from the original DICS [2] by considering only the imaginary part of the source-space cross-spectrum.

As a threshold-free performance metric, we used the area under the precision–recall curve [3]. At the n-th MC iteration we simulated a network defined by two nodes with coordinates $\mathbf{r}_1^n$ and $\mathbf{r}_2^n$. For each such node, we defined a set of indices of cortical mesh nodes Ω_1^n and Ω_2^n whose coordinates fall into the δ-neighborhood of $\mathbf{r}_1^n$ and $\mathbf{r}_2^n$, i.e. $\Omega_k^n = \{i\} : (\mathbf{r}_k^n - \mathbf{r}_i) < \delta$ for $k = 1, 2$, $\delta = 1$ cm. An estimated connection between a pair of nodes from Ω_1^n and Ω_2^n (but not within one subset) was considered correctly identified.

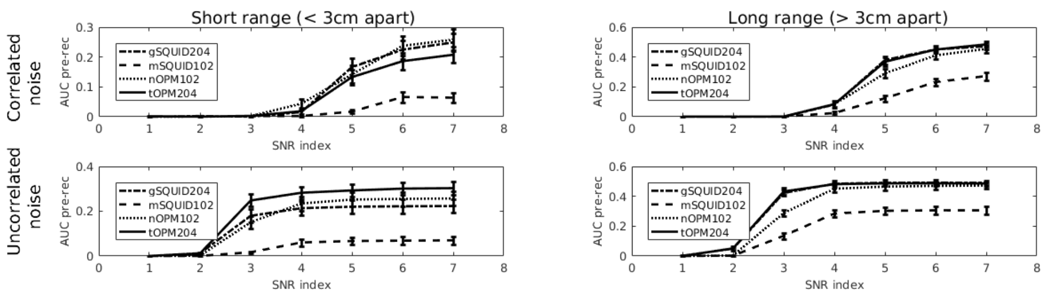

Fig. 1 Simulation results.

For brain networks comprising close-by nodes, the 102 sensor tOPM array delivers significantly better performance than all the other arrays in the white-noise scenario. In all four test cases, the nSQUID array performs worst; yet, 102 nOPM array presents a significant improvement in network detection for both noise models. Also, in the correlated noise case the gSQUID array pars with the 102 channel nOPM array in the short-range networks detection task and performs better in the long-range coupling scenario.

References

[1] J. Iivanainen, M. Stenroos, and L. Parkkonen, *Measuring MEG closer to the brain: Performance of on-scalp sensor arrays*, NeuroImage **147**, 542 (2017).

[2] J. Groß, J. Kujala, M. Hämäläinen, L. Timmermann, A. Schnitzler, and R. Salmelin, *Dynamic imaging of coherent sources: Studying neural interactions in the human brain.* Proceedings of the National Academy of Sciences **98**, 694 (2001).

[3] D. Powers, *Evaluation: From Precision, Recall and F-Measure to ROC, Informedness, Markedness and Correlation*, Journal of Machine Learning Technologies **2**(1), 37 (2011).

P34

Wide-Field Imaging of Magnetic Fields Using Nitrogen-Vacancy Centers in Diamond: Estimation of required sensitivity and resolution

Mürsel Karadas[1], Adam M. Wojciechowski[2], Nils Ole Dalby[2,3], Alexander Huck[2], Ulrik L. Andersen[2], and Axel Thielscher[1,4]

1. Department of Electrical Engineering, Technical University of Denmark, 2800 Kgs. Lyngby, Denmark
2. Department of Physics, Technical University of Denmark, 2800 Kgs. Lyngby, Denmark
3. Department of Drug Design and Pharmacology, Copenhagen University, 2100 Copenhagen, Denmark
4. Danish Research Center for Magnetic Resonance, Copenhagen University Hospital Hvidovre, 2650 Hvidovre, Denmark

Recently, magnetometry based on quantum measurements of the nitrogen-vacancy (NV) centers in diamond has been proposed to detect brain activity with high spatial and temporal resolution [1]. In NV magnetometry, a diamond chip with a thin and dense NV center layer is employed. The electronic spin of these NV centers is initialized (polarized) under laser illumination, altered by a microwave source and read out optically. Magnetic field is then inferred from the magnetic resonance signals in the NV fluorescence. In this study, we use computational simulations to explore the feasibility of wide-field imaging of magnetic fields caused by neural activity in rat brain slices with high spatial and temporal resolution by means of NV magnetometry.

Our goal was to determine the required measurement sensitivity and resolution in space and time of the NV sensors. We simulated the magnetic fields using realistic models of pyramidal neurons in the hippocampal CA1 region that would result from evoked events generated by stimulating Schaffer collateral axons. The thickness of the simulated brain slice was set to 400 μm (50 μm dead, 300 μm active, 50 μm dead cell layer at bottom, middle and top, respectively) which is similar to standard hippocampus samples prepared for electrophysiological experiments (Figure 1-a). The calculation of the transmembrane potential and currents was performed using the NEURON (v7.4) software package [2]. Then, the extracellular magnetic fields were determined in the diamond plane placed directly below the brain slice. Our simulation results indicate that the magnetic field has strong components orthogonal to the CA1 cells body layer and that it reaches up to 2.5 nT whenever the nerve excitation is strong enough to generate action potentials (Figure 1-b, c). Moreover, the temporal information is contained mostly within the bandwidth from DC to 0.5 kHz (Figure 1-d). Further analysis demonstrated that the optimal reconstruction of the neural current source requires a measurement resolution of around 10 μm (data not shown). If we consider a 5-μm thick NV layer, a 10×10 μm^2 sensing area and a 1 kS/s sampling rate, the next generation NV sensor proposed in [3] would have a magnetic field resolution of 167 $\mathrm{pT_{RMS}}$. These results suggest that magnetic fields caused by neural activity may be imaged using high-purity diamond sensors with a large NV concentration, combined with a fast and high signal-to-noise ratio camera.

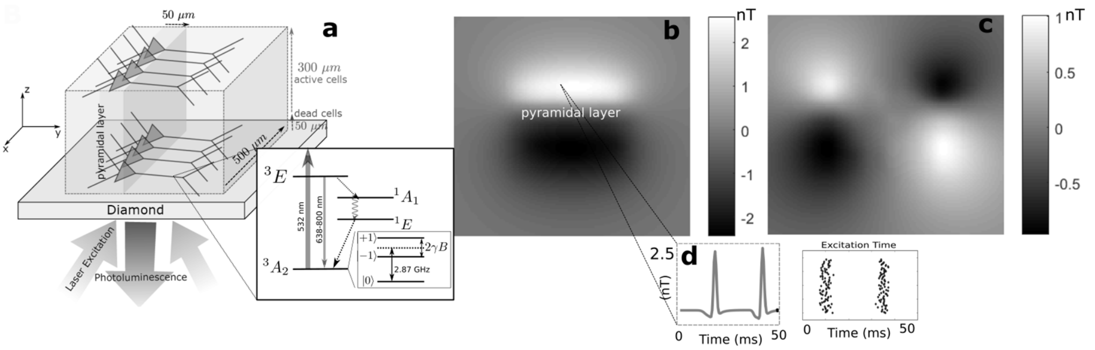

Fig. 1 (a) Simulation setup proposed for NV magnetometry. NV layer on diamond substrate detects the projection of the magnetic field generated by slice. (Inset) NV center energy level diagram. A small patch of 500 μm x 500 μm x 300 μm CA1 region is placed on the diamond sample. The soma location of each cell is equally distributed over a thickness of 50 μm in y direction. (b) Peak magnitude of X component of the magnetic field. (c) Z component of the magnetic field. (d) Time course of the signal for a given excitation pattern.

References

[1] L. T. Hall *et al.*, *High spatial and temporal resolution wide-field imaging of neuron activity using quantum NV-diamond*, Sci. Rep. **2**, 401 (2012).
[2] M. L. Hines and N. T. Carnevale, *NEURON: a tool for neuroscientists*, Neuroscientist **7**(2), 123 (2001).
[3] J. F. Barry *et al.*, *Optical magnetic detection of single-neuron action potentials using quantum defects in diamond*, Proc. Natl. Acad. Sci. **18**, 201601513 (2016).

Authors

Notes:

Elekta